

CIRCADIAN BEHAVIOR AND GENE EXPRESSION IN AN ESTUARINE
CNIDARIAN, *NEMATOSTELLA VECTENSIS*

by

Whitney B Leach

A dissertation submitted to the faculty of
The University of North Carolina at Charlotte
in partial fulfillment of the requirements
for the degree of Doctor of Philosophy in
Biology

Charlotte

2019

Approved by:

Dr. Adam Reitzel

Dr. Andrew Truman

Dr. Stan Schneider

Dr. Paola Duarte-Lopez

Dr. George Banks

ABSTRACT

WHITNEY B LEACH. Circadian behavior and gene expression in a burrowing estuarine cnidarian *Nematostella vectensis*. (Under the direction of ADAM M. REITZEL)

Animals respond to diurnal shifts in their environment with a combination of behavioral, physiological, and molecular changes to synchronize with regularly-timed external cues. The light:dark cycle is regarded as the most important entrainment cue for setting cycles in many bilaterian including mammals, fish, insects and other invertebrates; but the molecular mechanisms that may be responsible for these phenotypes in non-bilaterian phyla remain largely unknown. To improve our understanding of how the photoperiod impacts circadian oscillation in cnidarian organisms (sister group to bilaterians), the sea anemone *Nematostella vectensis* was used to develop transcriptional and behavioral profiles in response to different light conditions. *Nematostella* has oscillating patterns of locomotion and respiration, as well as the molecular components of a putative circadian clock that may provide a mechanism for these light-induced responses. Transcriptional profiling revealed large shifts in differential gene expression in response to light removal and to different wavelengths of light. Further, analysis revealed many circadian clock related genes shift expression or lose expression depending on the light cue, suggesting that this repertoire of genes may be photo-responsive rather than truly circadian and behavioral profiling of anemones in different wavelengths revealed a potential circatidal clock in anemones. Our data highlight the importance of diel light cycles on circadian mechanisms in this species, prompting new hypotheses for the role of photoreception in major biological processes, e.g., metabolism, immunity.

DEDICATION

To my partner, Maison Leach, for fiercely supporting me and irrevocably believing in me, even when I didn't believe in myself. This dissertation is dedicated to you.

ACKNOWLEDGMENTS

I would first like to acknowledge the support I have received the past 4 years from my advisor Dr. Adam M. Reitzel. You have supported my research goals and career aspirations in every way, providing mental and financial support to learn everything I wanted or needed to learn but most importantly you have been my ultimate inspiration as a human and a scientist. I only hope that one day I am able to impact the lives of others the way you have impacted mine. I must also express the upmost gratitude to Dr. Stan Schneider for allowing me the opportunity to do undergraduate research, which ultimately led to my love for animal behavior. Thank you for encouraging me to pursue graduate training, all of your support getting me there, and your continual mentorship over the past 10 years. I would also like to thank my other committee members Dr. Truman, Dr. Banks, and Dr. Lopez-Duarte for their invaluable advice, time, and encouragement. I would like to extend special thanks to Dr. Ann Tarrant for being my ‘home away from home’ during field work trips. I am so grateful for your endless kindness and willingness to provide advice, a microscope, or a couch. Furthermore, I acknowledge my lab mates, and colleagues, Remi Ketchum, Tyler Carrier, Devin Clegg, and Amy Klock, who contributed both intellectually and emotionally to my scientific journey. I thank you each for the courage to push me further than I would have gone on my own and for providing solace during the ups and downs. I would also like to thank all the other postdoctoral fellows, graduate and undergraduates that have assisted, inspired, and challenged me throughout my graduate program and those whose labs I’ve visited to work and receive training that made this dissertation possible. I also acknowledge the support from both the Department of Biological Sciences and the Graduate School at

UNC Charlotte. Finally, thank you to my parents and sister for teaching me hard work and perseverance, without which this work would not have been possible.

TABLE OF CONTENTS

LIST OF TABLES	xiv
LIST OF FIGURES	xvi
INTRODUCTION	1
1.1 Structure of Animal Circadian Clocks	1
1.2 Transcription-Translation Feedback Loop: Positive and Negative Elements	2
1.2.1 Insect Oscillator	2
1.2.2 Mammalian Oscillator	3
1.3 Transcription-Translation Feedback Loop: Feed-Forward Loop	4
1.3.1 PAR-bZIP Transcription Factors	4
1.4 Non-Model Organism Clocks	4
2.1 Cnidarians	5
2.1.1 The Ecology and Distribution of <i>Nematostella</i>	6
2.1.2 <i>Nematostella</i> in the Laboratory	7
2.1.3 Field Collections of <i>Nematostella</i>	9
3.1 Current Understanding of Cnidarian Circadian Clocks	9
4.1 Dissertation Aims and Objectives	11
CHAPTER 1: GENE EXPRESSION EFFECTS OF LIGHT CUE REMOVAL IN <i>NEMATOSTELLA VECTENSIS</i>	
Citation and Abstract	15
Introduction	16
Materials and Methods	20

Culturing and entrainment of <i>Nematostella vectensis</i>	20
Light-removal experiment	21
Tag-based RNA library preparation, sequencing, and processing	22
Data processing pipeline	22
Identification of cycling genes	23
Identification of differentially expressed genes (DEGs)	23
Gene ontology (GO) enrichment analysis	24
Gene co-expression	25
Results	26
Cycling gene expression	26
Cycling genes in LR1 and LR2	28
Differential gene expression	29
LD v DD	30
LD v LR1	31
LD v LR2	32
Weighted gene co-expression network analysis (WGCNA)	33
Discussion	34
‘Circadian’ gene expression dependent on light cues	34
Changes in light condition results in stress and changes to chromatin structure	36
Photoresponse versus circadian clock	37
References	39
Tables	48

Figures	50
---------	----

CHAPTER 2: ROLE OF LIGHT WAVELENGTH IN *NEMATOSTELLA VECTENSIS* BEHAVIOR AND GENE EXPRESSION

Abstract	63
Introduction	64
Results	68
Nocturnal behavior irrespective of light condition	68
Wavelength-inducible circadian or circatidal behavioral response	69
Spectrally insensitive gametogenesis of <i>Nematostella</i>	69
Wavelength and time-of-day dependent transcriptional response	70
Transcriptomic response combining wavelength and time	73
Expression of candidate circadian genes	75
Discussion	77
Conclusions	83
Materials and Methods	83
Animal culture	83
Experimental treatments	83
Behavioral assays and data analysis	84
Wavelength experiment	85
Tag-based RNA library preparation, sequencing, and processing	86
Gene expression analysis	86
References	89

Figures	104
CHAPTER 3: TEMPORAL SINGLE CELL GENE EXPRESSION OF <i>NEMATOSTELLA VECTENSIS</i>	
Abstract	111
Introduction	111
Materials and Methods	114
Transgenesis for cell/tissue-specific markers	115
Animal culturing and sampling	115
Tissue processing, cell sorting, and MARS-seq	115
Cyclic transcript expression analyses	117
Results and Discussion	118
References	123
Figures	129
CHAPTER 4: BACTERIAL RHYTHMS IN <i>NEMATOSTELLA VECTENSIS</i>	
Citation and Abstract	132
Introduction	133
Materials and Methods	137
Animal culturing and experimental conditions	137
Assaying microbial communities	139
Identification of oscillating OTUs	141
Results	141
Community-level dynamics	141
Composition of the bacterial community	142

Shared taxa between LD and DD	144
Patterns of abundance in LD and DD	144
Discussion	145
References	150
Tables	163
Figures	167
CHAPTER 5: GLOBAL TEMPORAL GENE EXPRESSION OF <i>NEMATOSTELLA</i> <i>VECTENSIS</i> ‘IN-SITU’	
Abstract	175
Introduction	176
Materials and Methods	179
Animal culture: in the laboratory and <i>in situ</i>	179
TagSeq: library preparation, sequencing, and processing	180
Expression variation between individual and pooled samples	181
Gene expression analyses	182
Results	
Differentially variable genes between pooled and individual samples	183
<i>Nematostella</i> ‘ <i>in-situ</i> ’ gene expression is correlated with time-of-day	184
Environmental conditions	187
<i>Nematostella</i> gene expression <i>in-situ</i> and in laboratory conditions	187
Discussion	188

References	191
Figures	199
OVERALL CONCLUSIONS	207
INTRODUCTION REFERENCES	209

LIST OF TABLES

CHAPTER 1

TABLE 1.1: Cycling and differential expression of candidate circadian clock genes resulting from DESeq2 and JTK_Cycle analysis of subgroups. 48

TABLE 2.1: Top significantly enriched gene ontology (GO) terms of contrasting treatment subgroups. 49

TABLE S1: Raw counts table for the samples reported in this study.

TABLE S2: Reads per sample for the samples reported in this study.

TABLE S3: JTK_Cycle analysis of *Nematostella* transcriptomes pre- and post-light removal.

CHAPTER 2

TABLE S1: Photoperiod vs. scotoperiod statistical comparisons of activity profiles in this study.

TABLE S2: Reads per sample reported in this study.

TABLE S3: Differentially expressed genes by color and time from DESeq2 analyses.

TABLE S4: Gene ontology enrichment for modules in gene co-expression analysis.

TABLE S5: Gene expression comparisons for the candidate circadian genes reported in this study.

CHAPTER 3

TABLE 1.3: Primers used in this study. 131

CHAPTER 4

TABLE 1.4: Taxonomic classification for differentially abundant OTUs associated with *Nematostella vectensis* in light:dark (LD) relative to constant darkness (DD) conditions. 163

TABLE 2.4: Taxonomy of OTUs with significant 24-hour periodicity associated with adult *Nematostella vectensis* in light:dark (LD) and constant darkness (DD) conditions, as determined by JTK_Cycle. 164

TABLE 3.4: Differential gene expression of candidate cnidarian innate immune genes between light:dark (LD) and constant darkness (DD) determined by DESeq2. NOD genes were arbitrarily given numbers and the order matches the order in Supplemental Table 1 from Lange et al. (2011). 165

LIST OF FIGURES

CHAPTER 1

FIGURE 1: Gene expression of <i>Nematostella vectensis</i> in diel and constant conditions.	50
FIGURE 2: Candidate circadian gene expression profiles over time.	51
FIGURE 3: Gene ontology analysis of differently expressed genes after light removal.	52
FIGURE 4: Eigengene expression across all treatment subgroups for light responsive WGCNA salmon module.	53
FIGURE S1: Experimental design of (1) diel and (2) long-term darkness treated <i>Nematostella</i> run in parallel.	54
FIGURE S2: DESeq2 analysis of <i>Nematostella</i> transcriptomes pre- and post-light removal.	55
FIGURE S3: WGCNA analysis of differentially expressed genes across all light treatment subgroups, individuals, and time.	56
FIGURE S4: Module-trait relationship heatmap and significance values of each module eigengene correlated to external traits.	57
FIGURE S5: Gene significance scatter plots for each light treatment subgroup.	58
FIGURE S6: Venn diagram of cycling genes from each light treatment subgroup generated by JTK_Cycle.	59
FIGURE S7: Gene ontology (GO) analysis of differentially expressed genes enriched between light:dark and dark:dark.	60
FIGURE S8: Gene ontology (GO) analysis of differentially expressed genes enriched between light removal day 1 and dark:dark.	61
FIGURES S9: Gene ontology (GO) analysis of differentially expressed genes enriched between light removal day 2 and dark:dark.	62

CHAPTER 2

FIGURE 1: Average locomotive activity (cm/hr) of <i>Nematostella vectensis</i> over a full light cycle.	104
---	-----

FIGURE 2: Normalized locomotive activity patterns of <i>Nematostella vectensis</i> over time.	105
FIGURE 3: Time-of-day and wavelength-dependent differential gene expression analysis of <i>Nematostella vectensis</i> .	106
FIGURE 4: <i>Nematostella vectensis</i> candidate circadian gene profiles over the 24-hour sequencing time course.	107
FIGURE 5: Heatmap of <i>Nematostella vectensis</i> candidate circadian genes across each light treatment.	108
FIGURE 6: Proposed model for the cnidarian circadian clock composed of two loops adapted from Reitzel et al. (2013) and associated behavior.	109
FIGURE S1: A. Light spectra intensity and energy values from the experimental treatments used in this study. Spectra were determined using a Qstick Subminiature Spectrometer (RGB Laser Systems). B. Energy values were determined using a radiometer (QSL 2100, Biospherical Instruments Inc.) at two positions in a 90mm petri dish, on the inner (left star) and outer (right star) edges. Measurements are in $\mu\text{mol}/\text{cm}^2/\text{sec}$ of photons.	110
CHAPTER 3	
FIGURE 1: Venn diagram of significant 24-hour cycling genes in the three lines: gland cells (Gd2K), neural cells (Elav_mOrange), and epithelial cells (Ep3K).	129
FIGURE 2: Time series transcript expression of <i>nvClock</i> (left) and <i>nvCIPC</i> (right) in the Gd2K (A), Ep3K (B), and Elav_mOrange (C) lines from two technical replicates (black and red lines).	130
CHAPTER 4	
FIGURE 1: Experimental design for light:dark (LD) and constant dark conditions (DD) and corresponding sampling.	167
FIGURE 2: Similarity amongst the bacterial community associated with light:dark (LD) and constant darkness (DD) entrained <i>Nematostella vectensis</i> .	168
FIGURE 3: Abundance plots of 24-hour cycling bacterial OTUs during light:dark and constant darkness over the time course.	169
FIGURE S1: Alpha rarefaction curves for LD and DD entrained <i>Nematostella vectensis</i> . Alpha rarefaction curves for the associated	170

microbiota for *N. vectensis* that were entrained to either a 12-hour light: 12-hour dark light cycle (red squares) or 24 hours of darkness (blue circles) based on the rarefaction depth (1,080 sequences) used for all PCoA plots.

- FIGURE S2: Number of OTUs for the ‘core’ bacterial community. Enumeration of the bacterial phylotypes of the ‘core’ bacterial community associated with *Nematostella vectensis* for LD and DD entrained individuals for 60%, 70%, 80%, 90%, and 100% of sampled anemones. 171
- FIGURE S3: Beta-diversity statistics for ‘core’ diversity analyses. Representation of statistical comparisons (ANOSIM) between the ‘core’ (at 60%, 70%, 80%, 90%, and 100%) bacterial communities associated with LD and DD entrained *Nematostella vectensis*. 172
- FIGURE S4: ‘Core’ bacterial taxa associated with adult *Nematostella vectensis* across treatments. Classes of bacteria associated with LD and DD entrained *N. vectensis* for the ‘core’ community at the 60%, 70%, 80%, 90%, and 100% level. 173

CHAPTER 5

- FIGURE 1: Map of field sampling site (A) and study species, adult *Nematostella vectensis* (B), at Great Sippewissett Marsh in Massachusetts (C). 199
- FIGURE 2: Principal Component Analysis (PCA) of samples collected between 08:00-12:00 (blue) and 13:00-17:00 (yellow). 200
- FIGURE 3: Weighted gene co-expression network analyses in this study. Gene dendrogram of modules based on correlation calculations from rlog transformed count data generated by DESeq2 and obtained by average linkage hierarchical clustering in WGCNA analysis. Colors of the dynamic tree cut represent the modules assigned for each gene, and the colors of the merged dynamic display the new modules after assigning a stringency threshold of 0.25 (A). Average linkage hierarchical cluster tree shows module eigengenes after clustering analysis. Each branch represents a meta-module that groups together the eigengenes that are positively correlated (B). Module-trait relationship heatmap and significance values of each module eigengene correlated to external traits from weighted gene co-expression network analysis (C). Gene co-expression network and module-trait relationships are represented by a heatmap of transcripts assigned to six modules (arbitrary colors on the left of the heatmap). Eigengenes were calculated for each module. The strength of the correlations between traits (time point and biological replicates) and gene expression, is indicated by the intensity of the colored blocks with red and blue indicating positive 201

and negative correlations, respectively. The numbers in each block represent the Pearson's correlation between the module eigengene and the trait and corresponding p-values.

FIGURE 4: (A) Module eigengenes with up-regulation in the afternoon (blue, brown, red) and (B) in the morning (black, pink, turquoise) with eigengene expression on the Y-axis and time on the X-axis. Each bar represents a single replicate. 202

FIGURE S1: Small pen used for *Nematostella vectensis* (A) deployment and recapture (B). 203

FIGURE S2: Gene ontology (GO) enrichment analysis for differentially expressed genes between morning and afternoon samples in the Molecular Function category. AM up-regulated genes are shown in red. PM up-regulated genes are shown in blue. 204

FIGURE S3: Gene ontology (GO) enrichment analysis for differentially expressed genes between morning and afternoon samples in the Biological Processes category. AM up-regulated genes are shown in red. PM up-regulated genes are shown in blue. 205

FIGURE S4: Gene significance scatter plots for the turquoise module. The plots represent gene significance (GS; y-axis) at t10AM (A) and t2PM (B) versus module membership (MM; x-axis). Gene significance and module membership are significant correlations that imply the genes of each module are highly correlated with the time of day sampled. 206

Introduction

1.1 Structure of Animal Circadian Clocks

Nearly all organisms on Earth exhibit biological rhythms driven by environmental cues, or *Zeitgebers*, set by biotic and abiotic factors (e.g., temperature and food availability), with solar (day/night) irradiance as a prominent natural cue. The endogenous, self-sustained oscillations in animals are propelled by a common mechanism involving three essential parts: the proteins that make up the clock itself, input environmental signals and regulatory proteins, and output genes/proteins (clock controlled genes, CCGs; Allada and Chung, 2010; Dunlap, 1999; Golden et al., 1997; Reitzel et al., 2010; Reppert, 2000). The genetic basis of circadian rhythmicity has been defined in several model animals, including insects (Allada and Chung, 2010; Yuan et al., 2007), mammals and other vertebrates (Buhr and Takahashi, 2013; Dodd et al., 2005; Panda et al., 2002), and more recently in sponges (Jindrich et al., 2017) and cnidarians (Hoadley et al., 2011; Reitzel et al., 2010; Vize, 2009, see below). Each of these studies identified several feedback loops, transcription factors, promoter regions, or regulator proteins related to circadian rhythmicity that share common functional domains, protein-protein interactions, and enhancer motifs (Allada and Chung, 2010; Sebens and DeRiemer, 1977; Yuan et al., 2007; Zhu et al., 2008a).

The molecular mechanisms underlying endogenous oscillations in animals are, in principle, a set of interlocking transcriptional-translational feedback loops (TTFL) – mostly transcription factors – that have cyclic expression patterns (Figure 1). The foundation of what is known about the molecular underpinnings of circadian networks

comes from studies using diverse insects and mammals, which is remarkably highly conserved. The general architecture of the circadian framework is composed of three components: negative elements, the positive elements, and feed-forward elements (Dunlap, 1999). Figure 1 shows this network of interacting loops, where the positive elements, also known as the core clock components, upregulate and promote transcription of elements in the feedback and feed-forward loops (along with other CCGs). Activation of these elements in turn provide positive (feed-forward elements) or inhibitory (negative elements) feedback to the core clock components, creating a pattern of activity leading to biological oscillation.

1.2 Transcription-Translation Feedback Loop: Positive and Negative Elements

1.2.1 Insect Oscillator

In 1971, the first circadian clock gene, *period*, was identified in the fruit fly *Drosophila melanogaster* (Konopka and Benzer, 1971). Decades of research since has paved the way for building the circadian framework in flies and other model organisms, which remarkably, is largely conserved among bilaterians and dates back to ancestors of deuterostomes and protostomes (Dunlap, 1999). It was in *Drosophila* that TTFLs were originally proposed as the mechanism that drives rhythmic gene expression controlling biological clocks (Hardin et al., 1990; Hardin et al., 1992). After extensive investigation of this hypothesis, the current understanding of TTFLs is shown in Figure 2.

In flies, as reviewed in Allada and Chung (2010), expression of transcriptional activators *Clock* and *Cycle* of the basic helix-loop-helix Per-ARNT-Sim (bHLH-PAS) family make up the core of the clock, or the positive elements (Figure 2). Light driven

rhythmic cytoplasmic expression of their encoded protein products CLK and CYC form heterodimers (CLK:CYC) via their PAS domains, that translocate back to the nucleus where they selectively bind to the E-box enhancer elements (CACGTG) in the DNA binding domain of target genes, including the transcriptional repressors *period* and *timeless*. In the cytoplasm, accumulation of CLK:CYC early in the photoperiod drives an increase of PER:TIM and by the end of the photoperiod, a decrease of CLK:CYC effectively terminates expression of *period* and *timeless*. As the balance of PER:TIM is greater in the cytoplasm late in the day, the remaining CLK and CYC proteins are degraded as PER and TIM proteins heterodimerize and translocate to the nucleus where they bind to and sequester CLK:CYC heterodimers via a PAS domain, keeping them from binding to E-boxes and essentially turning off their own transcription. By the next day, early light activates transcription of *Clock* and *Cycle* and the loop repeats itself.

1.2.2 Mammalian Oscillator

The positive elements *Clock* and *brain and muscle ARNT-like protein 1*, or *BMAL1* (ortholog of *Cycle*, in the bHLH family of transcription factors – also called MOP3), make up the core bilaterian oscillator [see reviews by Reppert (2000) and Reppert and Weaver (2002)]. One of the major differences between the molecular mechanisms of circadian clocks in mammals and flies is in the negative loop, where CLK:BMAL1 heterodimers drive expression of both conserved and unique CCGs as repressors: three orthologous PERIOD (PER1, PER2, or PER3) proteins and two orthologous Type II Cryptochromes (CRY1 or CRY2). Combinations of these transcriptional repressive CCGs form heterodimers, and provide negative feedback by

directly interacting with CLK:BMAL1 heterodimers through their PAS domains in a mechanism similar to *Drosophila*.

1.3 Transcription-Translation Feedback Loop: Feed-Forward Loop

1.3.1 PAR-bZIP Transcription Factors

Transcription factors in the proline- and acid-rich (PAR) subfamily of the basic leucine zipper bZIP family are common regulators of a broad range of biological processes, including development, reproduction, metabolism, and circadian cycles (Amoutzias et al., 2007; Reinke et al., 2013). In both insects and mammals, the feed-forward loop of the circadian architecture for some tissues is made up of PAR-bZIP genes (Reitzel et al., 2013b), although their function is better characterized in insects. The activity of this branch of the clock provides both positive and negative feedback to the core clock components to balance their transcription. In *Drosophila*, protein products of E-box containing PAR-bZIP genes *vriille* and *pdp1* (also target genes of CLK:CYC activation) bind to V/P-boxes in the promoter region of *Clock* genes, inhibiting (VRILLE) or activating (PDP1) its transcription (Cyran et al., 2003).

1.4 Non-Model Organism Clocks

Because studies of circadian oscillators in animals have mainly been conducted on mammals and insects, it has been inferred that many or all animal circadian clock mechanisms are highly conserved due to the level of similarity between these two disparate lineages (Dunlap, 1999). However, with the emergence of genomic resources for non-model organisms and mechanistic characterization of the circadian clock of more

species, divergence of the genes involved in the circadian clock has become increasingly apparent. In addition to gene duplications and deletions contributing to a broader repertoire of circadian genes than previously thought (Yuan et al., 2007), studies have also shown core clock components have involvement in processes other than time-keeping, for example: visual sensitivity (Horne and Renninger, 1988), symbiotic bioluminescence (Heath-Heckman et al., 2013), sun compass apparatus (Merlin et al., 2009; Zhu et al., 2008b), reproductive cycles (Levy et al., 2007), and diapause (Meuti et al., 2015) to name a few. Thus, while early efforts to compare circadian clockwork across bilaterian animals favored a hypothesis for deep conservation (Dunlap, 1999), recent studies with more species have revealed the variability in composition of this molecular time keeper (Rosbash, 2009). These studies resulted in less certainty with what we may actually call the "animal circadian clock" and what the core components are. Here, studies of outgroup taxa to the bilaterians would certainly be of value to understand what components were present and when in phylogenetic history and how they may interact in the origin and variation of the circadian clock in different lineages. Species in the phylum Cnidaria are informative for these comparisons.

2.1 Cnidarians

Cnidarians (corals, jellyfish, sea anemones, hydroids) form a phyla of marine invertebrates that, as an outgroup to Bilateria, comprise an insightful system to study circadian biology from a comparative and functional context. The starlet sea anemone, *Nematostella vectensis*, has been developed as a model cnidarian due to its ease of laboratory culture and sequenced genome (Hand and Uhlinger, 1992; Hand and Uhlinger,

1994; Putnam et al., 2007), becoming a focal species for cnidarian circadian research (Hendricks et al., 2012; Oren et al., 2015; Peres et al., 2014; Reitzel et al., 2010; Reitzel et al., 2013b). In addition to its informative phylogenetic position, *Nematostella* inhabits a highly variable estuarine environment, with seasonal and daily fluctuations in abiotic factors (Reitzel et al., 2013a; Sheader et al., 1997) known to influence behavior and physiology; e.g., gametogenesis, reproductive cycles, oxygen consumption and locomotion (Fritzenwanker and Technau, 2002; Hand and Uhlinger, 1994; Hendricks et al., 2012; Maas et al., 2016).

2.1.1 The Ecology and Distribution of *Nematostella*

Sea anemones are typically found in marine ecosystems; however, a few species have been identified in the brackish water of salt marsh habitats, including *Nematostella vectensis* of the family Edwardsiidae, commonly referred to as the starlet sea anemone. *Nematostella* is a small (~2 cm long), transparent infaunal species occupying the soft substrate in tidally restricted pools with extreme salinity and thermo-tolerance. Salinities and temperatures as low as 8.96 parts per thousand (PPT) and -1°C, respectively, and as high as 51.54 PPT and 28°C have been reported for *Nematostella* (Hand and Uhlinger, 1994; Reitzel et al., 2013a; Williams, 1983). Additionally, extreme daily temperature fluctuations greater than +/- 20°C are possible in these environments.

Kneib (1985) reported the only known predator of *Nematostella* as *Palaemonetes pugio*, a common marsh grass shrimp, but are themselves voracious predators (Posey and Hines, 1991). Based on laboratory and field observations, they naturally occur with their physa and body column burrowed into the thixotrophic sediments, with their oral disk

and tentacles exposed. This position allows them to opportunistically feed on passing adult crustaceans and their larvae (Frank and Bleakney, 1978), where their prey capture strategy involves injection of a battery of neurotoxins prior to ingestion.

The sexes of *Nematostella* are separate and can reproduce asexually through budding, or sexually. Female gametes are released in a gelatinous egg mass where upon external fertilization with sperm, will undergo a complete larval cycle in less than 7 days. Adult anemones will reach sexual reproductive age between 3-6 months in laboratory settings.

Nematostella is widely distributed and can be found all along the eastern, western and Gulf of Mexico coastline of the US, parts of eastern Canada and the southeast coast of England (Hand and Uhlinger, 1994). Population level genomic work suggests that *Nematostella* native range is the eastern coast of the US and has been anthropogenically introduced into other locations (Darling et al., 2004; Reitzel et al., 2008). Nonetheless, this broad geographic distribution with independent populations along a latitudinal cline requires anemones to tolerate a wide range of environmental conditions.

2.1.2 *Nematostella* in the Laboratory

The culturing of *Nematostella* in laboratory settings is well described, further lending towards this species as a model organism. With relatively little investment, anemones can be maintained in non-circulating artificial sea water in finger bowls at ambient light and temperature. Routine care involves weekly feedings of freshly hatched brine shrimp, or mussel for more rapid growth, followed by water replacement; however, animals are negligibly senescent and can be kept at ~16°C indefinitely if they are in clean

water. Although anemones are not sexually dimorphic, they are dioicous and can be induced to spawn in laboratory conditions. Reproductively active adults are capable of undergoing a complete reproductive cycle every 24-hours. Females release egg masses, or clutches, with up to thousands of eggs contained in a jelly-like matrix, which can be removed by washing in 2-4% cysteine solution. Once the eggs have been ‘de-jellied’, manipulation is straightforward (Genikhovich and Technau, 2009b). Females can be kept separate from males; thus fertilization can be controlled and each life history stage (egg, embryo, planula, juvenile polyp, adult) can be collected. Anemones also undergo asexual reproduction via physal budding or pinching, where, within a short period (<5 days), complete regeneration of each portion can occur. Animals can also be cut, which induces regeneration of each portion allowing controlled clonal populations to exist.

The genome of *Nematostella* was sequenced in 2007 (Putnam et al., 2007) revealing a high level of genomic complexity, including conservation of many pathways (e.g., developmental genes, immune genes – (Genikhovich et al., 2010; Layden et al., 2016). Since 2007, several molecular tools have been developed and matured, that in addition to its tractability in the lab, renders *Nematostella* a powerful cnidarian model. Among these tools are matured protocols for transgenesis (Renfer and Technau, 2017), knock-down and knock-out gene editing (He et al., 2018; Ikmi et al., 2014; Karabulut et al., 2019; Moran et al., 2014; Wolenski et al., 2013), and in-situ hybridization (Genikhovich and Technau, 2009a). Further, extensive transcriptome sequencing and gene methylation studies have increased the utility of the *Nematostella* genome (Schwaiger et al., 2014; Sebé-Pedrós et al., 2018; Zemach et al., 2010).

2.1.3 Field Collections of *Nematostella*

Because they are easily collected year-round from salt marsh sediments and occur in high densities, *Nematostella* field collections are relatively simple. Not only does this help with supplying animals for lab populations, but because the natural habitat of *Nematostella* is one that is typically undisturbed, ecological studies are feasible. However, few studies have leveraged their utility ‘*in-situ*’ (in this case, meaning ‘in the field’) from the perspective of evolutionary adaptation. Coastal estuaries are ecologically critical and highly dynamic and the physiological tolerance of *Nematostella*, in addition to limited gene flow between populations (Darling et al., 2004; Reitzel et al., 2008), makes them an attractive model for understanding the genetics and molecular mechanisms underlying local adaptation.

3.1 Current Understanding of Cnidarian Circadian Clocks

Our understanding of what molecular components are involved in the cnidarian clock is fairly limited (see reviews by Hoadley et al., 2016; Reitzel et al., 2013b). Initial studies have provided evidence that cnidarians possess light-sensing proteins responsible for photoreception and genes orthologous to core transcription factors, e.g., Clock and Cycle (Hoadley et al., 2011; Levy et al., 2007; Reitzel et al., 2010); they however lack the prototypical bilaterian clock repressors PER and TIM. Reitzel et al. (2010) described three cryptochromes in *Nematostella* and determined that expression of two (*NvCry1a* and *NvCry1b*) are diel and likely play a role in the circadian regulatory pathway, whereas the potential involvement of other light-sensing proteins like opsins is yet to be determined (Reitzel et al., 2010; Suga et al., 2008). Although circadian cycling as it

relates to light-dependent cues is responsible for numerous physiological, behavioral, and molecular processes, our understanding of which genes respond to daily signals is poor. Potential cnidarian CCGs have been studied in a few species of scleractinian corals: *Acropora cervicornis* (Hemond and Vollmer, 2015), *Acropora millepora* (Brady et al., 2011; Hoadley et al., 2011; Levy et al., 2007; Vize, 2009), and *Favia fragum* (Hoadley et al., 2011) as well as the sea anemone *Nematostella* (Oren et al., 2015; Reitzel et al., 2010). Oren et al. (2015) characterized changes in gene expression in *Nematostella* over a light:dark period and showed that approximately 180 genes had cyclic expression. Under light:dark conditions, potential CCGs that exhibit diel patterns of expression are from diverse gene families and can be categorized into particular functional subgroups; e.g., metabolism, cell cycle, immunity, sensory processes, and essential circadian CCGs. Previous studies that have compared gene expression in light:dark and constant dark conditions have suggested a mixed response in cnidarians. Reitzel et al. (2010) showed that long periods of darkness resulted in loss of cyclic gene expression for putative circadian clock genes in *Nematostella*. Peres et al. (2014) showed that this loss of cyclic expression occurred over a few days, in a gene-dependent manner. In corals, three days of constant darkness resulted in loss of oscillating gene expression for *F. fragum* (Hoadley et al., 2011). Similarly, Brady et al. (2011) showed that brief periods of total darkness (one day) resulted in loss of cyclical gene expression for circadian clock genes in *A. millepora*. It is presently unclear how the prolonged absence of light impacts transcriptome-wide diel gene expression in cnidarians. In this study, we aim to explore genes influenced by the photoperiod that putatively govern daily cycles and circadian regulation in sea anemones.

4.1 Dissertation Aims and Objectives

The objective of this dissertation research is to describe a suite of molecular and behavioral responses to variable light environments for *Nematostella* and determine the impact light has on entrainment of gene expression and activity levels. Previous research in this species and other cnidarians have shown that oscillations in gene expression dampen or disappear for several hypothesized circadian clock genes when exogenous light is removed. Based on these combined data, light perception is a likely mediator in many molecular pathways that work synergistically to coordinate gene expression. We further support these observations by temporally comparing across the transcriptome of dark-entrained sea anemones and have identified a subset of genes that did not retain significant differences in expression over a day period (Leach et al., 2018). The decrease in differentially expressed genes when sea anemones are cultured in constant darkness indicates that consistent light cues are required to maintain oscillations for particular groups of genes.

To further characterize gene expression and behavior to variable photic environments, this dissertation has five data chapters: Chapter 1 quantifies differential gene expression responses to light cue removal in *Nematostella* after 30 days of entrainment in cyclic or constant conditions. Chapter 2 integrates gene expression and behavior to measure the response of *Nematostella* to diel cycles of red, green, and blue light and to constant conditions. Chapter 3 utilizes a cell type specific approach at measuring transcriptomic responses of *Nematostella* to light:dark conditions in three cell types (i.e., neural, epithelial and gland cells). Chapter 4 uses 16S rDNA sequencing to

measure the abundance of bacterial associates of *Nematostella* over both light:dark and constant conditions to measure how symbiotic interactions may be influenced by diel lighting. Chapter 5, the final data chapter, establishes hourly transcriptomic profiles of *Nematostella* sampled '*in-situ*' from The Great Sippewissett Marsh in Massachusetts.

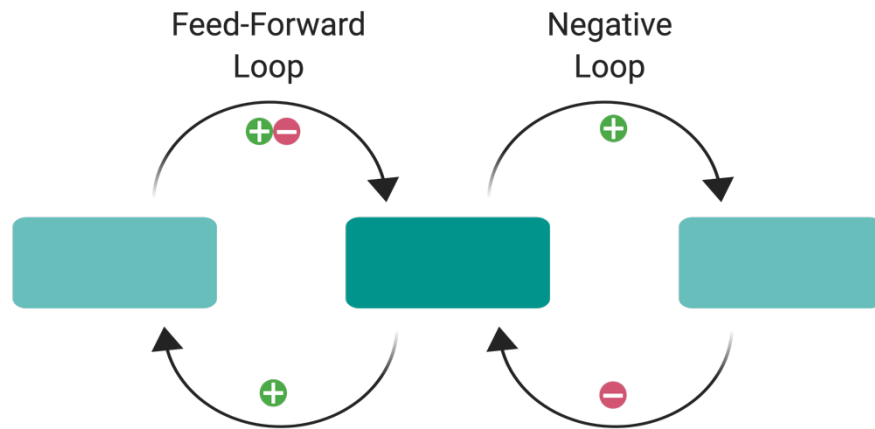


Figure 1. Transcription translation feedback loop architecture model. Model circadian clock oscillations involving feed-back and negative regulation of the circadian clock genes.

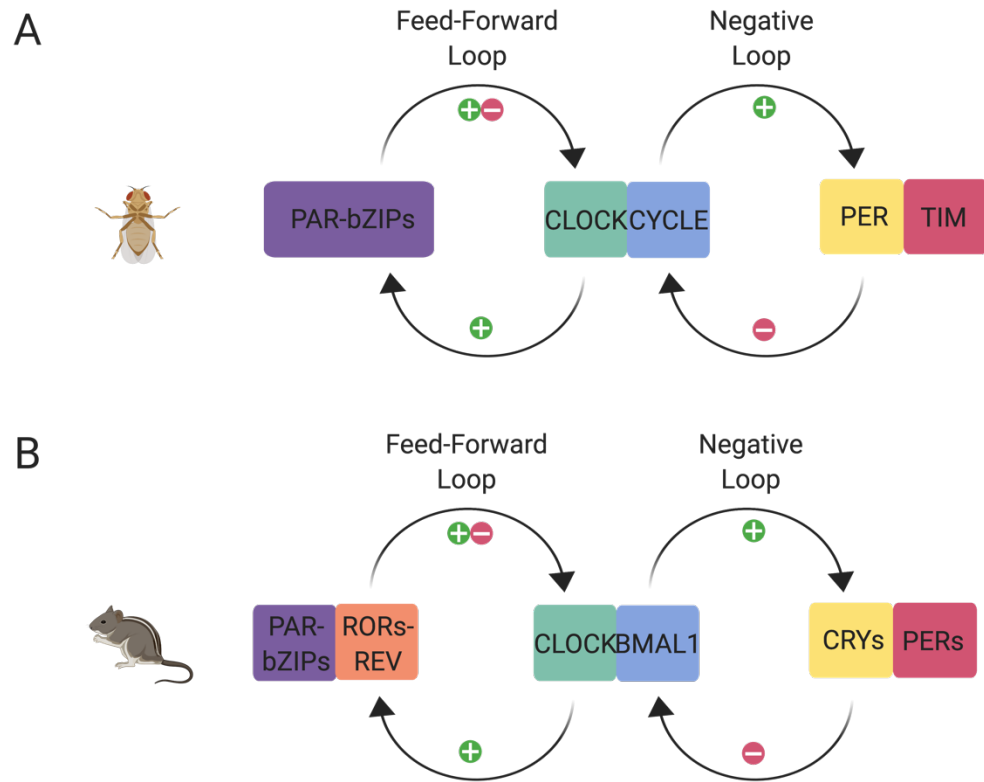


Figure 2. Transcription translation feedback loop in *Drosophila* (A) and mammals (B).

CHAPTER 1

GENE EXPRESSION EFFECTS OF LIGHT CUE REMOVAL IN *NEMATOSTELLA VECTENSIS*

Whitney B. Leach and Adam M. Reitzel

Citation

Leach WB, Reitzel AM. 2019. Transcriptional remodeling upon light removal in a model cnidarian: losses and gains in gene expression. Molecular Ecology **28.14**:3413-3426.

Abstract

Organismal responses to light:dark cycles can result from two general processes: (i) direct response to light or (ii) a free-running rhythm (i.e., a circadian clock). Previous research in cnidarians has shown that candidate circadian clock genes have rhythmic expression in the presence of diel lighting, but these oscillations appear to be lost quickly after removal of the light cue. Here, we measure whole-organism gene expression changes in 136 transcriptomes of the sea anemone *Nematostella vectensis*, entrained to a light:dark environment and immediately following light cue removal to distinguish two broadly defined responses in cnidarians: light entrainment and circadian regulation. Direct light exposure resulted in significant differences in expression for hundreds of genes, including more than 200 genes with rhythmic, 24-hour periodicity. Removal of the lighting cue resulted in the loss of significant expression for 80% of these genes after one day, including most of the hypothesized cnidarian circadian genes. Further, 70% of these candidate genes were phase shifted. Most surprisingly, thousands of genes, some of which are involved in oxidative stress, DNA damage response, and chromatin

modification, had significant differences in expression in the 24 hours following light removal, suggesting that loss of the entraining cue may induce a cellular stress response. Together, our findings suggest that a majority of genes with significant differences in expression for anemones cultured under diel lighting are largely driven by the primary photoresponse rather than a circadian clock when measured at the whole animal level. These results provide context for the evolution of cnidarian circadian biology and help to disassociate two commonly confounded factors driving oscillating phenotypes.

Introduction

Light is a principal environmental cue that shapes biological communities by influencing the behavior, physiology, and gene expression of individual organisms. For organisms living in photic environments, the presence, duration, and intensity of light is the most predictable cue for shaping time-dependent responses, whether they be at periods of hours, days, or seasons (Bradshaw & Holzapfel, 2007; Dunlap, Loros, & DeCoursey, 2004; Edmunds, 1988). Over evolutionary time, these responses to light have resulted in convergent behavioral and physiological phenotypes including diurnal and nocturnal activity patterns, reproductive windows, and migration patterns, to name a few (A. Brady, Hilton, & Vize, 2009; Gwinner, 1996; Mercier & Hamel, 2010; Tosches, Bucher, Vopalensky, & Arendt, 2014). These light-dependent phenotypes measured at the organismal level are the product of the differential expression of molecular pathways. How light exposure is translated by organisms into these diverse phenotypes has been a central focus for understanding how shifts in the environment can result in different phenotypic

outputs through particular changes in gene expression (Cheng, Tsunenari, & Yau, 2009; Fernandes, Fero, Driever, & Burgess, 2013; Roenneberg & Foster, 1997).

Organismal responses to a diel, or daily, light cue can result from two general processes: direct response to the exogenous light or a free-running rhythmic response due to an endogenous time keeper (circadian clock; Berson, Dunn, & Takao, 2002; Miyamoto & Sancar, 1998; D. L. Williams, 2016). Direct responses occur only when an organism responds post-illumination where the light impacts particular cells directly and the response does not continue in the absence of repeated light exposures. Direct light responses occur through ocular (Freedman et al., 1999; Lamb, Collin, & Pugh, 2007) or extra-ocular (Edwards et al., 2008; Porter, 2016) photosensors that may then transmit the light responses to other cells or tissues typically through neural cells. These responses may also occur in any cell exposed to light, which would be particularly common in translucent organisms. On the other hand, circadian clocks generate free-running rhythms as a result of molecular networks that maintain oscillations in phenotype after the entraining cue is removed (Dunlap, 1999; Hardin, 2006). In various animal species, circadian clocks are generally known to be transcription-translation feedback loops that are centrally located in neural cells in the brain or anterior structures (e.g., antennae in some insects) and maintain a free-running period of approximately 24 hours (Dunlap, 1999; Shearman et al., 2000). The central circadian clock can regulate the periodicity of additional tissues through hormonal or other endocrine signaling mechanisms (Gamble, Berry, Frank, & Young, 2014; J. Williams & Sehgal, 2001). Categorization between direct light responses and the endogenous circadian clock can be challenging because these two responses can be causally connected. For example, changes in the timing or duration of the daily light cue

can influence the timing of the circadian clock and result in resetting (jet lag; Davis & Mirick, 2006; Mendlewicz, 2009).

Species from early diverging animal phyla have been studied to characterize the mechanisms of photoreception and signal transduction as well as the potential for a circadian clock (Plachetzki, Fong, & Oakley, 2010). Research with sponges has shown that various species have light-dependent behavior (Leys, Cronin, Degnan, & Marshall, 2002) as well as the molecular components for photoreception (cryptochromes; Rivera et al., 2012), components of the classic bilaterian circadian clock (Jindrich et al., 2017; Simionato et al., 2007), and cyclical oscillations in gene expression of these clock genes under diel lighting conditions (Jindrich et al., 2017). Similarly, light has a significant impact on the behavior of ctenophores and previous studies have shown they have various light sensing proteins encoded in their genome (Schnitzler et al., 2012), but the potential for a circadian clock has not yet been studied (Reitzel et al., 2014). Cnidarians have emerged as an informative group of animals to study the evolution of the circadian clock and the role of daily light exposure on behavior, physiology, and gene expression (Hoadley, Vize, & Pyott, 2016; Reitzel, Tarrant, & Levy, 2013). It has been known for decades that light:dark cycles impact the reproduction, movement, and physiology of various cnidarian species (Chalker, Barnes, Dunlap, & Jokiell, 1988). More recently, phylogenomic studies have shown cnidarians have many of the genes that compose the core bilaterian clockwork (Levy et al., 2007; Reitzel, Behrendt, & Tarrant, 2010; Vize, 2009), most of which are expressed in an oscillating pattern under diel lighting conditions (A. K. Brady, Snyder, & Vize, 2011; Oren et al., 2015; Reitzel et al., 2010). Additional studies, primarily with corals, have also shown that hundreds of genes are differentially expressed under light:dark (A. K. Brady et al.,

2011; Ruiz-Jones & Palumbi, 2015), and lunar (Oldach, Workentine, Matz, Fan, & Vize, 2017) conditions, many of which appear to dissipate once the entraining cue is removed (A. K. Brady et al., 2011; Peres et al., 2014). It remains unclear how much of the differential gene expression is a product of a direct light response or from an endogenous oscillator (Oldach et al., 2017).

In this study, we utilized comparative transcriptomics to investigate the role of direct light exposure and endogenous circadian oscillations on the gene expression of the starlet sea anemone, *Nematostella vectensis* (hereafter referred to as just *Nematostella*). *Nematostella* has developed into a focal species to determine the potential mechanisms for responses to diel lighting and the circadian clock in cnidarians (Hendricks, Byrum, & Meyer-Bernstein, 2012; Maas, Jones, Reitzel, & Tarrant, 2016). This nocturnal species has clear circadian behavior and physiology with differential activity in diel lighting that is maintained upon removal of the entraining cue. *Nematostella* has orthologs (bHLH-PAS members *Clock* and *Cycle/Bmal*) or homologs (cryptochromes, PAR-bZIP) to genes centrally involved in the bilaterian circadian clock, many of which have oscillating expression under light:dark conditions (Reitzel et al., 2010; Reitzel et al., 2013). In addition, hundreds of genes show differential expression under diel lighting (Leach, Macrander, Peres, & Reitzel, 2018; Oren et al., 2015), but many of these have no evidence for differential expression when animals are cultured under extended periods of darkness (Leach et al., 2018; Peres et al., 2014). Together, these previous studies have shown this species has a diverse transcriptional response to light but the maintenance of these oscillations in gene expression are largely unknown, except after long periods of time (>20 days; Leach et al., 2018; Peres et al., 2014; Reitzel et al., 2010; Reitzel et al., 2013).

Understanding how time-dependency of loss of rhythmic expression in genes with removal of the entraining light cue is thus important to discern between direct light effects and those resulting from a free-running circadian clock.

Here, we measure whole organism gene expression changes in *Nematostella* entrained to a light:dark environment and immediately following light cue removal to distinguish two broadly defined responses in cnidarians: (i): light entrainment and (ii) circadian regulation. By comparing transcriptional patterns before and after exogenous light removal, we report hundreds of cycling light responsive genes including those predicted to be involved in a core clock mechanism, followed by a stress response in constant conditions. Finally, we compared co-expressed genes over time and in each light regime to reveal that light condition, rather than time-of-day, most significantly influences gene expression.

Materials and Methods

Culturing and entrainment of *Nematostella vectensis*

Adult sea anemones from an outbred population of the genome strain (Maryland, USA) were cultured in glass dishes containing 15 parts per thousand (ppt) artificial seawater (ASW). These animals were fed haphazardly three times per week with freshly hatched *Artemia* nauplii and the water was changed weekly. Animals were maintained at these conditions for ≥ 1 month in an incubator at 25°C in one of two treatment groups: either a diel light cycle using full spectrum lights (MINGER) or in constant long-term darkness (DD; Fig. S1). Diel conditions were defined as cycles of 12-hour light: 12-hour

dark. Zeitgeber time, or ZT = 0/ “lights on” was at 7:00 AM and ZT = 12/ “lights off” was at 7:00 PM.

Light-removal experiment

Individual sea anemones (2-3 cm in length) were sampled from both treatment groups (diel and long-term darkness; Fig. S1) in parallel every 4 hours over a 3-day period, then immediately preserved in RNAlater (Ambion). Four biological replicates were sampled at each time point from both treatment groups for a total of 136 individual samples (n = 68 per treatment group). To measure the time-dependent effects of light removal on gene expression in *Nematostella*, the light cue was removed from the diel light cycle group after the first 24 hours (at ZT = 0 on the second day) and sampling continued for 44 additional hours. This sampling regime effectively created three treatment subgroups from diel entrained anemones: day 1 of the experiment or ‘light:dark’ (LD), day 2 of the experiment or ‘light removal day 1’ (LR1; i.e., the first day post-light removal), and day 3 of the experiment or ‘light removal day 2’ (LR2; i.e., the second day post-light removal). Thus, samples from the first 24 hours of the experiment will subsequently be referred to as light treatment ‘LD’, samples from the following 24 hours of the experiment will be referred to as LR1, and samples from the last 20 hours of the experiment will be referred to as LR2. Conditions for animals in the long-term darkness (DD) treatment group remained constant during each sampling day (DD1, DD2, and DD3; Fig. S1, Supporting information). We were unable to sample a sixth time at the end of sampling day 3 because of insufficient animals in some treatments, hence why there are only 17 time points over 68 hours rather than a full 72-hour time course (Fig. S1).

Tag-based RNA library preparation, sequencing, and processing

Total RNA was isolated from 136 samples (4 biological replicates * 17 time points * 2 treatment groups) using the RNAqueous kit (Ambion) according to the manufacturer's protocol. Briefly, after pipetting off and discarding RNAlater from each sample, whole animals were lysed by pipetting in lysis buffer for <2 minutes, washed 2-3 times, and eluted on a column. Genomic DNA was removed using DNA-free kit (Invitrogen), and RNA was assessed using a NanoDrop 2000 spectrophotometer (Thermo Fisher Scientific). RNA was shipped for tag-based library preparation at the University of Texas at Austin's Genomic Sequencing and Analysis Facility (GSAF) as in Meyer et al. (2011) and adapted for Illumina HiSeq 2500. Briefly, total RNA was heat-fragmented and then reverse transcribed into first-strand cDNA. The cDNA was purified using AMPure beads, and PCR-amplified for 18 cycles. Unique Illumina barcodes were added in an additional PCR step for indexing of each sample. After an additional purification step, libraries were pooled, spot checked for quality on a Bioanalyzer (Agilent and Pico), and size-selected using BluePippin (350-550bp fragments). A full version of the library preparation protocol can be found at https://github.com/z0on/tag-based_RNAseq.

Data processing pipeline

Raw sequence data (100 bp, single-end) were delivered from the UT Austin GSAF. Raw reads were trimmed and quality-filtered using the FastX-toolkit (Pearson, Wood, Zhang, & Miller, 1997). Trimmed reads were mapped against the *Nematostella* Vienna transcriptome (see 'Data Accessibility' for link to gene models) using the Bowtie2 aligner (Langmead & Salzberg, 2012) and a read-counts-per-gene file was generated retaining only

reads mapping to a single gene (Table S1, Supporting information). Lastly, counts were imported into the R environment for all downstream statistical analysis (R3.5.0, R Core Team 2015).

Identification of cycling genes

Oscillating transcripts were identified with `JTK_CYCLEv3.1` in R (Hughes, Hogenesch, & Kornacker, 2010), which determines p-values based on Kendall's rank correlation coefficient and effectively distinguishes rhythmic and non-rhythmic patterns. `JTK_Cycle` p-values were Bonferroni-adjusted for multiple testing. Raw counts from 4-hour sampling intervals across all treatment subgroups were used as input data in the `JTK_Cycle` script, and the 'period' parameter was set to '5:7' to identify genes cycling every 20-28 hours. We compared peak expression times for genes with significantly oscillating expression over multiple days to identify potential shifts in peak transcription with light removal.

Identification of differentially expressed genes (DEGs)

Normalization and differential expression analysis of read counts was performed using a negative binomial generalized linear model in the R package `DESeq2` (Fig. S2A-C, Supporting information; Love, Huber, & Anders, 2014). Transcripts with low abundances (mean count <3) were filtered to improve the rate of differential gene discovery as implemented in the `DESeq2` pipeline. The `arrayQualityMetrics` package (Kauffmann, Gentleman, & Huber, 2009) was used to detect outlier transcripts with counts significantly higher than the rest of the total counts, and were discarded from subsequent analysis (Fig. S3A, Supporting information). `DESeq2` normalized count data were regularized log

transformed using the *rlog* function. Normalized and rlog transformed counts were used for principal coordinate analysis based on Manhattan distances and significance was evaluated using the *vegan* package in R (Fig. S2, Supporting information; Dixon, 2003). Gene expression heatmaps were created using the *pheatmap* package in R with hierarchical clustering of expression patterns (Kolde, 2018). Gene expression graphs were generated with the *ggplot2* function in R (Wickham, 2009).

We performed pairwise contrasts between each treatment subgroup, and between each timepoint using Wald tests in DESeq2. P-values were calculated using the Benjamini-Hochberg procedure and false discovery rate (FDR) adjusted for multiple testing. The differentially expressed gene (DEG) lists from each contrast, including adjusted and unadjusted p-values and log₂ fold changes, were used for downstream analyses.

Gene ontology (GO) enrichment analysis

Functional summaries of DEGs from each contrast were determined by rank based Gene Ontology (GO) enrichment analysis, using signed, unadjusted log-transformed p-values (positive if up-regulated, negative if down-regulated) with the *GO_MWU* (https://github.com/z0on/GO_MWU) package. This method utilizes the Mann-Whitney U (MWU) test and measures whether each GO term is significantly enriched in up- or down-regulated genes based on their delta rank (quantitative shift in rank) rather than looking for GO terms among “significant” genes only.

Gene co-expression

We next identified groups (“modules”) of highly correlated genes from each contrast in an unbiased way using weighted gene correlation network analysis (WGCNA;

Langfelder & Horvath, 2008). We used genes with an unadjusted p-value <0.1 (5,678 genes) determined by the generalized linear model in DESeq2. The resulting modules were then related to external traits (i.e., sampling day/treatment subgroup, individual, and time) using the eigengene network methodology (Langfelder & Horvath, 2008). This method does not use information regarding how the samples were distributed within experimental conditions to ensure that the module eigengenes correlate with gene expression patterns that reflect biological processes. A sample network identified outlying samples ($n = 5$, Fig. S3A, Supporting information) with a connectivity score less than -2.5 and were removed from the analysis. A signed co-expression network was built using a soft threshold power of 6 (Fig. S3B, Supporting information) and modules were merged if their eigengene expression correlated with the Pearson correlation coefficient greater than 0.42 (Fig. S3C, Supporting information). Each module's eigengene expression (the first principal component of all of the genes within that module) was correlated to the day sampling occurred (i.e., treatment subgroup), biological replicate, and time point (Fig. S4, Supporting information). Significant correlations between the membership of the genes in each module and their significance indicates a strong association of the module with a trait (i.e. genes in a particular module are positively or negatively associated with day of sampling, individual, or time; Fig. S5, Supporting information). Module eigengenes were functionally characterized with the GO_MWU package using a transcriptome-wide Fishers exact test for the genes in each module (https://github.com/z0on/GO_MWU).

Results

Transcriptome sequencing produced >396 million raw reads, with an average of 2.9 million reads per sample (each time point had 4 biological replicates, barcoded and sequenced individually). After quality filtering and removal of PCR duplicates, an average of 889,112 reads per sample remained (Table S2, Supporting information). After trimming and deduplication of transcripts, the reads were mapped to the Vienna *Nematostella* transcriptome (see ‘Data Accessibility’ section for link) with an average mapping efficiency of 74.5%. The mapped reads were converted into a counts per sample table, representing a total of 24,392 genes (Table S1, Supporting information). A generalized linear model in DESeq2 identified unique DEGs normalized with sampling day/treatment subgroup as the covariate. In order to explore gene expression patterns specific to each treatment subgroup, pairwise comparisons between each treatment subgroup were run using Wald statistics to contrast each subgroup to the other two (LD, LR1, LR2). A principal coordinate analysis of the entire rlog transformed dataset separated samples by subgroup and showed distinct clustering of LD, LR1, and LR2 (Fig. 1A). Further, consecutive time points during day and night sampling events tended to cluster within subgroups.

Cycling gene expression

To quantify how many genes were cycling on each sampling day, we analyzed the normalized counts by subgroup with non-parametric JTK_Cycle (Table S3, Supporting information). In total, we identified 1,073 cycling genes over the 3-day time course. The number of genes with signatures of cycling differed between subgroups: 228 genes were

identified to be significantly cycling (period = 24; p-value <0.01) in LD, 865 genes in LR1, and only 40 genes in LR2. Fifty-two genes were shared between LD and LR1, eight genes were shared between LR1 and LR2, and no genes were shared between LD and LR2 (Fig. S6, Supporting information). Cycling genes in LD

To explore the genes JTK_Cycle identified as cycling on the first day of the experiment prior to light removal, we isolated genes from the LD subgroup with a significant period of 24 hours (228 genes; p-value <0.01). There were 487 cycling genes at $p < 0.05$, and 35 cycling genes at $p < 0.001$. Only a subset of the 24-hour cycling genes from LD continued to oscillate on the second day and third days, after the light cue was removed (54 genes from subgroups LR1 and LR2). The remaining 174 genes (p-value <0.01) uniquely cycling in LD included light responsive genes (e.g., cryptochromes and rhodopsin) and signal transduction genes (e.g., protein kinase C, and G-protein couple receptor). Several genes previously reported to exhibit rhythmic expression over a diel light cycle in cnidarians (A. K. Brady et al., 2011; Hemond & Vollmer, 2015; Hoadley, Szmant, & Pyott, 2011; Oren et al., 2015) showed expression patterns consistent with a 24-hour rhythm in LD (Fig. 2; Table 1.1); *Clock*, *Cry1a*, *Cry1b*, *PAR-bZIPa*, *PAR-bZIPc*, a Hes/Hey-like transcription factor *helt*, and a putative *clock-interacting circadian pacemaker* homolog (*CiPC*) were expressed with a significant circadian period of 24 hours and all had daytime peaks in expression except *PAR-bZIPc* (ZT = 18) and *CiPC* (ZT = 24; Table 1.1). *PAR-bZIPb* had a significant period of 28 hours with peak expression in mid-afternoon (Table 1.1, Fig. 2). The transcription factor *helt* and the *CiPC* homolog each had a significant period of 24 hours and were previously identified to have diel expression under LD conditions in cnidarians (Oren et al., 2015; Shoguchi, Tanaka, Shinzato,

Kawashima, & Satoh, 2013). Consistent with those earlier studies, *helt* and *CiPC* expression peaked mid-morning (ZT = 6) and during subjective night (ZT = 24), respectively (p-value <0.01; Table 1.1). The subset of significantly cycling genes identified in both the LD and LR1 subgroups included environmental response genes (e.g. peroxiredoxin 5, thioredoxin), genes involved in metabolic processes (e.g., malate dehydrogenase, adenylate cyclase, aspartate aminotransferase) and transcription (e.g., six homeobox). Upon light removal, all but one gene (NVE15806; unidentified protein) phase shifted peak expression. Most of these genes (69%) peaked later in the day, but the remaining genes peaked earlier (28%).

Cycling genes in LR1 and LR2

In addition to genes cycling under normal conditions (identified in treatment subgroup LD), we also ran JTK_Cycle on gene counts from the LR1 and LR2 subgroups to reveal expression patterns unique to the first and second days after light removal. During LR1, 1,693 genes were cycling at $p < 0.05$ and 117 genes were cycling at $p < 0.001$. During LR2, 90 genes were cycling at $p < 0.05$ and four genes were cycling at $p < 0.001$. The number of cycling genes at $p < 0.01$ tripled on the first day of light removal compared to LD (Table 1.1, Fig. S6, Supporting information).

After light cue removal, genes related to signal transduction (e.g., protein phosphatase and protein kinases), metabolism and stress response (e.g., superoxide dismutase, glutathione peroxidase, and HSP70) were uniquely cycling. The bZIP family transcription factors *CREB* and *Maf* showed a significant ($p < 0.01$) period of 24 hours during the first day following light cue removal along with DNA regulatory factors (e.g.,

ARNT and *HIF*; Table S3, Supporting information). The circadian-associated genes *Clock* and *Cry1a* lost signatures of a 24-hour rhythm in the absence of a diel light cue (*Clock*: period = 0, p-value = 1; *Cry1a*: period = 2, p-value = 0.33), and the peak expression of *Cry1b* shifted from ZT = 12 to ZT = 20 in LR1 but was no longer identified by JTK_Cycle to have a significant cycling period (period = 24, p-value = 0.31). *PAR-bZIPb* maintained a period of 28 hours in the first day following light cue removal (p-value = 0.05), however peak expression shifted from ZT = 6 in LD to ZT = 20 and *helt* lost evidence of any rhythmicity (period = 0, p-value = 0.52).

Of the previously identified genes hypothesized to be involved in the circadian-clock, only *PAR-bZIPb* retained a consistent period of 28 hours throughout each treatment subgroup (LD, LR1, LR2; Table 1.1). However, on the second day after light removal, peak expression of *PAR-bZIPb* shifted to ZT = 4 (Fig. 2; p-value = 0.01). The remaining 71 uniquely cycling genes during LR2 were sparsely annotated, but included mostly cellular component genes (e.g., ribosomal proteins, solute carrier proteins).

After constant and prolonged exposure to darkness (DD), *PAR-bZIPb* and *PAR-bZIPc* were identified by JTK_Cycle to have significant cycling periods of 28 hours (p-value = 0.005 and p-value = 0.02, respectively). The circadian-related tryptophan hydroxylase, or *TPH* (Peres et al., 2014), did not show evidence of cycling in any diel treatment subgroup (LD, LR1, or LR2) but during DD had a period of 28 hours (p-value = 0.08).

Differential gene expression

After comparing genes that show signatures of circadian rhythmicity from each subgroup, we used DESeq2 to analyze differential gene expression of pairwise comparisons between subgroups. These comparisons expose time-dependent transcriptional changes in response to a changing light environment. A total of 2,562 DEGs were differentially expressed over all subgroup comparisons (LD, LR1, LR2; FDR = 0.1, log₂ fold-change >1.5). Of these, 350 genes were unique to the contrast of subgroup LD and LR1, 667 genes were unique to the LD v LR2 subgroups, and only 10 genes were shared between the three subgroups. We also compared gene expression between each subgroup and DD. These specific pairwise comparisons establish a baseline for the response of gene expression before and after light cue removal, when compared to a constant condition control (DD). Interestingly, when compared to DD, a nearly 2-fold increase in DEGs was observed in the first 24 hours following light removal (1,649) over the number of DEGs in LD (876). On the second day after light cue removal (LR2) there was a reduction in the number of DEGs (734). This observation is consistent with differential expression between LD and DD (Fig. 1B) and is similar to the pattern of 24-hour cycling genes identified by JTK_Cycle (Fig. S6, Supporting information). Each of these results were in contrast to the patterns of expression for anemones under constant conditions (DD1 v DD2, for example). Pairwise comparisons between each sampling day during DD revealed a total of 66 significant DEGs that were consistently differentially expressed between days (DD1 v DD2, DD1 v DD3, DD2 v DD3; FDR = 0.1, absolute log₂ fold-change >1.5).

LD v DD

The contrast of light:dark and long-term darkness allowed us to characterize genes that are differentially expressed during a diel light cycle, before light cue removal. Using a relaxed FDR of 10%, DESeq2 generated 1,160 DEGs (Fig. 1B), predominately comprised of genes up-regulated in LD compared to DD (971 genes). These were genes involved in transcription (e.g., bHLH transcription factors *Clock* and *helt* and bZIP transcription factors in the HLF and PAR subfamilies) as well as DNA-photolyase activity (e.g., cryptochromes; Fig. 1C). A GO analysis of genes differentially expressed under diel lighting showed ‘endopeptidase’ and ‘chromatin binding’ as the most enriched terms in up- and down-regulated genes, respectively in the molecular function category (Table 2.1; Fig. S7, Supporting information). Among biological processes enriched in light:dark conditions, ‘positive regulation of immune system process’ and ‘regulation of immune response’ were upregulated and ‘chromosome organization’ was down-regulated compared to constant conditions (Fig. S7, Supporting information).

LD v LR1

The comparison of light:dark conditions and the first day post light cue removal revealed 876 DEGs (449 up-regulated and 427 down-regulated after light removal compared to LD) that exceeded the Benjamini-Hochberg FDR cutoff of 10%. Of these, 125 genes were also cycling (identified by JTK_Cycle, Table S3, Supporting information). A survey of circadian-related genes found *Clock*, *Cry1a*, *PAR-bZIPa*, *PAR-bZIPb*, and *PAR-bZIPc* to be down-regulated immediately after light removal compared to diel conditions, along with *helt* and an additional *PAR-bZIPd*, previously called NV16 (Fig. 1D; Reinke, Baek, Ashenberg, & Keating, 2013). Genes identified to be up-regulated following light cue removal compared to diel conditions include several environmental

response genes, particularly factors involved in the oxidative stress pathway (e.g., hypoxia inducible factor and one cytochrome P450), and heavy metal detoxification (e.g., one phytochelatin synthase; Fig. 1C). Genes involved in metabolic pathways, specifically central enzymes in the citric acid cycle (e.g., malate dehydrogenase and isocitrate dehydrogenase) were also significantly up-regulated after light removal compared to LD. Other essential gene regulatory enzymes, primarily those involved in chromatin organization, were up-regulated in LR1 compared to LD (e.g., histone methyltransferase (HMT), histone deacetylase (HDAC), and transcriptional regulator of ATRX; Fig. 1C, Fig. 3).

Gene ontology (GO) enrichment analysis of DEGs between LD and LR1 found significantly enriched terms in genes up-regulated after light removal to be ‘structural constituent of ribosome’ in the molecular function category and ‘cellular respiration’ in the biological process category (Table 2.1). The most significantly enriched terms in genes down-regulated after light removal was ‘actin binding’ of molecular function and ‘lipid metabolic process’ of the biological process category (Table 2.1). We also compared LR1 to DD, where GO analysis revealed ‘chromosome organization’, ‘cellular response to DNA damage stimulus’, and ‘DNA metabolic process’ as significantly enriched terms from the biological process category for genes up-regulated after light removal compared to long-term darkness (Fig. 3).

LD v LR2

DESeq2 identified 1,181 DEGs passing the Benjamini-Hochberg FDR cutoff of 10% in the contrast between light:dark and the second day after light removal (353 up-

regulated and 828 down-regulated after two days of darkness compared to LD). GO enrichment analysis of DEGs between LD and LR2 identified the most significantly enriched GO term in up-regulated genes after two days of light removal as ‘structural constituent of ribosome’ in the molecular function category, and ‘RNA catabolic process’ of biological processes. The most significantly enriched GO term in the molecular function category of down-regulated genes after two days of light removal was ‘oxidoreductase’, and in the biological process category ‘fatty acid metabolism’ was the most enriched. Additionally, comparing DEGs between LR2 and DD, ‘chromatin binding’ and ‘endopeptidase’ were the most enriched GO terms in up- and down-regulated genes, respectively, in the molecular function category (Table 2.1, Fig. S9, Supporting information).

Weighted gene co-expression network analysis (WGCNA)

After identifying differently expressed gene patterns between subgroups, we performed a weighted gene co-expression network analysis (WGCNA; Langfelder & Horvath, 2008) to isolate groups of genes that show correlated expression across samples without the consideration of experimental conditions. Two modules were significantly and uniquely correlated to light:dark (LD: brown - Pearson’s $R^2 = 0.35$, p-value $<4e-05$; salmon - Pearson’s $R^2 = 0.81$, p-value $<1e-08$; Fig 4; Fig. S5, Supporting information). The brown module (1,201 genes) showed GO enrichment for ‘chromatin binding’ in the molecular function category, and ‘chromatin’ in the cellular component category, which were different genes than those with higher expression in the comparison of LR1 and LD. The salmon module (33 genes), also unique to LD, showed significant GO enrichment for ‘transcription factor, RNA polymerase II’ (Fig. 4). One module was significantly correlated

to the first day of light removal (LR1: green - Pearson's $R^2 = -0.2$, p-value <0.02 ; Fig. S5, Supporting information). GO enrichment analysis of the green module (170 genes) showed enrichment for 'cytoskeletal protein binding' and 'actin binding' of the molecular function category and 'cell-to-cell junction' in the cellular component category. The remaining three modules were significantly and uniquely correlated to the second day of light removal (LR2: turquoise - Pearson's $R^2 = 0.22$, p-value <0.01 ; red - Pearson's $R^2 = 0.31$, p-value $<3e-04$; purple - Pearson's $R^2 = 0.31$, p-value $<4e-04$; Fig. S5, Supporting information). GO analysis of the turquoise module (2,766 genes) showed enrichment for 'respiratory electron transport chain' and 'cellular respiration' in the biological process category. The red (156 genes) and purple modules (91 genes) were not enriched for any GO terms.

Discussion

Our quantitative analysis of transcriptomes for anemones during consistent light:dark cycles and after removal of the lighting cue revealed unique gene expression profiles over 24-hour periods in the presence of light, after 24 hours of removal, and after longer periods of light removal. Consistent with previous analyses of candidate genes or the whole transcriptome, long-term culturing in all dark conditions resulted in near loss of any differential gene expression over a 24-hour period. The light dependency of the differentially expressed gene sets suggests that many genes under diel lighting are direct response genes and not the product of a circadian timekeeper, at least when measured at the whole individual level. Upon light removal, we measured a large number of genes that

were uniquely expressed when the cue was absent for 24 or 44 hours, which appears to be a type of stress response given the types of genes with increased expression.

'Circadian gene' expression dependent on light cues

A central finding from our analyses is that the expression of the candidate "circadian clock genes" identified in previous studies is strongly dependent on consistent light:dark cycling, at least when measured in whole animals. Earlier studies by Reitzel et al. (2010), Peres et al. (2014), Oren et al. (2015), and Leach et al. (2018) had shown that *Nematostella* orthologs to genes central to the circadian clock of bilaterians have oscillating expression in light:dark conditions. Our transcriptome comparisons are consistent with these earlier studies where the bHLH-Pas gene *Clock* and the bZIP transcription factors in the PAR family had rhythmic expression. Another transcription factor previously identified in corals to be differentially expressed in diel lighting, *eyes absent (eya)*, showed differential expression following light removal (A. K. Brady et al., 2011). Our analyses identified additional PAR-bZIP genes that fit a diel expression pattern, particularly *PAR-bZIPd* (called NV16 in Reinke et al., 2013) with robust expression in the light period, with peak expression at the beginning of the photoperiod (ZT = 2; Fig. 1C, Fig. 2). This particular PAR-bZIP is a heterodimer partner with other PAR-bZIP proteins from *Nematostella* previously identified by Reitzel et al. (2013) with different peak expression periods, suggesting the potential for complex gene regulation over a diel period, similar to *Drosophila* (Cyran et al., 2003). After the removal of the light cue, *PAR-bZIPd* maintained significant differences throughout light treatments; however, its expression dampened each day following light removal, suggesting light dependency rather than true circadian regulation (Fig. 2). The remaining hypothesized cnidarian circadian genes were not

differentially expressed in the absence of a light cue (Fig. 2). Interestingly though, after light cue removal a few of these candidates shifted peak expression time. *PAR-bZIPb* continued to cycle every 28 hours, but peak expression was phase shifted by 12 hours. Cryptochromes previously identified to have differential expression in response to diel lighting [*NvCry1a* and *NvCry1b* in Reitzel et al. (2010)] also experienced peak shifts after light removal. Consistent with previous studies, the hypothesized repressive Type 2 cryptochrome, *Nvcry2*, showed no response to diel lighting in *Nematostella*, similar to insect and mammal clocks (Fig. 2; Griffin, Staknis, & Weitz, 1999; Kume et al., 1999; Reitzel et al., 2010; Zhu et al., 2008). Presently, it is unclear what role cryptochromes and PAR-bZIP transcription factors play in the clock of cnidarians; thus, future mechanistic experiments would provide more insight to the potential suppressive role of these proteins and regulatory role of these transcription factors, respectively.

Changes in light condition results in stress and changes to chromatin structure

The large and unique set of differentially expressed genes after one or two days of light removal are broadly consistent with an environmental stress response that involves a number of genes related to cellular stress and chromatin remodeling (Fig. 3, Fig. S8-S9, Supporting information). Removal or time-shifting of entraining cues is broadly known to disrupt physiology and behavior for various animals (Davis & Mirick, 2006; Garaulet & Madrid, 2010; Rhoades, Nayak, Zhang, Sehgal, & Weljie, 2018). Unlike in light:dark conditions, genes involved in cellular and aerobic respiration and cellular response to DNA damage were differentially expressed upon removal of the light cue (Fig. 3). Additionally, *Nematostella* sampled in constant conditions upregulate hypoxia inducible factor (HIF), cytochrome c oxidase, monoamine oxidase, and aquaporin 4 (Fig. 1D). Genes related to

chromatin remodeling that were significantly up regulated after light removal include histone deacetylase and histone methyltransferase (Fig. 4). Broadly, these enzymes regulate gene expression by making modifications to the chromatin structure, ultimately increasing compaction within DNA and reducing transcription factor activity and thus, gene expression.

Photoresponse versus circadian clock

Previous studies in cnidarians have typically relied on a comparison of consistent light:dark cycles and a single day of all darkness immediately after in which to determine if genes are likely "circadian". The period of free-running behavior or physiology varies between organisms with well-described circadian oscillators but typically last for days or weeks with removal of the entraining cue. Our gene expression results with *Nematostella* that showed large shifts in the transcriptional profile with removal of light differ from the consistency of a free-run period previously reported for locomotion (Hendricks et al., 2012; Oren et al., 2015) and physiology (Maas et al., 2016). At present, we hypothesize the cause for this discrepancy is the use of whole animals for our sample material when the mechanisms driving cyclic phenotypes are conceivably restricted to a subset of cells, likely neurons. Combining gene expression information from multiple tissues in one sample has the potential to diminish oscillating gene expression signals if present in a small number of cells or if tissues have rhythmic gene expression in different phases, as is known in vertebrates (Albrecht, 2012). *Nematostella*, like other cnidarians, has a complex but diffuse nervous system without a centralized concentration of neurons (Marlow, Srivastava, Matus, Rokhsar, & Martindale, 2009), which presumably arose in a later common ancestor (Arendt, Tosches, & Marlow, 2015). Recent work (Sebé-Pedrós et al., 2018) has revealed

the complex transcriptional differences of the more than eight broad cells types of *Nematostella*. Moving forward, these cell-type specific analyses of oscillating gene expression will be useful to identify what cells in heterogeneous cell populations may be driving the circadian phenotypes of cnidarians.

Acknowledgements

We would like to thank members of the Reitzel and Tarrant (WHOI) laboratories for discussions during the course of this study. We would also like to thank Misha Matz (UT Austin) for assistance with gene expression analyses.

References

1. Albrecht, U. (2012). Timing to perfection: The biology of central and peripheral circadian clocks. *Neuron*, 74(2), 246-260. doi:10.1016/j.neuron.2012.04.006
2. Arendt, D., Tosches, M. A., & Marlow, H. (2015). From nerve net to nerve ring, nerve cord and brain — evolution of the nervous system. *Nature Reviews Neuroscience*, 17, 61. doi:10.1038/nrn.2015.15
3. Berson, D. M., Dunn, F. A., & Takao, M. (2002). Phototransduction by retinal ganglion cells that set the circadian clock. *Science*, 295(5557), 1070-1073. doi:10.1126/science.1067262
4. Bradshaw, W. E., & Holzapfel, C. M. (2007). Evolution of animal photoperiodism. *Annual Review of Ecology Evolution and Systematics*, 38, 1-25. doi:10.1146/annurev.ecolsys.37.091305.110115
5. Brady, A., Hilton, J., & Vize, P. (2009). Coral spawn timing is a direct response to solar light cycles and is not an entrained circadian response. *Coral Reefs*, 28(3), 677-680.
6. Brady, A. K., Snyder, K. A., & Vize, P. D. (2011). Circadian cycles of gene expression in the coral, *Acropora millepora*. *PLoS ONE*, 6(9), e25072.
7. Chalker, B. E., Barnes, D. J., Dunlap, W. C., & Jokiel, P. L. (1988). Light and reef-building corals. *Interdisciplinary Science Reviews*, 13(3), 222-237. doi:10.1179/isr.1988.13.3.222
8. Cheng, N., Tsunenari, T., & Yau, K. W. (2009). Intrinsic light response of retinal horizontal cells of teleosts. *Nature*, 460(7257), 899-U139. doi:10.1038/nature08175

9. Cyran, S. A., Buchsbaum, A. M., Reddy, K. L., Lin, M.-C., Glossop, N. R. J., Hardin, P. E., . . . Blau, J. (2003). Vrille, Pdp1, and dClock form a second feedback loop in the *Drosophila* circadian clock. *Cell*, 112(3), 329-341.
10. Davis, S., & Mirick, D. (2006). Circadian disruption, shift work and the risk of cancer: A summary of the evidence and studies in Seattle. *Cancer Causes & Control*, 17(4), 539-545. doi:10.1007/s10552-005-9010-9
11. Dixon, P. (2003). VEGAN, a package of R functions for community ecology. *Journal of Vegetation Science*, 14(6), 927-930. doi:10.1111/j.1654-1103.2003.tb02228.x
12. Dunlap, J. C. (1999). Molecular bases for circadian clocks. *Cell*, 96(2), 271-290.
13. Dunlap, J. C., Loros, J. J., & DeCoursey, P. J. (2004). *Chronobiology: biological timekeeping*: Sinauer Associates.
14. Edmunds, L. N., Jr. (1988). Cellular and molecular bases of biological clocks. Models and mechanisms for circadian timekeeping. Springer.
15. Edwards, S. L., Charlie, N. K., Milfort, M. C., Brown, B. S., Gravlin, C. N., Knecht, J. E., & Miller, K. G. (2008). A novel molecular solution for ultraviolet light detection in *Caenorhabditis elegans*. *Plos Biology*, 6(8), 1715-1729. doi:10.1371/journal.pbio.0060198
16. Fernandes, A. M., Fero, K., Driever, W., & Burgess, H. A. (2013). Enlightening the brain: Linking deep brain photoreception with behavior and physiology. *Bioessays*, 35(9), 775-779. doi:10.1002/bies.201300034
17. Freedman, M. S., Lucas, R. J., Soni, B., von Schantz, M., Munoz, M., David-Gray, Z., & Foster, R. (1999). Regulation of mammalian circadian behavior by non-rod, non-cone, ocular photoreceptors. *Science*, 284(5413), 502-504. doi:10.1126/science.284.5413.502

18. Gamble, K. L., Berry, R., Frank, S. J., & Young, M. E. (2014). Circadian clock control of endocrine factors. *Nature Reviews Endocrinology*, 10, 466. doi:10.1038/nrendo.2014.78
19. Garaulet, M., & Madrid, J. A. (2010). Chronobiological aspects of nutrition, metabolic syndrome and obesity. *Advanced Drug Delivery Reviews*, 62(9–10), 967-978. doi:10.1016/j.addr.2010.05.005
20. Griffin, E., Staknis, A., & Weitz, C. J. (1999). Light-independent role of CRY1 and CRY2 in the mammalian circadian clock. *Science*, 286, 768-771.
21. Gwinner, E. (1996). Circadian and circannual programs in avian migration. *Journal of Experimental Biology*, 199(1), 39-48.
22. Hardin, P. E. (2006). Essential and expendable features of the circadian timekeeping mechanism. *Current Opinion in Neurobiology*, 16(6), 686-692.
23. Hemond, E. M., & Vollmer, S. V. (2015). Diurnal and nocturnal transcriptomic variation in the Caribbean staghorn coral, *Acropora cervicornis*. *Molecular Ecology*, 24(17), 4460-4473. doi:10.1111/mec.13320
24. Hendricks, W. D., Byrum, C. A., & Meyer-Bernstein, E. L. (2012). Characterization of circadian behavior in the starlet sea anemone, *Nematostella vectensis*. *PLoS ONE*, 7(10), e46843. doi:10.1371/journal.pone.0046843
25. Hoadley, K. D., Szmant, A. M., & Pyott, S. J. (2011). Circadian clock gene expression in the coral *Favia fragum* over diel and lunar reproductive cycles. *PLoS ONE*, 6(5), e19755.
26. Hoadley, K. D., Vize, P. D., & Pyott, S. J. (2016). Current understanding of the circadian clock within Cnidaria. In S. Goffredo & Z. Dubinsky (Eds.), *The Cnidaria, Past, Present and Future: The world of Medusa and her sisters* (pp. 511-520). Cham: Springer International Publishing.

27. Hughes, M. E., Hogenesch, J. B., & Kornacker, K. (2010). JTK_CYCLE: An efficient nonparametric algorithm for detecting rhythmic components in genome-scale data sets. *Journal of Biological Rhythms*, 25(5), 372-380. doi:10.1177/0748730410379711
28. Jindrich, K., Roper, K. E., Lemon, S., Degnan, B. M., Reitzel, A. M., & Degnan, S. M. (2017). Origin of the animal circadian clock: diurnal and light-entrained gene expression in the sponge *Amphimedon queenslandica*. *Frontiers in Marine Science*, 4(327). doi:10.3389/fmars.2017.00327
29. Kauffmann, A., Gentleman, R., & Huber, W. (2009). arrayQualityMetrics--a bioconductor package for quality assessment of microarray data. *Bioinformatics (Oxford, England)*, 25(3), 415-416. doi:10.1093/bioinformatics/btn647
30. Kolde, R. (2018). Pretty Heatmaps. Comprehensive R Archive Network.
31. Kume, K., Zylka, M. J., Sriram, S., Shearman, L. P., Weaver, D. R., Jin, X., . . . Reppert, S. M. (1999). mCRY1 and mCRY2 are essential components of the negative limb of the circadian clock feedback loop. *Cell*, 98(2), 193-205.
32. Lamb, T. D., Collin, S. P., & Pugh, E. N., Jr. (2007). Evolution of the vertebrate eye: opsins, photoreceptors, retina and eye cup. *Nature reviews. Neuroscience*, 8(12), 960-976. doi:10.1038/nrn2283
33. Langfelder, P., & Horvath, S. (2008). WGCNA: an R package for weighted correlation network analysis. *BMC Bioinformatics*, 9, 13. doi:10.1186/1471-2105-9-559
34. Langmead, B., & Salzberg, S. L. (2012). Fast gapped-read alignment with Bowtie 2. *Nature Methods*, 9(4), 357-U354. doi:10.1038/nmeth.1923
35. Leach, W. B., Macrander, J., Peres, R., & Reitzel, A. M. (2018). Transcriptome-wide analysis of differential gene expression in response to light:dark cycles in a model

- cnidarian. *Comparative Biochemistry and Physiology Part D: Genomics and Proteomics*, 26, 40-49. doi:10.1016/j.cbd.2018.03.004
36. Levy, O., Appelbaum, L., Leggat, W., Gothlif, Y., Hayward, D. C., Miller, D. J., & Hoegh-Guldberg, O. (2007). Light-responsive cryptochromes from a simple multicellular animal, the coral *Acropora millepora*. *Science*, 318(5849), 467-470. doi:10.1126/science.1145432
37. Leys, S. P., Cronin, T. W., Degnan, B. M., & Marshall, J. N. (2002). Spectral sensitivity in a sponge larva. *Journal of Comparative Physiology A*, 188(3), 199-202.
38. Love, M. I., Huber, W., & Anders, S. (2014). Moderated estimation of fold change and dispersion for RNA-seq data with DESeq2. *Genome Biology*, 15(12). doi:10.1186/s13059-014-0550-8
39. Maas, A. E., Jones, I. T., Reitzel, A. M., & Tarrant, A. M. (2016). Daily cycle in oxygen consumption by the sea anemone *Nematostella vectensis* Stephenson. *Biology Open*, 5(2), 161.
40. Marlow, H. Q., Srivastava, M., Matus, D. Q., Rokhsar, D., & Martindale, M. Q. (2009). Anatomy and development of the nervous system of *Nematostella vectensis*, an anthozoan cnidarian. *Developmental Neurobiology*, 69. doi:10.1002/dneu.20698
41. Mendlewicz, J. (2009). Disruption of the circadian timing systems. *CNS Drugs*, 23(2), 15-26. doi:10.2165/11318630-000000000-00000
42. Mercier, A., & Hamel, J. F. (2010). Synchronized breeding events in sympatric marine invertebrates: role of behavior and fine temporal windows in maintaining reproductive isolation. *Behavioral Ecology and Sociobiology*, 64(11), 1749-1765. doi:10.1007/s00265-010-0987-z

43. Meyer, E., Aglyamova, G. V., & Matz, M. V. (2011). Profiling gene expression responses of coral larvae (*Acropora millepora*) to elevated temperature and settlement inducers using a novel RNA-Seq procedure. *Molecular Ecology*, 20(17), 3599-3616. doi:10.1111/j.1365-294X.2011.05205.x
44. Miyamoto, Y., & Sancar, A. (1998). Vitamin B2-based blue-light photoreceptors in the retinohypothalamic tract as the photoactive pigments for setting the circadian clock in mammals. *Proceedings of the National Academy of Sciences of the United States of America*, 95(11), 6097-6102. doi:10.1073/pnas.95.11.6097
45. Oldach, M. J., Workentine, M., Matz, M. V., Fan, T. Y., & Vize, P. D. (2017). Transcriptome dynamics over a lunar month in a broadcast spawning acroporid coral. *Molecular Ecology*, 26(9), 2514-2526. doi:10.1111/mec.14043
46. Oren, M., Tarrant, A. M., Alon, S., Simon-Blecher, N., Elbaz, I., Appelbaum, L., & Levy, O. (2015). Profiling molecular and behavioral circadian rhythms in the non-symbiotic sea anemone *Nematostella vectensis*. *Scientific Reports*, 5, 11418. doi:10.1038/srep11418
47. <https://www.nature.com/articles/srep11418#supplementary-information>
48. Pearson, W. R., Wood, T., Zhang, Z., & Miller, W. (1997). Comparison of DNA sequences with protein sequences. *Genomics*, 46(1), 24-36. doi:10.1006/geno.1997.4995
49. Peres, R., Reitzel, A. M., Passamaneck, Y., Afeche, S. C., Cipolla-Neto, J., Marques, A. C., & Martindale, M. Q. (2014). Developmental and light-entrained expression of melatonin and its relationship to the circadian clock in the sea anemone *Nematostella vectensis*. *EvoDevo*, 5, 26. doi:10.1186/2041-9139-5-26

50. Plachetzki, D. C., Fong, C. R., & Oakley, T. H. (2010). The evolution of phototransduction from an ancestral cyclic nucleotide gated pathway. *Proceedings of the Royal Society B-Biological Sciences*, 277(1690), 1963-1969. doi:10.1098/rspb.2009.1797
51. Porter, M. L. (2016). Beyond the eye: molecular evolution of extraocular photoreception. *Integrative and Comparative Biology*, 56(5), 842-852. doi:10.1093/icb/icw052
52. Reinke, A. W., Baek, J., Ashenberg, O., & Keating, A. E. (2013). Networks of bZIP protein-protein interactions diversified over a billion years of evolution. *Science*, 340(6133), 730. doi:10.1126/science.1233465
53. Reitzel, A. M., Behrendt, L., & Tarrant, A. M. (2010). Light entrained rhythmic gene expression in the sea anemone *Nematostella vectensis*: the evolution of the animal circadian clock. *PLoS ONE*, 5(9), e12805.
54. Reitzel, A. M., Passamaneck, Y. J., Karchner, S. I., Franks, D. G., Martindale, M. Q., Tarrant, A. M., & Hahn, M. E. (2014). Aryl hydrocarbon receptor (AHR) in the cnidarian *Nematostella vectensis*: comparative expression, protein interactions, and ligand binding. *Development Genes and Evolution*, 224(1), 13-24. doi:10.1007/s00427-013-0458-4
55. Reitzel, A. M., Tarrant, A. M., & Levy, O. (2013). Circadian clocks in the Cnidaria: Environmental entrainment, molecular regulation, and organismal outputs. *Integrative and Comparative Biology*, 53(1), 118-130. doi:10.1093/icb/ict024
56. Rhoades, S. D., Nayak, K., Zhang, S. L., Sehgal, A., & Weljie, A. M. (2018). Circadian- and light-driven metabolic rhythms in *Drosophila melanogaster*. *Journal of Biological Rhythms*, 33(2), 126-136. doi:10.1177/0748730417753003
57. Rivera, A. S., Ozturk, N., Fahey, B., Plachetzki, D. C., Degnan, B. M., Sancar, A., & Oakley, T. H. (2012). Blue-light-receptive cryptochrome is expressed in a sponge eye

- lacking neurons and opsin. *The Journal of Experimental Biology*, 215(Pt 8), 1278-1286.
doi:10.1242/jeb.067140
58. Roenneberg, T., & Foster, R. G. (1997). Twilight times: Light and the circadian system. *Photochemistry and Photobiology*, 66(5), 549-561. doi:10.1111/j.1751-1097.1997.tb03188.x
59. Ruiz-Jones, L. J., & Palumbi, S. R. (2015). Transcriptome-wide changes in coral gene expression at noon and midnight under field conditions. *Biological Bulletin*, 228(3), 227-241. doi:10.1086/BBLv228n3p227
60. Schnitzler, C. E., Pang, K., Powers, M. L., Reitzel, A. M., Ryan, J. F., Simmons, D., . . . Baxevanis, A. D. (2012). Genomic organization, evolution, and expression of photoprotein and opsin genes in *Mnemiopsis leidyi*: a new view of ctenophore photocytes. *BMC Biology*, 10, 107-107. doi:10.1186/1741-7007-10-107
61. Seb e-Pedr os, A., Saudemont, B., Chomsky, E., Plessier, F., Mailh e, M.-P., Renno, J., . . . Marlow, H. (2018). Cnidarian cell type diversity and regulation revealed by whole-organism single-cell RNA-Seq. *Cell*, 173(6), 1520-1534.e1520.
doi:10.1016/j.cell.2018.05.019
62. Shearman, L. P., Sriram, S., Weaver, D. R., Maywood, E. S., Chaves, I., Zheng, B. H., . . . Reppert, S. M. (2000). Interacting molecular loops in the mammalian circadian clock. *Science*, 288(5468), 1013-1019. doi:10.1126/science.288.5468.1013
63. Shoguchi, E., Tanaka, M., Shinzato, C., Kawashima, T., & Satoh, N. (2013). A genome-wide survey of photoreceptor and circadian genes in the coral, *Acropora digitifera*. *Gene*, 515(2), 426-431. doi:10.1016/j.gene.2012.12.038

64. Simionato, E., Ledent, V., Richards, G., Thomas-Chollier, M., Kerner, P., Coornaert, D., . . . Vervoort, M. (2007). Origin and diversification of the basic helix-loop-helix gene family in metazoans: insights from comparative genomics. *BMC Evolutionary Biology*, 7(1), 33.
65. Tosches, M. A., Bucher, D., Vopalensky, P., & Arendt, D. (2014). Melatonin signaling controls circadian swimming behavior in marine zooplankton. *Cell*, 159(1), 46-57.
doi:10.1016/j.cell.2014.07.042
66. Vize, P. D. (2009). Transcriptome analysis of the circadian regulatory network in the coral *Acropora millepora*. *Biological Bulletin*, 216(2), 131-137.
67. Wickham, H. (2009). ggplot2.
68. Williams, D. L. (2016). Light and the evolution of vision. *Eye*, 30(2), 173-178.
doi:10.1038/eye.2015.220
69. Williams, J., & Sehgal, A. (2001). Molecular components of the circadian system in *Drosophila*. *Annual Review of Physiology*, 63(1), 729-755.
doi:10.1146/annurev.physiol.63.1.729
70. Zhu, H., Sauman, I., Yuan, Q., Casselman, A., Emery-Le, M., Emery, P., & Reppert, S. M. (2008). Cryptochromes define a novel circadian clock mechanism in monarch butterflies that may underlie sun compass navigation. *PLoS Biology*, 6(1), e4.

Table 1.1: Cycling and differential expression of candidate circadian clock genes resulting from DESeq2 and JTK_Cycle analysis of subgroups.

ID	Annotation	DESeq2 p-value ^a	JTK_Cycle periodicity ^b	Peak expression ^c		
				LD	LR1	LR2
NVE2080	<i>Clock</i>	1.20459E-08	24 (0.07)	ZT10	-	-
NVE1138	<i>Cry1a</i>	1.66397E-18	24	ZT10	ZT4	ZT4
NVE24214	<i>Cry1b</i>	0.03511226	24	ZT12	ZT20	ZT4
NVE14677	<i>PAR-bZIPa</i>	1.27133E-12	24	ZT6	ZT2	ZT6
NVE20636	<i>PAR-bZIPb</i>	0.052867218	28	ZT6	ZT20	ZT4
NVE8107	<i>PAR-bZIPc</i>	0.007379136	24	ZT18	ZT22	ZT6
NVE8679	<i>helt</i>	1.40066E-11	24	ZT6	ZT4	ZT4
NVE8085	<i>PAR-bZIPd</i>	2.2241E-52	24	ZT10	ZT4	ZT20
NVE4116	<i>CIPC</i>	0.000118936	24	ZT24	-	-

^aBenjamini-Hochberg-adjusted.

^bPeriodicity significance in LD.

^cPeak expression values in LD correspond to a significant JTK_Cycle period.

Table 2.1: Top significantly enriched gene ontology (GO) terms of contrasting treatment subgroups

Comparison ^a	Direction	No. of DEGs ^b	Top GO term (No. of sig. genes/all genes in category) ^c		
			Molecular function	Biological process	Cellular component
LD versus DD	Up	971	Endopeptidase (13/150) $p < .05$	Cellular amide metabolic process (33/367) $p < 1e-04$	Cytosolic ribosome (5/79) $p < .001$
	Down	189	Chromatin binding (19/144) $p < .05$	Regulation of cell cycle process (51/352) $p < 1e-04$	Chromosome (54/389) $p < 1e-04$
LR1 versus DD	Up	1,391	ATPase (57/215) $p < 1e-04$	Chromosome organization (109/322) $p < 1e-09$	Chromosome (126/394) $p < 1e-06$
	Down	258	Structural molecule (82/237) $p < 1e-04$	Protein localization to ER (20/99) $p < 1e-09$	Small ribosomal subunit (30/53) $p < 1e-06$
LR2 versus DD	Up	434	Chromatin binding (135/144) $p < .05$	Histone modification (121/130) $p < .001$	Axoneme (53/54) $p < 1e-04$
	Down	300	Endopeptidase (134/142) $p < .05$	NA	Endoplasmic reticulum lumen (57/61) $p < 1e-04$
LD versus LR1	Up	427	Actin binding (128/135) $p < 1e-05$	Actin filament-based process (269/296) $p < 1e-05$	Endoplasmic reticulum lumen (60/61) $p < 1e-05$
	Down	449	Structural constituent of ribosome (105/111) $p < 1e-05$	Translation initiation (111/113) $p < 1e-05$	Large ribosomal subunit (61/63) $p < 1e-05$
LD versus LR2	Up	828	Oxidoreductase (242/266) $p < .001$	Fatty acid metabolic process (97/102) $p < .001$	Endoplasmic reticulum lumen (59/61) $p < .001$
	Down	353	Structural constituent of ribosome (101/111) $p < 1e-05$	Spindle elongation (68/69) $p < 1e-05$	Cytosolic part (133/139) $p < 1e-05$
LR1 versus LR2	Up	372	Electron transfer (50/52) $p < .001$	Mitochondrial ATP synthesis-coupled electron transport (32/32) $p < 1e-05$	Mitochondrial respiratory chain (33/33) $p < 1e-05$
	Down	133	Signalling receptor (136/145) $p < 1e-05$	Biological adhesion (212/228) $p < 1e-05$	Synapse (242/261) $p < 1e-05$

^aPairwise comparisons using Wald tests in DESeq2.

^bBenjamini-Hochberg FDR cut-off of 10%.

^cMann-Whitney U test corrected p -value.

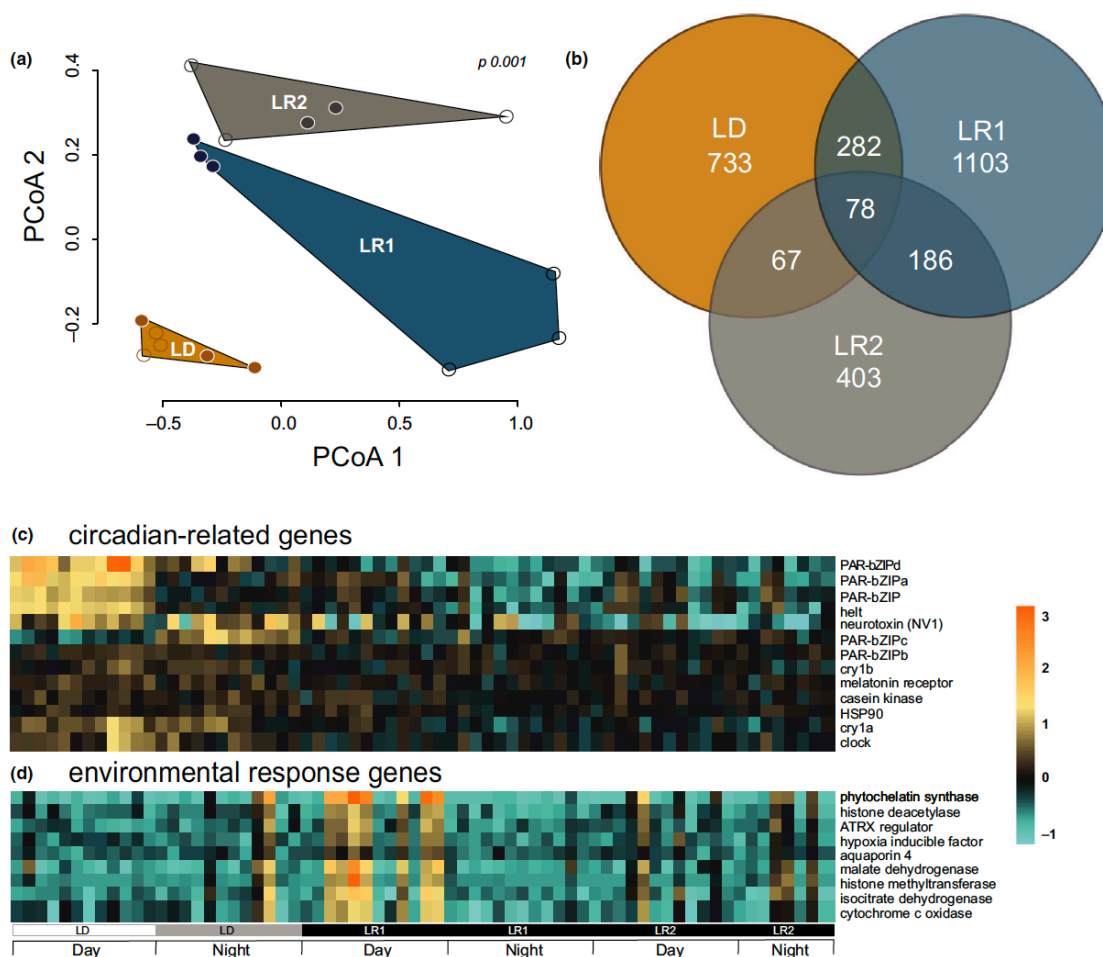


Figure 1. Gene expression of *Nematostella vectensis* in diel and constant conditions. (A) Principal coordinate analysis based on Manhattan distances. Clusters are grouped by diel treatment subgroups (light:dark or LD, light removal day 1 or LR1, light removal day 2 or LR2) and by time of day (open circles – ‘day’, closed circles – ‘night’; pPERMANOVA = 0.001). (B) Venn diagram of the total number of differentially expressed genes resulting from each pairwise comparison between the diel treatment subgroups (LD, LR1, LR2) and control animals kept in long-term constant darkness determined by DESeq2 (Benjamini-Hochberg FDR <0.01). (C) Heatmap of circadian related genes and (D) environmental response genes differentially expressed in light:dark conditions (LD), and after one or two days of light removal (LR1, LR2) determined by DESeq2 (Benjamini-Hochberg FDR <0.01). The experiment key at the bottom identifies the subgroups of the diel light treatment and the ‘day’ and ‘night’ periods of each 24-hour cycle for both C and D. Each row of the heatmaps represent a single annotated gene, and each column represents a single individual in each time point (n = 4 per time point). The color scale is log₂ fold change.

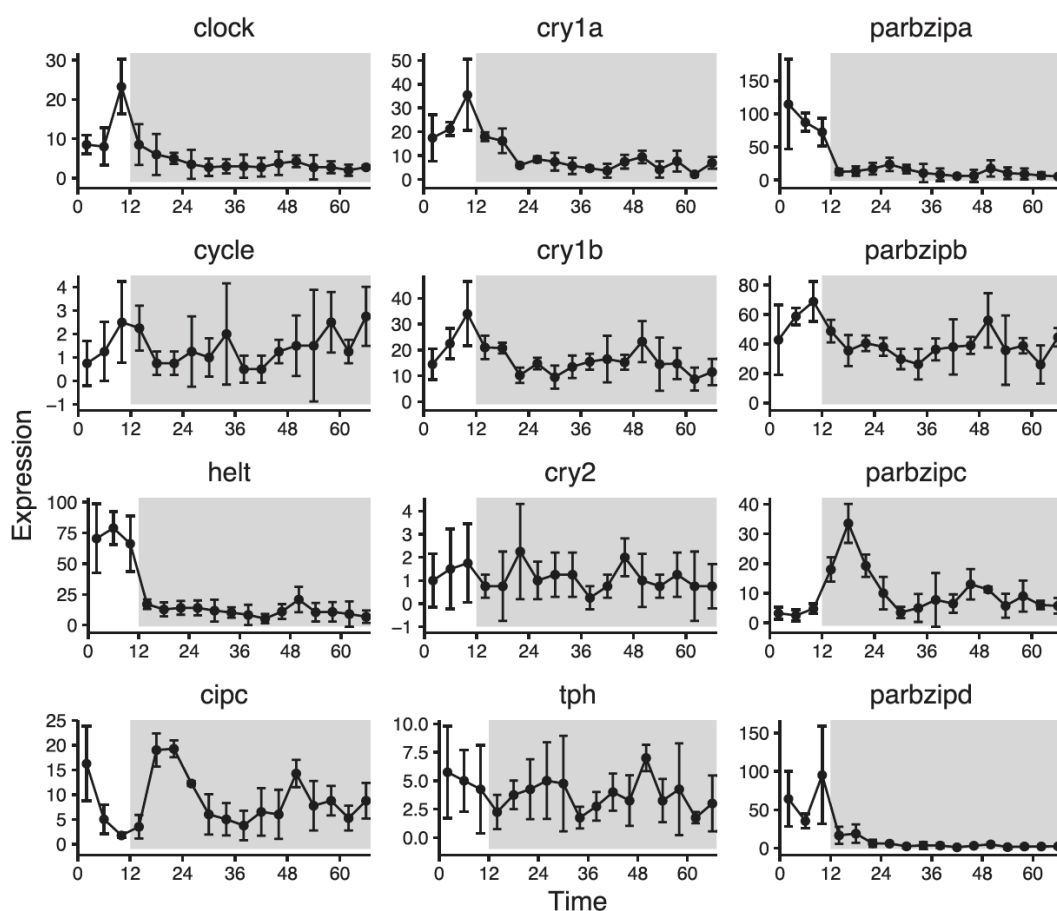


Figure 2. Candidate circadian gene expression profiles over time. Each graph plots a single gene's expression over the three-day sampling time course for light:dark entrained anemones. Each data point represents the mean of four individually sequenced replicates. Error bars are calculated from the standard deviation for each data point ($n=4$). The relative expression (y-axis) is shown for each gene over the sampling period (x-axis). The grey shading in each plot indicates light removal.

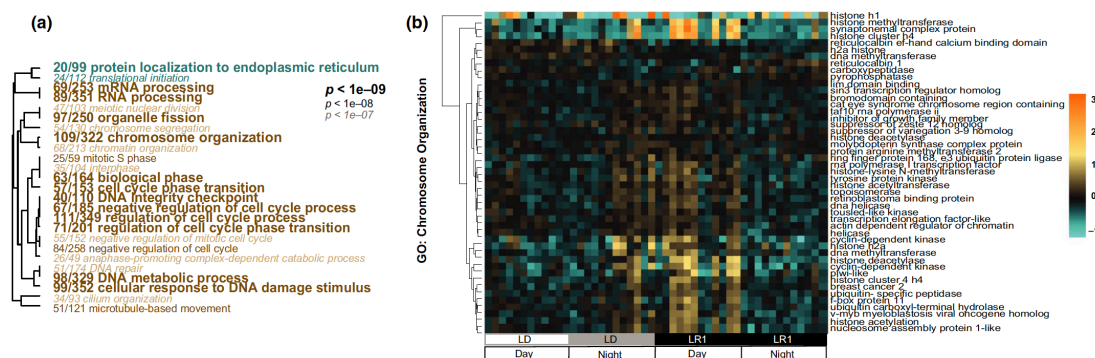


Figure 3. Gene ontology analysis of differentially expressed genes after light removal. (A) Significantly up (tan) or down (cyan) -regulated genes related to ‘biological process’ based on a Mann-Whitney U test of the pairwise comparison between the first day following light removal and constant conditions. The font size corresponds to smaller FDR-adjusted p-values, the smallest font is equivalent to a p-value $< 1e-07$, the largest font is equivalent to a p-value $< 1e-09$. Dendrograms represent hierarchical clustering of GO terms based on shared genes in this data set and the ratios in front of each GO term represent the number of genes from that specific GO term in this data set over all genes belonging to that GO term. (B) Clustered heatmap of the top genes (log2 fold change > 1.5 , DESeq2 p-value < 0.001) from the GO term ‘chromosome organization’ (GO:0006325) during light:dark (LD) and one day post light removal (LR1). The color scale is log2 fold change. The experiment key at the bottom identifies the subgroup and the ‘day’ and ‘night’ periods of each 24-hour cycle.

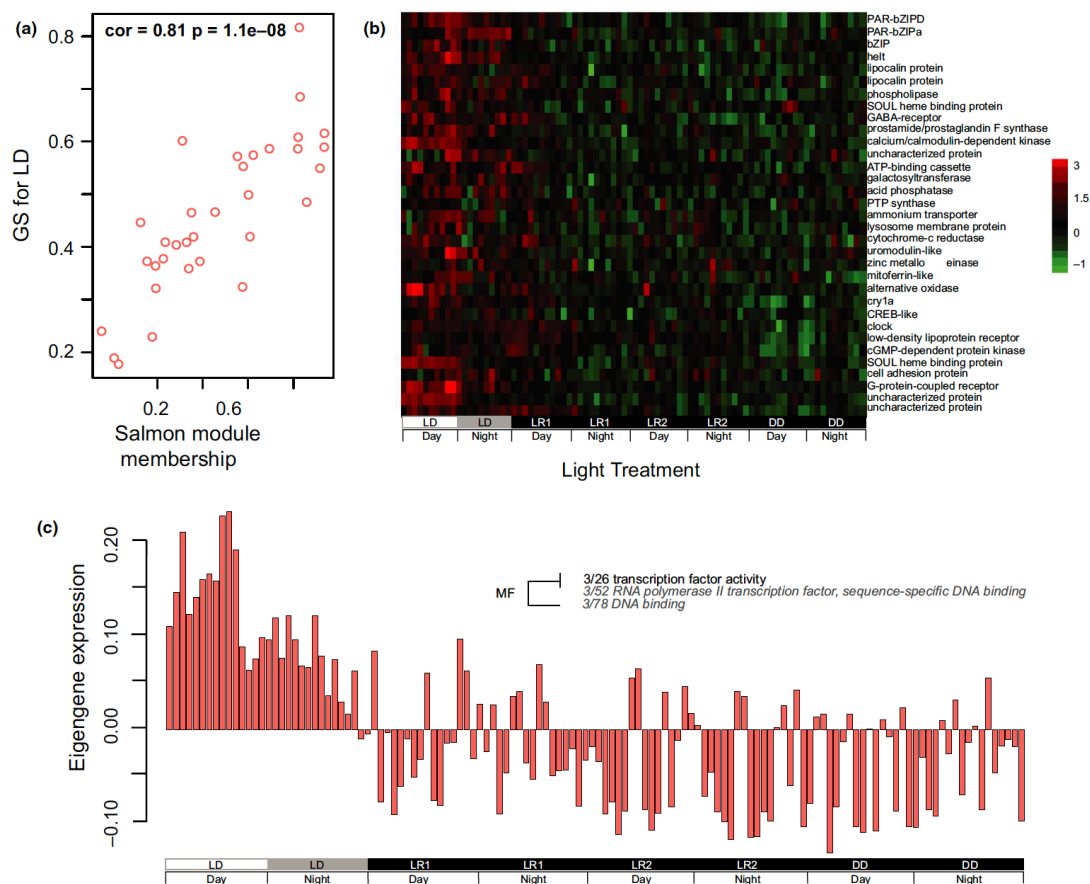
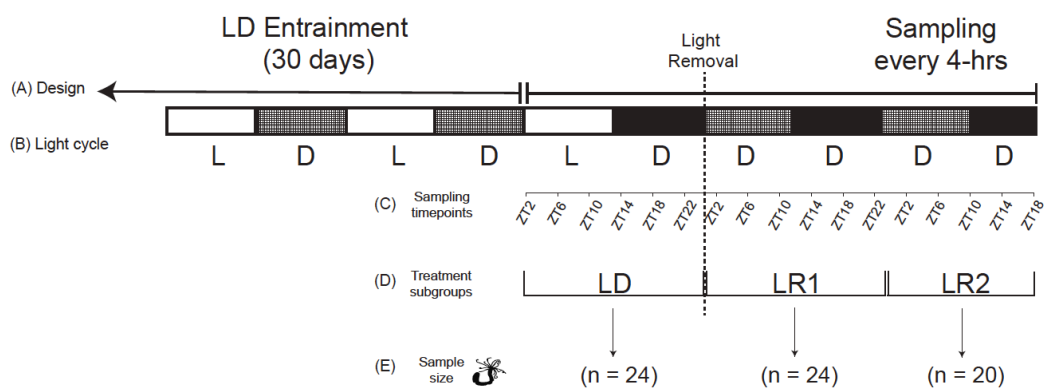


Figure 4. Eigengene expression across all treatment subgroups for light responsive WGCNA salmon module. (A) Scatterplot of the salmon module contains genes co-expressed and positively correlated with light:dark conditions determined by WGCNA analysis and illustrates the genes module membership score along the x-axis and the gene's significance (GS) for the light treatment trait along the y-axis. A high correlation ($cor = 0.81$) between these measures indicates a strong association of the module with the trait (i.e. genes in the salmon module are strongly associated with light:dark conditions). (B) Heatmap of genes in the salmon module across each treatment subgroup. The experiment key at the bottom identifies the subgroups and the 'day' and 'night' periods of each 24-hour cycle. Each row of the heatmap represents a single annotated gene, and each column represents a single individual in each time point ($n = 4$ per time point). The color scale is log2 fold change. (C) Eigengene expression across all treatment subgroups and long-term darkness with corresponding Gene Ontology. Each bar represents a single individual. The experiment key at the bottom identifies the subgroups and the 'day' and 'night' periods of each 24-hour cycle. Positive eigengene expression values indicate positive correlation and negative eigengene expression values indicate negative correlation of the module to the light treatment trait. A fisher's exact test was used to identify significantly enriched GO terms (presence or absence) of the eigengene and categories enriched for molecular function (MF) were assigned. The size and color of the font increases as significance increases, as shown in the inset.

(1) 12:12 LD + Light Removal



(2) Long-Term Constant Darkness

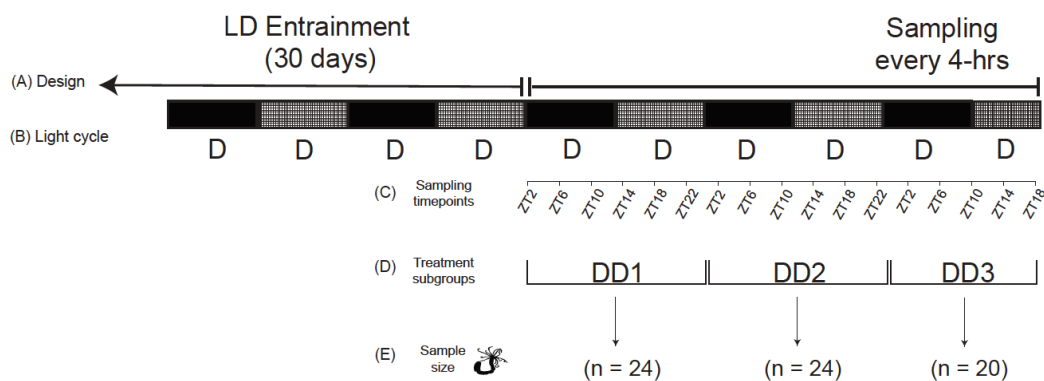


Figure S1. Experimental design of (1) diel and (2) long-term darkness treated *Nematostella*. The design of diel (1A; top) and long-term darkness (2A; bottom) experimental treatment groups shows the identical entrainment period and sampling time course running in parallel. Solid colored boxes represent the ‘day’ period, hatched boxes represent the ‘night’ period, and below the corresponding light cycle is shown by the letters ‘L’ and ‘D’ (light and dark, respectively; 1B, 2B). In the diel-entrained group (1A), the light cue was removed after the first 24 hours of the sampling period as indicated by the horizontal dashed line. The sampling points are shown in Zeitgeber time (ZT; 1C, 2C). ZT2 corresponds to 9:00AM. The 3-day sampling time course corresponds to assigned treatment subgroups (1D, 2D). Treatment subgroups are identified as: LD – light:dark, LR1 – light removal day 1, LR2 – light removal day 2, DD1-DD3 – constant darkness day 1 – 3. 1E and 2E show the sample size (n) of each subgroup (4 anemones per time point * 17 time points = 68 anemones per treatment). *Note: on day 3 of sampling (LR2 and DD3), anemones were only collected at 5 time points.

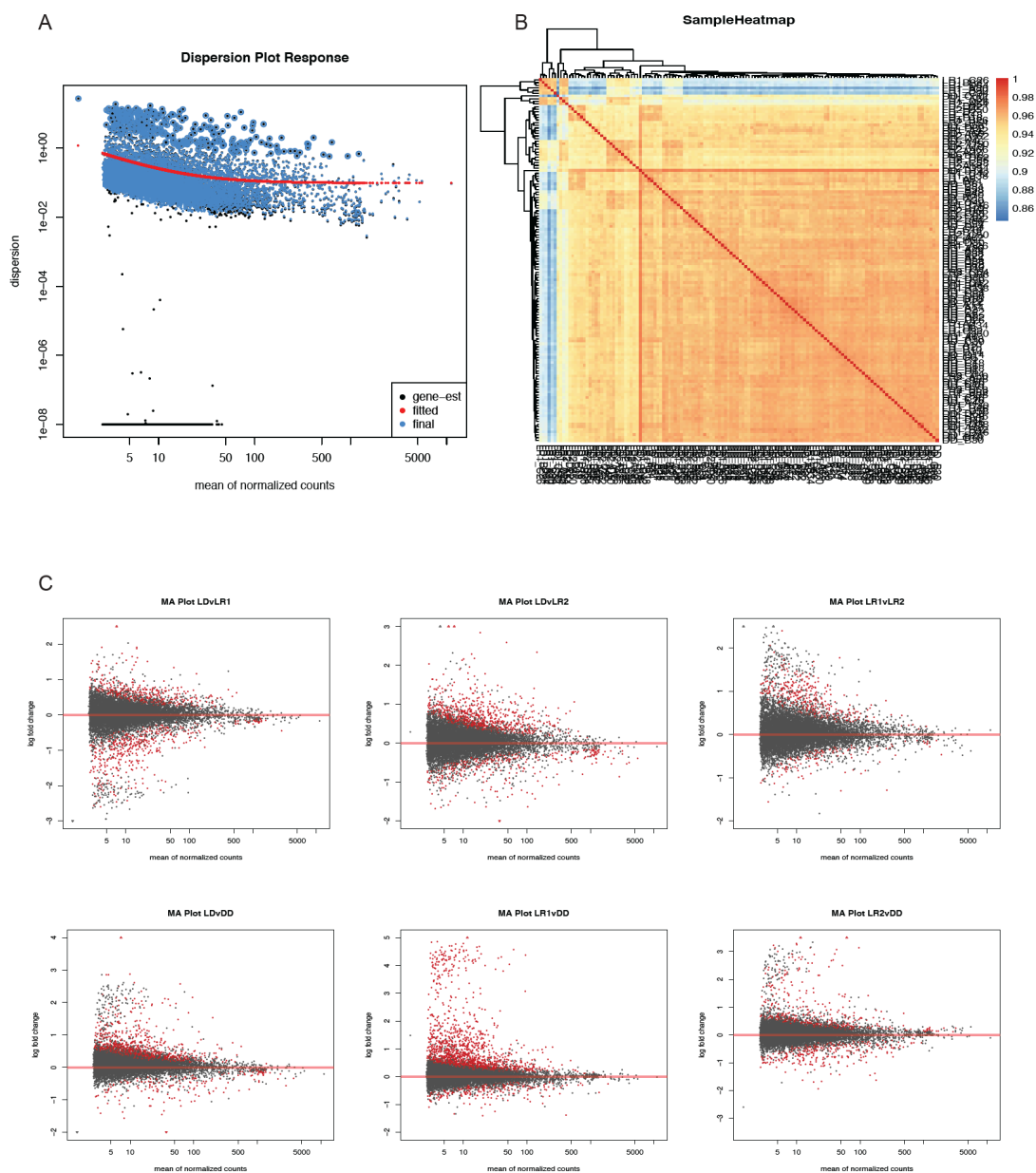


Figure S2. DESeq2 analysis of *Nematostella* transcriptomes pre- and post-light removal. A. DESeq2 plot of dispersion estimates over the average expression strength for the entire dataset. Data points near the bottom are from genes which the observed variance is below the variance expected under the Poisson model. B. Manhattan plots of each contrasting treatment subgroup (LD, LR1, LR2, DD). Each point represents a single gene. The x-axis is the average expression over all samples in the dataset, and the y-axis is the log₂ fold change between the two treatment subgroups. Genes shown in red have pass the 10% FDR threshold.

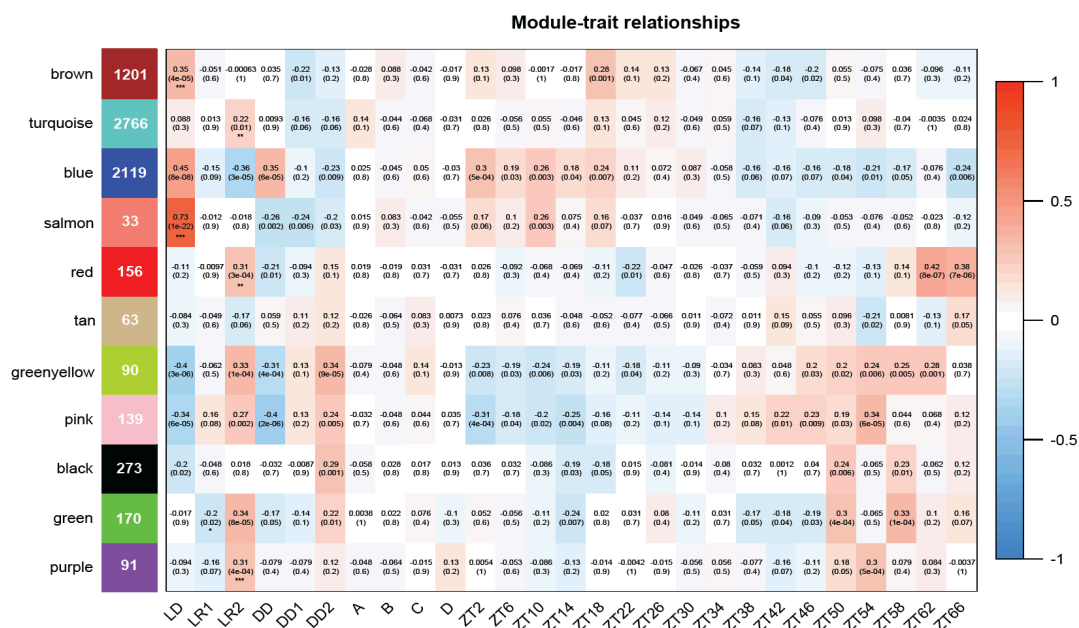


Figure S4. Module-trait relationship heatmap and significance values of each module eigengene correlated to external traits. Gene co-expression network and module-trait relationships are represented by a heatmap of transcripts (5,678) assigned to 11 modules (arbitrary colors on the left of the heatmap). Eigengenes were calculated for each module. The strength of the correlations between traits (light treatment subgroup, time, biological replicates) and gene expression, is indicated by the intensity of the colored blocks with red and blue indicating positive and negative correlations, respectively. The numbers in each block represent the Pearson's correlation between the module eigengene and the trait and corresponding p-values. Modules that are specifically correlated with each of the light conditions are marked with asterisks.

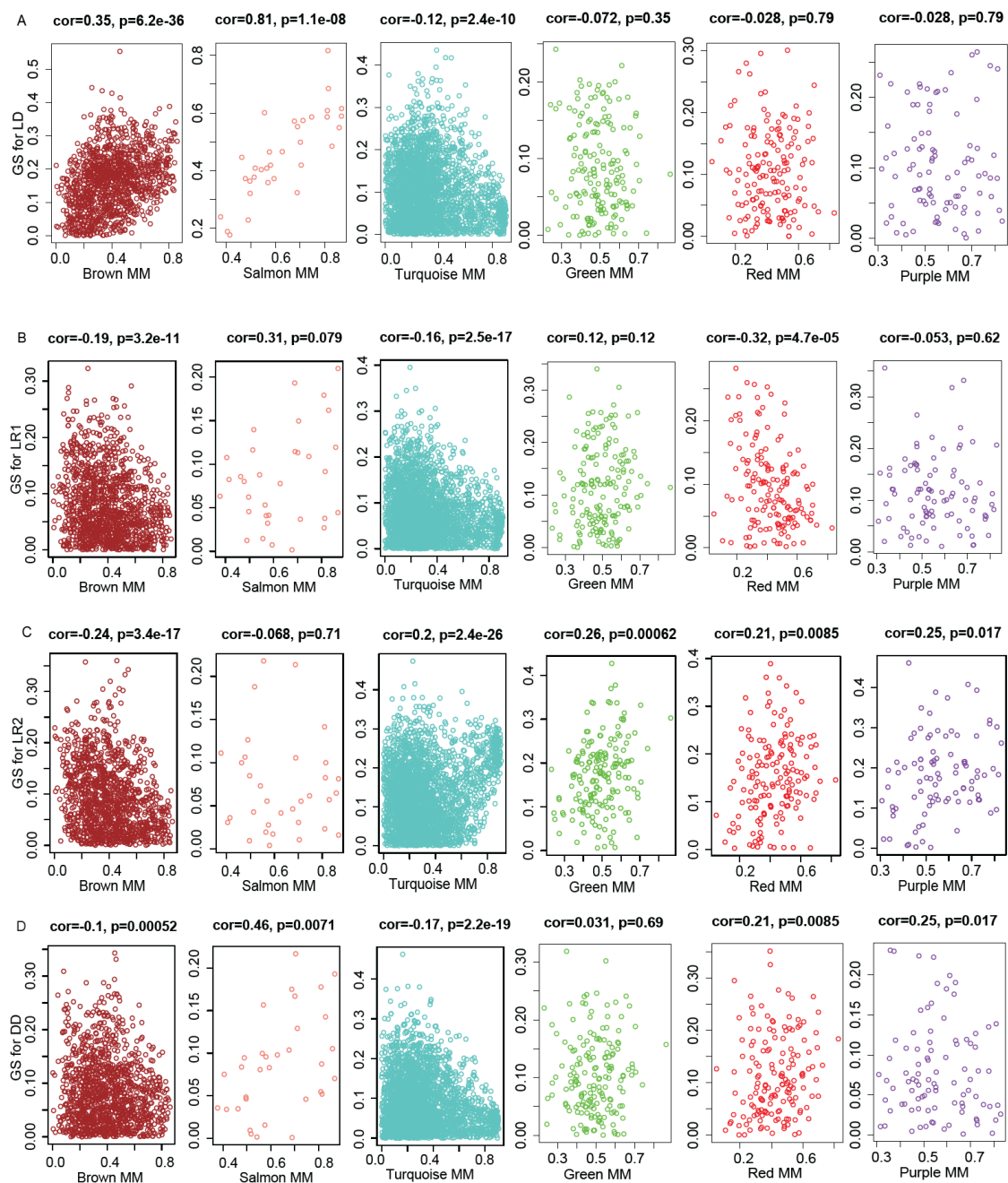


Figure S5. Gene significance scatter plots for each light treatment subgroup: LD (A), LR1 (B), LR2 (C), and (D) DD for each module (brown, salmon, turquoise, green, red, and purple). The plots represent gene significance (GS; y-axis) for each light treatment subgroup versus module membership (MM; x-axis). Gene significance and module membership are significant correlations that imply the genes of each module are highly correlated with the light treatment subgroup.

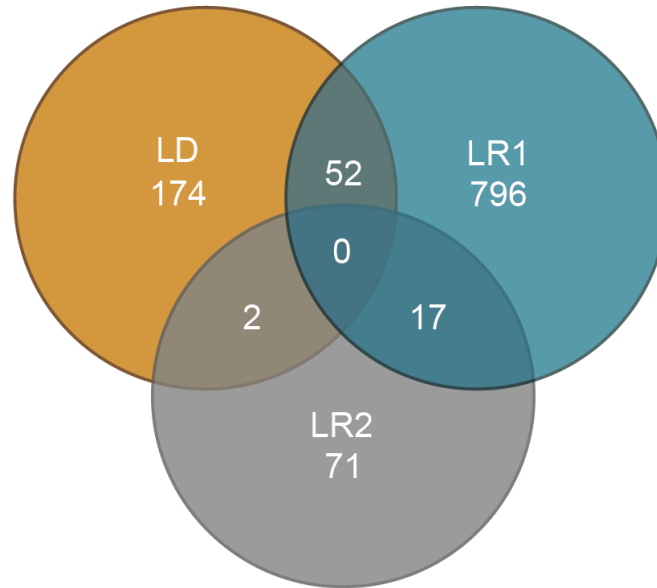
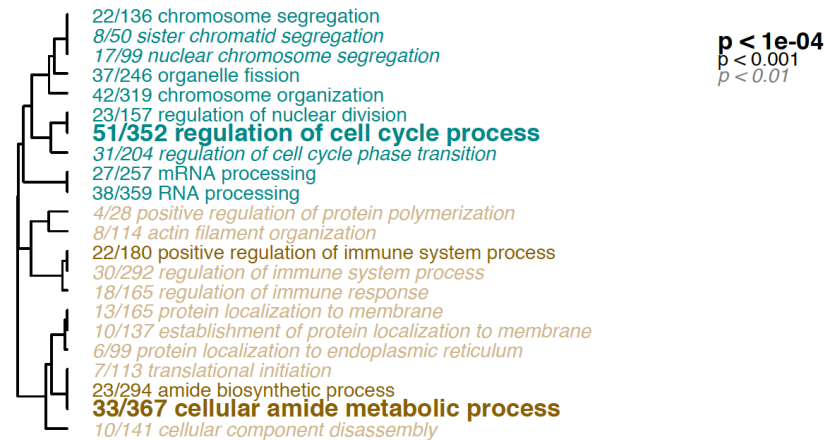
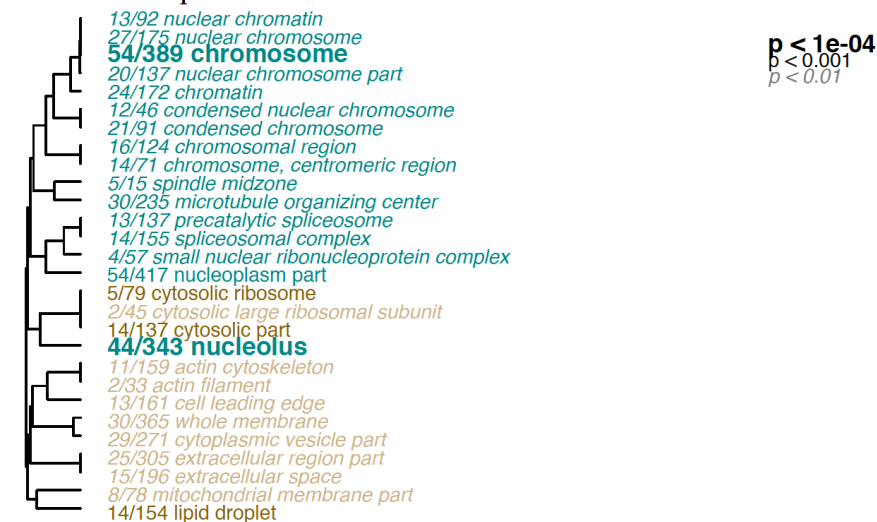


Figure S6. Venn diagram of cycling genes from each light treatment subgroup generated by JTK_Cycle (period = 24, Bonferroni-corrected p-value < 0.01).

Biological Process



Cellular Component



Molecular Function

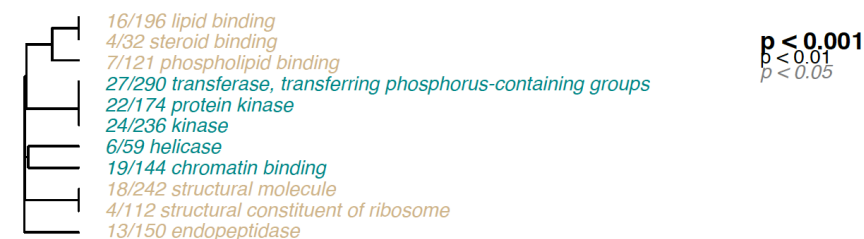
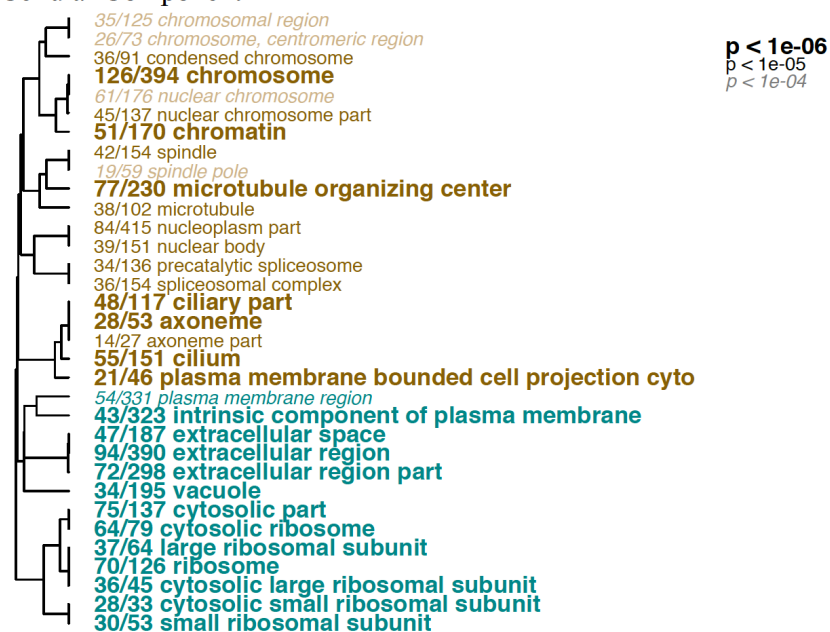


Figure S7. Gene ontology (GO) analysis of differentially expressed genes enriched between light:dark and dark:dark.

Cellular Component



Molecular Function

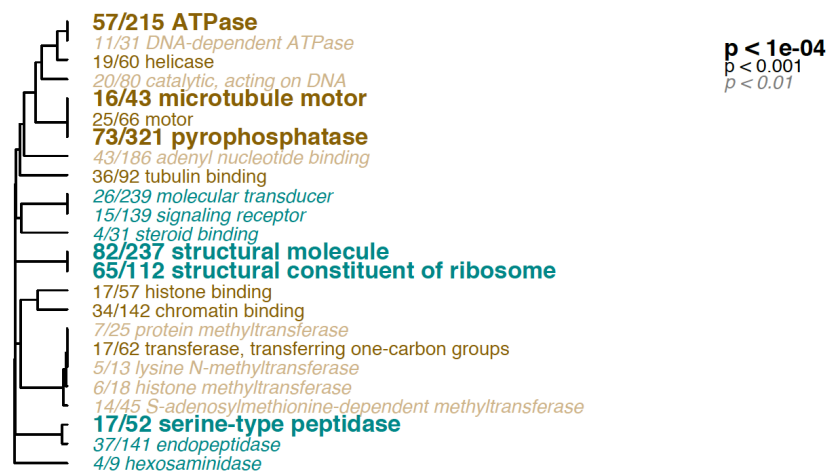
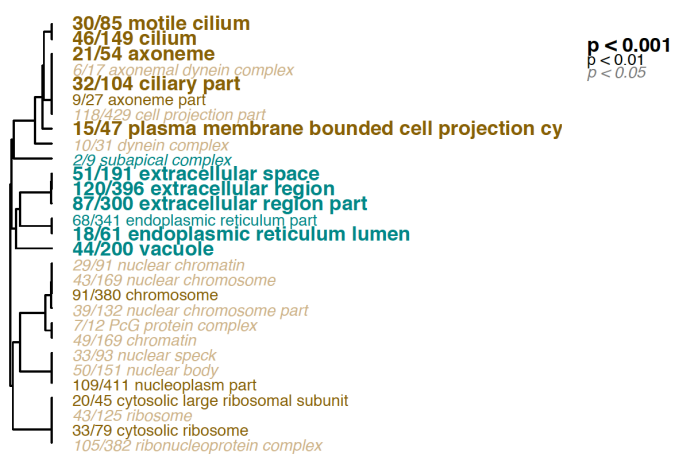


Figure S8. Gene ontology (GO) analysis of differentially expressed genes enriched between light removal day 1 and dark:dark.

Biological Process



Cellular Component



Molecular Function



Figure S9. Gene ontology (GO) analysis of differentially expressed genes enriched between light removal day 2 and dark:dark.

CHAPTER 2

ROLE OF LIGHT WAVELENGTH IN *NEMATOSTELLA VECTENSIS* BEHAVIOR
AND GENE EXPRESSION

Whitney B. Leach and Adam M. Reitzel

In review, *Journal of Experimental Biology*.

Abstract

Animals have specific molecular, physiological, and behavioral responses to isolated portions of the visible light spectrum. The ability to distinguish between different wavelengths of light with particular photoreactive proteins has been a focus for understanding how species respond to a shifting light environment and how light-dependent responses can evolve through both ocular and extraocular surfaces. Cnidarians have been a focal group to discern the evolution of light responsiveness due to their phylogenetic position to understand the emergence of vision in bilaterian animals, as well as the diverse role of light in the behavior and physiology of species throughout the phylum. Much of this previous research has focused on light reception through ocular photoreception, but extraocular mechanisms are more common and likely shared throughout the phylum. Here, we utilize the eyeless sea anemone *Nematostella vectensis* to compare behavioral and molecular responses of individuals exposed to red, green, and blue light. Quantitative measures of locomotion clearly showed that this species responds to shorter, high intensity wavelengths (blue and green) with a circadian activity profile, in contrast to a circatidal activity profile in longer wavelengths (red) and in constant darkness. Differences in average day/night locomotion were significant in each condition, with overall peak activity during the dark period. Comparative analyses of 96

transcriptomes revealed complex differences in gene expression under each lighting condition, and across time including many of the genes likely involved in the cnidarian circadian clock. Temporal transcriptional profiling showed the majority of genes are differentially expressed between mid-day and mid-night, and of the 512 differentially expressed genes, 68% were uniquely expressed in red light. Together, these analyses reveal *Nematostella* is capable of photo-entrainment to a broad range of wavelengths resulting in divergent transcriptional and behavioral responses.

Introduction

Light can be a rich source of environmental information depending on an organism's ability to sense it. Light intensity and duration are indicative of the time of day and season, respectively, which provides a central signal for regulating behavior and physiology (Giese, 1959; Hastings et al., 1985; Saunders, 2008). The particular wavelengths that compose visible light represent complex information. For example, light attenuation in water, where longer wavelengths are absorbed more quickly over depth, provides a signal for position in the water column. The spectral composition of light also varies depending on the relative position of the sun so that light quality is indicative of time of day (Endler, 1993). Spectral irradiance from moonlight is also a source of information that varies in intensity dependent on the phase of the moon (Johnsen et al., 2006). Reflected light from the moon is a widely utilized cue for regulating the behavior, physiology, and reproductive cycle of many animals (Fox, 1932; Giese, 1959; Grant et al., 2013; Takeuchi et al., 2018). In deep sea environments where solar or lunar illumination is not present,

species are also able to receive and respond to bioluminescence emitted from other animals for locating prey and behavioral evasion (Garm et al., 2016).

Light detection is generally driven by a combination of photoreceptive proteins and, depending on the species, pigment molecules used for visual and non-visual photoreception. Opsins compose a diverse family of G-protein-coupled receptors that have been studied for decades for their role in light absorption and G-protein activation (e.g., reviewed by Imamoto and Shichida, 2014; Wang et al., 2014). Phylogenomic studies of this family of photoreceptors has revealed they are present in nearly all phyla and have undergone multiple, independent radiations (Feuda et al., 2012; Ramirez et al., 2016; Schnitzler et al., 2012). As a result, opsin proteins have evolved different spectral sensitivities (Imamoto and Shichida, 2014). Opsin expression is not always spatially restricted to eyes and occurs in both ocular and extraocular tissues, although functional studies have focused primarily on ocular opsins from bilaterian species. Cryptochromes are photoabsorptive proteins with a central role in the circadian clocks of many animals through light-dependent repression of transcription factors or their co-factors (Yuan et al., 2007; Zhu et al., 2005), where their expression correlates with solar and lunar periodicity (Fukushiro et al., 2011). Type I cryptochromes, first characterized in *Drosophila* but present in most animals except vertebrates, contain a flavin co-factor which is reduced upon exposure to blue light, thus their designation as blue-light sensitive proteins (Chaves et al., 2011). Visual shading and filtering pigments are another type of molecule used in ocular photoreception to attenuate light before it is encountered by the photoreceptor (Cronin and Porter, 2014; Nilsson, 2009). Shading pigments shade the photoreceptor, providing information on the direction of illumination, thus facilitating a positive or

negative response, or phototaxis (as in planarians and annelids; Arendt et al., 2002; Lapan and Reddien, 2011; Thumann et al., 2013). Filtering pigments restrict particular colors to increase sensitivity of the photoreceptors (Cronin and Caldwell, 2002; Cronin and Porter, 2014).

Cnidarians have been a critical taxonomic lineage for understanding the evolution of photoreception in animals and the impacts of light on behavior and physiology. Cnidarians have evolved eyes multiple times (Picciani et al., 2018) and those with compound eyes express diverse ocular opsin proteins, that where characterized, have maximum absorbance in narrow wavelengths corresponding to blue-green (Garm et al., 2007a; Martin, 2004). In species with ocular photoreception, the sensitivity of the visual structure and environmental light contrast correlate with swimming behavior for orientation and obstacle avoidance (Garm et al., 2013; Garm et al., 2007b; Gershwin and Dawes, 2008). Most cnidarians lack eyes and thus the reception and transduction of light signals is performed extraocularly with non-visual components. In these species, light has been shown to be a central entraining cue for a broad range of behavioral and molecular responses (Hoadley et al., 2016; Kanaya et al., 2019; Oldach et al., 2017). For example, the diel vertical migrations of jellyfish are timed to daily light oscillations (Dupont et al., 2009; Kaartvedt et al., 2007; Schuyler and Sullivan, 1997), and the reproduction of many reef building corals is entrained to lunar moonlight cycles (Kaniewska et al., 2015) [but see (Wolstenholme et al., 2018)], which correlates with expression of cryptochromes (Levy et al., 2007). Moreover, individual wavelengths of light have been shown to result in specific behaviors, including larval settlement (Foster and Gilmour, 2016; Strader et al., 2015), tentacle expansion and contraction (Levy et al., 2003), and cnidocyte (stinging cells)

discharge (Plachetzki et al., 2012). Opsins have also been identified with tissue restricted expression in the gonads (Artigas et al., 2018), oral region, and tentacles (Suga et al., 2008) of certain species, which may be associated with specific physiological processes. The connections between light or wavelength-dependent behaviors and molecular responses remain poorly understood in any cnidarian, particularly for species with only extraocular photoreception.

Previous research with the sea anemone *Nematostella vectensis* (hereafter, *Nematostella*) has shown that light exposure impacts reproduction (Genikhovich and Technau, 2009), respiration (Maas et al., 2016), and locomotion (Hendricks et al., 2012), similar to other cnidarians. Much of this research has focused on the potential for light entrainment to impact gene expression, where repeated light exposure results in differential expression of hundreds of genes including those in a hypothesized circadian clock (Leach et al., 2018; Oren et al., 2015). A gene expression study by Reitzel et al. (2010) has been the only previous research to suggest that different wavelengths of light may exert specific effects on this species. Transcription factors and the Type I cryptochromes of *Nematostella* had differential expression depending on the portion of light spectrum (e.g., blue vs. longer wavelength), suggesting that a cnidarian with extraocular photoreception responds differently to portions of the light spectrum. Unlike most cnidarians, this translucent species occupies an estuarine habitat, typically distributed at shallow depths (< 1m), where they experience a broader range of wavelengths than those in deeper benthic habitats.

Here, we utilize an integrative organismal and molecular approach testing two hypotheses regarding extraocular light entrainment in *Nematostella*. First, we hypothesized that in response to narrow portions of the visible light spectrum, *Nematostella* would

exhibit higher activity at night, or during the scotoperiod, and lower activity during the day, or photoperiod. Secondly, exposure to narrow light spectra would result in observable behavioral shifts that correlate to transcriptional remodeling of circadian clock-related genes (e.g., *Clock*, *PAR-bZIPs*) or differential expression of extraocular light-responsive genes or proteins (e.g., cryptochromes, opsins). We measured behavior of sea anemones exposed to light:dark (12:12) cycles of either 1) red (630 nm); 2) green (510 nm); 3) blue (450 nm); or constant darkness (DD). We quantitatively measured locomotor activity during each light cycle, as well as qualitatively monitored female reproductive output. We used tag-based RNA-sequencing to transcriptionally profile animals and compared gene expression from each condition and over time. Comparing between light spectra at these intensities allowed us to identify expression patterns that might reveal expression of unique photoreceptors and comparing between time points in each light treatment further provided an opportunity to look for light and temporal-dependent molecular responses. Together, our results show that *Nematostella* is capable of behavioral entrainment in each light condition but exhibits different activity profiles dependent on the light cue. Interestingly, in the red light treatment and in constant darkness, *Nematostella* was observed exhibiting a twice-daily cycle, similar to those seen in animals with circatidal clocks.

Results

Nocturnal behavior irrespective of light condition

We monitored behavioral output using an animal tracking software (see Methods), in which each sea anemone was measured individually after entrainment in red, green, or blue light:dark (LD) conditions (here after referred to as ‘X color light’) or dark:dark (DD)

conditions during two consecutive light cycles (or constant darkness in DD). Plotting locomotion over time for all treatments (red light, green light, blue light, and DD) revealed that the average activity of sea anemones was higher during the scotoperiod than during the photoperiod for each condition (Figure 1). Locomotion increased with shorter wavelengths and higher intensity (Figure S1), with animals in blue light displaying the highest overall movement (Figure 1). Average movement in both the photo-and scotoperiod was significantly different within and between treatments (Table S1).

Wavelength-inducible circadian or circatidal behavioral response

Sea anemones in blue and green light exhibited locomotor oscillations that parallel circadian behavior of animals under full spectrum diel conditions (Hendricks et al., 2012). This response was signified by nocturnal movement, with peak activity occurring during the scotoperiod (Figure 2A, Figure 2B). Animals in red light and in DD displayed behavioral patterns consistent with circatidal oscillations, or twice-daily rhythms. In addition to nocturnal peaks of activity during the scotoperiod, a second peak during the photoperiod was observed (Figure 2C, Figure 2D). We used chi-squared analysis to determine periodicity of animals in each light treatment using a confidence level of 0.01. Over the 48-hour time course, animals entrained to blue and green light had a circadian periodicity of 23.8-hours (Figure 2E, Figure 2F). A circatidal periodicity of 11.8-hours and 12.4-hours was observed for red light and DD, respectively (Figure 2G, Figure 2H).

Spectrally insensitive gametogenesis of *Nematostella*

Groups of adult female sea anemones were induced to spawn in red, green, and blue light conditions, otherwise following reliable spawning procedures determined by

Fritzenwanker & Technau (2002). Qualitative measurements of gametogenesis (i.e., egg output) from each group were recorded weekly and showed sea anemone spawning occurred in all light treatments, but not in DD.

Wavelength and time-of-day dependent transcriptional response

To identify genes differentially expressed in each light treatment, we sequenced transcriptomes of 96 sea anemones: 24 individuals per condition, where four biological replicates were sampled (i.e., individual anemones cultured in separate bowls) every four hours for the period of one day (6 time points). Tag-based RNA sequencing produced >225 million reads (Table S2). On average, there were 2.3 million 100-base single-end reads per sample. Using a standard bioinformatic processing pipeline, reads were quality filtered and PCR duplicates were removed, leaving an average of 621,629 reads per sample (Table S2; Leach and Reitzel, 2019; Meyer et al., 2011). After trimming, reads were mapped to the Vienna *Nematostella* transcriptome (~24,000 genes) with an average mapping efficiency of 75.17%. Using DESeq2, raw count data were filtered, transformed, and normalized prior to statistical analysis employing Wald tests. Over the 24-hour sampling period of all light treatments, 512 transcripts were identified to have diel patterns of expression passing a Benjamini-Hochberg FDR cutoff of 10%. Of these diel genes, light treatment (red, green, blue) and time-of-day were contributing factors for their expression. Of the 512 genes, 441 (86%) were differentially expressed between ZT = 6 vs. ZT = 18 (mid-day and midnight contrast); 18 genes differentially expressed between ZT = 2 vs. ZT = 14 (early photoperiod and early scotoperiod contrast); and 52 genes were differentially expressed between ZT = 10 vs. ZT = 22 (late photoperiod and late scotoperiod contrast) (Figure 3D-E). Of the 512 time-of-day dependent diel genes, 348 (68%) were differentially expressed in red light;

102 (20%) were differentially expressed in blue light, 60 (12%) were differentially expressed in green light; and 2 were differentially expressed in dark conditions, with minimal overlap between light treatments. A list of differentially expressed genes from each comparison can be found in Table S3.

The majority of diel genes from the mid-day and mid-night contrast, 419 out of 441 (95%), were up-regulated during the photoperiod (Figure 3B). More than two-thirds of these diel genes were unique to red light (285 out of 441, 68%), and less than one percent of these genes were down-regulated during the photoperiod (22 out of 441). Notably, *nvTimeout*, the *timeless* homolog, was uniquely differentially expressed under red light and was 1.5-fold higher during the photoperiod. Further, several heat shock proteins were up-regulated mid-day in red light only (i.e., *nvHSP70E*, *nvHSP90A*, and *nvHSP90B*). Twenty-four out of 441 diel genes were unique to blue light, 75% of which were upregulated during the photoperiod, and included the circadian clock candidate genes *nvPAR-bZIPa*, *nvPAR-bZIPd*, and *nvhelt*. The transcription factor *nvPAR-bZIPc* was one of eight genes down-regulated during the photoperiod of blue light, and decreased > 2.5-fold after the light-dark transition, consistent with findings from Leach and Reitzel (2019) and Reitzel et al. (2013). Diel genes with the strongest changes in expression under blue light were core histone proteins, with a >7-fold increase during the photoperiod. Few diel genes (13 out of 441) were uniquely expressed in green light and 53% were upregulated during the photoperiod (7 genes). Only one gene, *supervillin*, was differentially expressed in DD, and was >3-fold higher mid-day. A small proportion of diel genes were shared between all light treatments (19 out of 441; Figure 3), and primarily consisted of cytoskeletal proteins (i.e., *alpha-tubulin*, *supervillin*). Nineteen diel genes (of 441) were shared between red light and blue

light, including *nvPAR-bZIPa*, a previously characterized diurnal gene (Reitzel et al., 2013). In both conditions, *nvPAR-bZIPa* transcription was >2-fold greater during the photoperiod.

Although more than 85% of all diel genes were differentially expressed between mid-day and mid-night, a portion of diel genes (18 out of 512; < 1%) were only identified in the contrast between early morning and early night following the light-dark transition. Of these 18 diel genes, 83% were up-regulated during the photoperiod (Figure 3A). Three diel genes were uniquely expressed in red light: a perilipin-like protein, a selenoprotein precursor, and an unannotated gene. One diel gene, a protease inhibitor, was uniquely expressed in blue light. Nine diel genes were uniquely expressed in green light and primarily consisted of unannotated proteins. No genes were shared between all treatments, red light/blue light or red light/green light (Figure 3D); however, two genes, both PAR-bZIP transcription factors, were shared between the blue light and green light: *nvPAR-bZIPa* and another PAR-bZIP with high sequence similarity to *nvPAR-bZIPa*, up-regulated during the photoperiod of each light condition, as was also seen in the mid-day and mid-night comparison. One gene was differentially expressed in constant darkness and was unannotated (Table S3).

Fifty-two diel genes were differentially expressed between late day and late night; the time point just prior to the transitions in lighting. Of these, < 35% were up-regulated during the photoperiod (Figure 3C). Unique to blue light was the transcription factor *nvPAR-bZIPd* and a heat shock protein *nvHSP70C*, both up-regulated during the photoperiod (Table S3). Two genes were shared between all conditions, with the same directionality of expression up during the scotoperiod (an unannotated gene and

collagenase). One gene, *ester hydrolase*, was shared between blue light and green light and four genes were shared between red light and blue light (2 unannotated genes, *carboxypeptidase*, and a ribosomal protein; Table S3). There were no genes in DD that were differentially expressed late in the light cycle.

Gene ontology (GO) enrichment analysis of genes differentially expressed in response to each treatment revealed that under red light, down-regulated genes enriched in the biological process category were related to ‘G-protein coupled receptor signaling’ and ‘regulation of response to stress’. Conversely, up-regulated molecular function genes were enriched for ‘mRNA metabolic process’ and ‘methylation’ in red light. GO enrichment analysis discovered in both red light and green light genes relating to ‘activation of immune response’ were down-regulated, and ‘cellular respiration’ genes were up-regulated. Enriched terms in blue light included up-regulated genes involved ‘DNA binding’, ‘chromatin binding’, and ‘amide biosynthetic process’, and down-regulated genes in the ‘signaling receptor binding’ category. In each light condition, there was enrichment amongst up-regulated genes of the GO terms ‘biological phase’ and ‘oxidation-reduction’.

Transcriptomic response combining wavelength and time

Weighted gene co-expression networks were constructed using 4,965 filtered genes (see Methods) to classify systems-level molecular responses to different wavelengths. Each gene in the data set was assigned to an expression module, pairing them based on similarity of expression profiles using a weighted gene correlation network and given an arbitrary color name. In total, 10 co-expression modules resulted from the analysis, and eight were highly enriched for genes corresponding to specific wavelengths. Three module eigengenes were composed of enriched genes negatively

associated, or down-regulated, with blue light (greenyellow: -0.27, $p < 0.009$; lightcyan: -0.36, $p < 0.0004$; purple: -0.36, $p < 0.0005$), while one eigengene was positively associated, or up-regulated, with blue light (grey60: 0.32, $p < 0.002$). The strongest module negatively associated with blue light (purple) exhibited GO enrichment of 'receptor regulator activity' and 'activation of immune response'. GO analysis of genes from the module eigengene positively associated with blue light (grey60) did not find any enriched terms. The co-expression network returned two modules that were enriched for genes specific to green light conditions, both of which were up-regulated (greenyellow: 0.26, $p < 0.01$; pink: 0.3, $p < 0.004$). GO analysis of green light specific modules identified functional enrichment of the terms 'cation binding' and 'immune system development'. Two modules containing genes enriched for red light conditions were identified, and each of these were up-regulated in response to red light (turquoise: 0.31, $p < 0.002$; lightcyan: 0.22, $p < 0.04$); however, expression of the turquoise module eigengene was down-regulated in DD conditions and the lightcyan module contained genes that were down-regulated in blue light and up-regulated in DD. The GO terms 'DNA-binding transcription factor activity', 'signaling receptor activity' and 'molecular transducer activity' were positively enriched in response to red light. Several modules were positively associated with DD (midnightblue: 0.29, $p < 0.006$; black: 0.37, $p < 0.0003$; lightcyan: 0.23, $p < 0.02$; purple: 0.43, $p < 0.00002$) and negatively associated with DD (grey60: -0.21, $p < 0.05$; pink: -0.22, $p < 0.03$; turquoise: -0.29, $p < 0.004$). The purple and black modules were most strongly up-regulated in DD and were enriched for GO terms related to 'activation of immune response' and 'antioxidant/peroxidase activity', respectively. A list of all modules is provided in Table S4.

Although some modules were not positively or negatively associated with a specific light treatment, the co-expression network identified modules that were associated with a specific time point during the day (Table S4). The blue module contained genes that were up-regulated during the photoperiod ($ZT = 6$, 0.28 , $p < 0.006$), and down-regulated the scotoperiod ($ZT = 14$, -0.21 , $p < 0.04$). GO analysis of this module found the terms ‘NADH dehydrogenase activity’ and ‘cellular respiration’ to be enriched at specific points of the day, consistent with previous respirometry data (Maas et al., 2016). The salmon module was not enriched for specific GO terms, however genes in this module were downregulated during the scotoperiod ($ZT = 18$, -0.27 , $p < 0.009$).

Expression of candidate circadian genes

Diel patterns of expression for genes previously described as circadian were observed differently across light conditions. Transcription of *nvClock* was highest during the late photoperiod ($ZT = 10$) of blue light and decreased immediately following the light to dark transition, consistent with previous studies (Leach and Reitzel, 2019; Peres et al., 2014; Reitzel et al., 2010) (Figure 4; Figure 5A). Diel expression of *nvClock* was not observed in anemones cultured in DD, and was significantly different from blue light at each sampling point during subjective day. In green light and red light, *nvClock* expression was not significantly different from DD at any time point, but were both significantly different from blue light at $ZT = 10$ ($p < 0.0001$). At $ZT = 6$, *nvClock* expression was also significantly different between blue light and green light ($p < 0.0001$; Figure 4, Figure 5A-B, Table S5). *nvPAR-bZIPa* expression was highest early in the photoperiod of each color: at $ZT = 2$ of blue light and green light, and $ZT = 6$ of red light (Figure 5C). At $ZT = 2$, *nvPAR-bZIPa* expression was significantly different from dark

conditions in both blue light and green light, but not red light (Figure 5). Further, at ZT = 6 each color was significantly different from all others (Table S5) excluding red light vs. dark. Transcription began decreasing during the late photoperiod and reached an expression trough just after the start of the scotoperiod of each color (ZT = 14). Transcription increased as the dark to light transition occurred (Figure 4). This pattern was not observed under DD (Figure 5D). Similarly, transcription of *nvPAR-bZIPd* peaked during the early photoperiod (ZT = 2) and decreased steadily into the scotoperiod. Diel expression of *nvPAR-bZIPd* was only observed in blue light, but transcription in both red and green light was significantly different than blue light at ZT = 6 ($p < 0.0001$) and no differential expression was measured in DD. Conversely, *nvPAR-bZIPc* peak expression occurred during mid- and late-scotoperiod of blue light (ZT = 18) and green light (ZT = 22), respectively; however, transcription was not sustained during late subjective night into the photoperiod. While *nvPAR-bZIPc* expression was diel in blue and green light, expression was constant in red light and dark conditions. Similarly, a Hes/Hey-like gene, *nvhelt*, was diurnal only under blue light and green light, however transcription was much higher in blue light overall (Figure 4). *nvhelt* transcription was highest at the beginning of the photoperiod (ZT = 2) and decreased over subjective day to a trough at ZT = 22. The diel expression of *nvCry1a* and *nvCry1b* was highest mid-photoperiod (ZT = 6) of blue and green light, however significant oscillations were not measured under red light or dark conditions. Diurnal expression of the *circadian interacting pacemaker protein*, *nvCiPC*, was only observed under blue light (Figure 5, Table S5). As previously shown by Reitzel et al. (2010) cyclic expression of *nvCycle* and *nvCry2* was not observed.

Discussion

Animal phototransduction cascades are highly diverse and predate bilaterian animals (Arendt, 2003; Shichida and Matsuyama, 2009). As a sister group to bilaterians, a number of studies have investigated the photoreceptive pathway of cnidarians to understand the evolution of vertebrate vision (Garm et al., 2007a; Garm et al., 2013). Most of these studies have focused on ocular photoreception, leaving relatively unknown the light-sensitivity and behavior of species with extraocular mechanisms, particularly in anthozoans [reviewed by Martin (2002)]. In contrast to ocular photoreception, non-visual or extra ocular photoreception does not occur in eyes or similar structures but through cells diffusely distributed in tissues of the animal or concentrated within particular regions (e.g., the nervous system) (Vigh et al., 2002; Wolken and Mogus, 1981). Behaviors attributed to light perception in cnidarians include diel vertical migrations in the water column (Arkett, 1989; Dupont et al., 2009; Kaartvedt et al., 2007; Kim et al., 2016; Mills, 1983), rhythmic contractional bursts (Passano and McCullough, 1963; Plachetzki et al., 2010), phototaxis and photokinesis (Garm and Mori, 2009; Garm et al., 2007b; Hamner et al., 1995; Stewart, 1996), gametogenesis (Grawunder et al., 2015; Harrison et al., 1984), cnidocyte discharge (Plachetzki et al., 2012), tentacle expansion and contraction (Abe, 1939; Gladfelter, 1975; Levy et al., 2003; Pearse, 1974; Sebens and DeRiemer, 1977), and feeding (Lewis and Price, 1975). While sensitivity to blue and green light is common, more variation in spectral sensitivity (including red) has been suggested for some species of corals (Mason et al., 2011; Mason and Cohen, 2012), where spectral cues from both the water column and substrate influence larval positioning for settlement and metamorphosis (Gleason et al., 2006; Mundy and Babcock, 1998; Strader et al., 2015).

The described photobehaviors of cnidarians has been attributed to the presence of light sensing opsins and cryptochromes, however investigations of the suggested photoreceptors are lacking. Some studies have suggested opsin-mediated pathways are responsible for photobehaviors in corals (Anctil et al., 2007; Mason et al., 2012), *Hydra* (Plachetzki et al., 2012), and jellyfish (Artigas et al., 2018; Koyanagi et al., 2008; Suga et al., 2008). In the only biochemical study to explicitly measure the absorptive range of a cnidarian photoreceptor, Koyanagi et al. (2008) characterized a single, green-light sensitive opsin (absorption maximum at 500 nm) responsible for initiating the phototransduction cascade in box jellyfish *Charybdea*, however the entire retinal opsin repertoire was not examined. While extraocular light sensing mechanisms of cnidarians have not been tested, screening of the *Nematostella* genome has identified 31 candidate opsins (Plachetzki et al., 2007; Suga et al., 2008), more than the number in other cnidarians (Picciani et al., 2018). A survey of the opsin genes identified by Suga et al. (2008) in this study did not show cyclic or light-dependent expression in any light treatment. Additional transcript mining from published time course data in full spectrum diel light conditions Leach and Reitzel (2019) also did not reveal differential expression of *Nematostella* opsins. Further, qPCR validation of select opsins did not show light-dependent expression (data not shown), but this result is not conclusive to exclude opsins' role in the photobehavior of *Nematostella*. We postulate this lack of light-dependent expression could be due to post-translational modifications required for opsin, which would not be picked up when measuring at the transcript level. Modifications to core circadian proteins and photoreceptors have been described for several species, including *Drosophila*, mammals, and cyanobacteria (reviewed in Mehra et al., 2009). Biochemical experiments examining the spectral

sensitivity of these proteins and their potential modifications will help elucidate their role in *Nematostella* light detection.

Cryptochrome evolution and function is poorly described for marine invertebrates (Haug et al., 2015; Mei and Dvornyk, 2015; Oliveri et al., 2014), but these proteins likely have roles in phototaxis by sponge larva (Rivera et al., 2012) and reproduction of some coral species (Hoadley et al., 2011; Levy et al., 2007). Both light-sensitive and insensitive cryptochromes (Type I and Type II, respectively) are present in anthozoans based on phylogenetic distribution. Unlike cnidarian opsins, our data presented here and previous transcriptomic data show that expression of Type I cryptochromes (i.e., *nvCry1a*, *nvCry1b*) in *Nematostella* and corals are light-dependent with peak expression during the photoperiod, but lose rhythmicity in prolonged darkness (this study; Brady et al., 2011; Hoadley et al., 2011; Leach et al., 2018; Leach and Reitzel, 2019; Levy et al., 2007; Peres et al., 2014; Reitzel et al., 2010; Shoguchi et al., 2013). Expression of Type I cryptochromes from corals, *AmCry1* and *FfCry1* (from *A. millepora* and *F. fragum*, respectively) are strongly diurnal in response to light cycles (Brady et al., 2011; Hoadley et al., 2011; Levy et al., 2007), particularly moonlight which is a major contributing cue in mass spawning for many reef corals. There is variation with reports of Type II cryptochrome expression in *Nematostella*. For example, *nvCry2* does not show a strong diurnal response in any light treatment of this study, as is similarly reported in Leach and Reitzel (2019) and Reitzel et al. (2010), as this gene is most closely related to insect light-insensitive cryptochromes (Griffin et al., 1999; Kume et al., 1999; Yuan et al., 2007; Zhu et al., 2008; Zhu et al., 2005). These data are in contrast to a study by Peres et al. (2014), in which *nvCry2* expression displayed rhythmic oscillations in response to light:dark treatment.

Furthermore, cryptochromes have been hypothesized to form feedback loops in the circadian circuitry of cnidarians acting as transcriptional repressors (discussed further below; Reitzel et al., 2013), however their absorbance spectra has not been measured. Future work incorporating measurements of the action spectra in predicted cnidarian photopigments, like opsins and cryptochromes, will certainly help determine their extraocular functionality.

Diel light cycles synchronize predictable patterns of behavior, physiology and gene expression, generating rhythmicity via two general processes: a direct response to light or through modulation by a molecular mechanism (i.e., a circadian clock). Broadly, the molecular basis for animal circadian clocks involves interlocked transcription-translation feedback loops with positive and negative elements (Dunlap, 1999). Through a combination of phylogenomics and light-dependent gene expression assays, Reitzel et al. (2013) proposed a model for the cnidarian circadian clock composed of two loops (Figure 6): the feedback loop where light dependent cryptochromes are involved in negative regulation of the CLOCK:CYCLE dimer and a feedforward loop where PAR-bZIPs activate and repress transcription of *clock* or *cycle* [as in *Drosophila*, see Cyran et al. (2003)]. In our study of light-dependent gene expression, we observed progressive loss of gene expression differences for these proposed clock components from blue to green to red light treatments. In blue light, components of each loop are differentially expressed in light:dark conditions suggesting robust diel gene expression for all genes, some of which have different phases (e.g., *nvPAR-bZIPa* and *nvPAR-bZIPc*). In green light, individual genes in each component (i.e., *nvPAR-bZIPc*, *nvClock*, *nvCry1a*) no longer showed significant differences in expression. However, anemones maintained rhythmic activity

with 24-hour periodicity. In red light, only *nvPAR-bZIPa* maintained differential gene expression in light:dark, which was restricted to just a narrow time comparison (early day vs early night). *nvCiPC* showed a similar pattern of light-dependent differential gene expression as *nvClock*, the protein that it regulates through phosphorylation in mammalian species (Yoshitane et al., 2009). *Timeout* (not shown in Figure 6) is a sister gene to *Timeless*, a critical component of the *Drosophila* circadian clock, but the role, if any, of *Timeout* in cnidarian clocks is unknown. In our study, *nvTimeout* showed diel expression only under red light, and was up-regulated during the day. In the facultatively symbiotic sea anemone, *Exaiptasia diaphana*, *Timeless* expression [*Timeout* in other cnidarians, see Reitzel et al. (2010)] was dependent on the presence or absence of symbionts and had a circatidal (12-hour) rhythmic expression in the absence of *Symbiodinium* (Sorek et al., 2018).

While we are unable to precisely determine if it is wavelength or intensity that impacts the oscillating organismal and molecular responses demonstrated here, behavioral studies in other cnidarians report similar light energies where light between 40 and 300 $\mu\text{mol}/\text{m}^2/\text{sec}^{-1}$ of photons elicits behavioral rhythmicity. For example, Levy et al. (2001) reported diel coral tentacle expansion occurring at intensities as low as 40 $\mu\text{mol}/\text{m}^2/\text{sec}^{-1}$ photons and Sorek et al. (2018) reported diel activity in the sea anemone *Aiptasia* (*Exaptasia*) *diaphana* in response to light at 70 $\mu\text{mol}/\text{m}^2/\text{sec}^{-1}$ photons, which are magnitudes lower than full spectrum light intensity. Although different species may respond to distinct intensities, we speculate the changes in activity in our study are likely due to discrepancies in wavelength, rather than intensity. One hypothesis for these shifts in global gene expression and differences in behavior under longer wavelengths (630 nm) and

lower intensity ($160\text{-}184 \mu\text{mol}/\text{m}^2/\text{sec}^{-1}$) is masking, where under typical daylight conditions, full spectrum illumination overrides or ‘masks’ other cues, eliminating the potential for differential wavelength- or intensity-dependent behaviors. The blue light responses commonly seen amongst cnidarians are likely due to the action of cryptochromes, opsins and/or rhodopsin (Arkett, 1989; Musio, 1997). Ours and other data lends support for *Nematostella* having maximal sensitivity in the 420-510 nm range, however we report a novel response to light near 630 nm that suggests the possibility of additional pigments or proteins capable of detecting low-intensity, higher-wavelengths may be present in this species.

In coastal habitats, organisms experience complex environmental signals including solar, lunar, and tidal cues. To accommodate this diverse set of potential cues, some marine invertebrates exhibit twice-daily oscillations in activity (Chabot et al., 2004; Last et al., 2009; Palmer, 2000) and have even evolved separate circadian and circatidal oscillators (Warman and Naylor, 1995; Zantke et al., 2013; Zhang et al., 2013). While no evidence to date has supported the presence of a circatidal clock in cnidarians, Hendricks et al. (2012) observed a similar twice daily activity pattern in *Nematostella* maintained in constant darkness similar to what we report in this study. Together, these results suggest the presence of a second oscillator within cnidarians, which may be masked by stronger competing entrainment cues. Deciphering between mechanisms of these two time keeping mechanisms would be an impactful area of future investigation, providing a novel evolutionary perspective on cnidarian clocks.

Conclusions

The data presented here contributes to our limited knowledge of non-visual photo behavior and gene expression in an eyeless cnidarian from an integrative organismal and molecular context. Combined with our report of differential transcriptomic responses to light spectra and intensity, these data support a hypothesis that *Nematostella* is capable of light entrainment in a broad range of wavelengths, despite lacking ocular photoreceptors, most notably in red light. Additionally, the activity profile of animals maintained in diel red light conditions suggests longer wavelengths may elicit circatidal behavior in this species. Future studies deciphering between wavelength-dependent or intensity-dependent responses in *Nematostella* would be informative to understanding if this species is capable of discriminating between discrete wavelengths.

Methods

Animal culture

Adult *Nematostella vectensis*, originally collected and outbred from Maryland (Putnam et al., 2007), were maintained in a laboratory setting as described in Hand & Uhlinger (1992). Sea anemones were kept in glass Pyrex dishes with 15 parts per thousand (ppt) artificial seawater (ASW). Individuals were fed haphazardly three days each week with freshly hatched brine shrimp (*Artemia sp.*) and the water was changed bi-weekly.

Experimental treatments

Animals were split into four experimental light treatment groups and culture conditions were adjusted to simulate a diel light cycle (12-hour light: 12-hour dark; LD) or constant darkness (DD) inside a light- and temperature-controlled room. For one

month, during the ‘entrainment period’, sea anemones were exposed to one of four isolated light treatments of different wavelengths using Minger LED strip lights: (i) red LD, (ii) green LD, (iii) blue LD, and (iv) 24-hour constant darkness. Light spectra were measured using a Qstick Subminiature Spectrometer (RGB Laser Systems) and light intensity was determined using a quantum scalar laboratory spherical radiometer (QSL-2100, Biospherical Instruments, Inc., San Diego, CA, USA). The irradiance of each light treatment ($\mu\text{mol photons m}^{-2}/\text{sec}^{-1}$) was measured from two locations within a single dish (Figure S1). Intensity of blue light in the range of 420-515 nm (peak at 450 nm) was measured at 396-401 $\mu\text{mol}/\text{m}^{-2}/\text{sec}^{-1}$ photons, intensity of green light ranging from 480-580 nm (peak at 510 nm) was 247-258 $\mu\text{mol}/\text{m}^{-2}/\text{sec}^{-1}$ photons, and the intensity of red light in the range of 600-650 nm (peak at 630 nm) was 169-184 $\mu\text{mol}/\text{m}^{-2}/\text{sec}^{-1}$ photons (Figure S1). For LD groups, light cycling began at 7:00 AM EST or Zeitgeber time (ZT) = 0 with “lights on”, and “lights off” at 7:00 PM EST or ZT = 12. During the entrainment period, animals were cultured on the same feeding and water change schedule as previous and care was taken for all groups during to limit stress to the animals. Animals in the DD group were fed and water changed during “lights off” to eliminate the potential for light contamination. All animals were starved for two days prior to data collection.

Behavioral assays and data analysis

Noldus Ethovision (Noldus Information Technology) was used to record and quantify the movement of sea anemones in each light condition independently. An infrared 850 nm 5050 LED strip light (Environmental Lights) was used to facilitate recordings in both light and dark conditions. For each experiment, animals were measured in individual glass petri (9 cm across) dishes with 50 mL ASW. Video

recordings were obtained for 12-16 animals in each light condition over 48 hours (n = 60), beginning at ZT = 0. Animals were not fed during data collection, and recording time was minimized to reduce the impact of starvation on the measurements.

Each video recording was analyzed using Noldus Ethovision XT9 with the area of each petri dish set as the 'tracking arena'. To avoid including light reflected off of the glass dish inside the tracking arena, all arenas were drawn with a 1 cm buffer from the edges of the dish (tracking arena area \square 50.27 cm²). In the case of animal movement into this region, the sample was discarded. Detection settings were set as follows: center-point detection, grey scaling (30-65), high pixel smoothing with contour erosion set to 1, and a sampling rate of 5.0 to ensure animal movement was detected throughout the collection period. Measurements of locomotion or 'distance traveled' in centimeters every 5 seconds was binned into hourly intervals (cm/hour) and analyzed with ClockLab software (Actimetrics).

Female populations were induced to spawn under red, green, and blue light cycles, following the animal care protocol outlined in Fritzenwanker & Technau (2002). Egg production was qualitatively recorded weekly to determine reproductive entrainment to individual wavelengths.

Wavelength experiment

For whole-organism gene expression analysis, animals were entrained in the same four experimental groups as described above for 1 month. After a starvation period of two days, individual sea anemones were sampled from each condition (4 biological replicates per time point) every 4 hours over 24 hours for a total of six timepoints (n = 96, replicates

were not pooled), beginning at ZT = 2. Samples were immediately preserved in RNAlater (Ambion) and stored at 4°C until processing.

Tag-based RNA library preparation, sequencing, and processing

Total RNA was isolated from 96 samples using the RNAqueous kit (Ambion) according to the manufacturer's protocol. Briefly, after pipetting off and discarding RNAlater from each sample, whole animals were lysed by pipetting in lysis buffer for <2 minutes, washed 2-3 times, and eluted on a column. Genomic DNA was removed using DNA-free kit (Invitrogen), and RNA was assessed using a NanoDrop 2000 spectrophotometer (Thermo Fisher Scientific). RNA was shipped for tag-based library preparation at the University of Texas at Austin's Genomic Sequencing and Analysis Facility (GSAF) as in Meyer et al. (2011) and adapted for Illumina HiSeq 2500. Briefly, total RNA was heat-fragmented and then reverse transcribed into first-strand cDNA. The cDNA was purified using AMPure beads, and PCR-amplified for 18 cycles. Unique Illumina barcodes were added in an additional PCR step for indexing of each sample. After an additional purification step, libraries were pooled, quality checked using a Bioanalyzer (Agilent), and size-selected using BluePippin (350-550bp fragments). Raw sequence data from 100 base paired, single-end reads were delivered from the UT Austin GSAF. Raw reads were trimmed and quality-filtered using the FastX-toolkit (Pearson et al., 1997). Trimmed reads were mapped against the *Nematostella* Vienna transcriptome using the Bowtie2 aligner (Langmead and Salzberg, 2012) and a read-counts-per-gene file was generated retaining only reads mapping to a single gene. Lastly, counts were imported into the R environment for all downstream statistical analysis (R3.5.0, R Core Team 2015). A

full version of the library preparation protocol and associated bioinformatic tools can be found at https://github.com/z0on/tag-based_RNAseq.

Gene expression analysis

Normalization and differential expression analysis of read counts was performed using the R package DESeq2 (Love et al., 2014). To enhance the rate of differential gene discovery, transcripts with low abundances (mean count <3) were independently filtered as per the DESeq2 pipeline described in Love et al. (2014). The arrayQualityMetrics package (Kauffmann et al., 2009) was used to detect outlier transcripts. DESeq2 normalized count data were regularized log transformed using the *rlog* function. Wald statistical tests were performed to identify diel transcription patterns in contrasts between all conditions and time points. P-values were Benjamini-Hochberg-adjusted to determine significance of contrasts (10% FDR cutoff). A rank-based gene ontology (GO) enrichment analysis was performed using signed, unadjusted log-transformed p-values (positive if up-regulated, negative if down-regulated) with the GO_MWU R package (https://github.com/z0on/GO_MWU) for all contrasts. We used the weighted correlation network analysis package in R to determine gene co-expression, using a soft threshold power of 11.5 (Langfelder and Horvath, 2008). Modules with expression patterns that were correlated greater than Pearson's $R > 0.45$ were merged and GO enrichment analysis was performed using a Fisher's exact test in the GO_MWU package. The R packages ggplot2 and pheatmap were used to generate graphs and heatmaps, respectively (Kolde, 2018; Wickham, 2009).

Acknowledgements

We would like to thank members of the Reitzel and Tarrant (WHOI) laboratories for discussions during the course of this study. We would also like to thank Misha Matz (UT Austin) for assistance with gene expression analyses. Finally, we would like to thank the handling editor and two anonymous reviewers for their many helpful suggestions that improved the originally submitted manuscript.

References

1. Abe, N. (1939). On the expansion and contraction of the polyp of a reef-coral, *Caulastraea furcata* Dana. Palao Tropical Biological Station Studies [Tokyo] 1, 651-669.
2. Anctil, M., Hayward, D. C., Miller, D. J. and Ball, E. E. (2007). Sequence and expression of four coral G protein-coupled receptors distinct from all classifiable members of the rhodopsin family. *Gene* 392, 14-21.
3. Arendt, D. (2003). Evolution of eyes and photoreceptor cell types. *International Journal of Developmental Biology* 47, 563-571.
4. Arendt, D., Tessmar, K., de Campos-Baptista, M. I. M., Dorresteyjn, A. and Wittbrodt, J. (2002). Development of pigment-cup eyes in the polychaete *Platynereis dumerilii* and evolutionary conservation of larval eyes in Bilateria. *Development* 129, 1143-1154.
5. Arkett, S. A. (1989). Hydromedusan photophysiology - an evolutionary perspective. *Evolution of the First Nervous Systems* 188, 373-392.
6. Artigas, G. Q., Lapebie, P., Leclere, L., Takeda, N., Deguchi, R., Jekely, G., Momose, T. and Houlston, E. (2018). A gonad-expressed opsin mediates light-induced spawning in the jellyfish *Clytia*. *Elife* 7.
7. Brady, A. K., Snyder, K. A. and Vize, P. D. (2011). Circadian cycles of gene expression in the coral, *Acropora millepora*. *PLoS ONE* 6, e25072.
8. Chabot, C. C., Kent, J. and Watson, W. H. (2004). Circatidal and circadian rhythms of locomotion in *Limulus polyphemus*. *Biological Bulletin* 207, 72-75.

9. Chaves, I., Pokorny, R., Byrdin, M., Hoang, N., Ritz, T., Brettel, K., Essen, L.-O., van der Horst, G. T. J., Batschauer, A. and Ahmad, M. (2011). The cryptochromes: blue light photoreceptors in plants and animals. *Annual Review of Plant Biology* 62, 335-364.
10. Cronin, T. W. and Caldwell, R. L. (2002). Tuning of photoreceptor function in three mantis shrimp species that inhabit a range of depths. II. Filter pigments. *Journal of Comparative Physiology a-Neuroethology Sensory Neural and Behavioral Physiology* 188, 187-197.
11. Cronin, T. W. and Porter, M. L. (2014). The evolution of invertebrate photopigments and photoreceptors. Boston, MA: Boston, MA: Springer US.
12. Cyran, S. A., Buchsbaum, A. M., Reddy, K. L., Lin, M.-C., Glossop, N. R. J., Hardin, P. E., Young, M. W., Storti, R. V. and Blau, J. (2003). Vrille, Pdp1, and dClock form a second feedback loop in the *Drosophila* circadian clock. *Cell* 112, 329-341.
13. Dunlap, J. C. (1999). Molecular bases for circadian clocks. *Cell* 96, 271-290.
14. Dupont, N., Klevjer, T., Kaartvedt, S. and Aksnes, D. (2009). Diel vertical migration of the deep-water jellyfish *Periphylla periphylla* simulated as individual responses to absolute light intensity. *Limnology and Oceanography* 54, 1765.
15. Endler, J. A. (1993). The color of light in forests and its implications. *Ecological Monographs* 63, 1-27.

16. Feuda, R., Hamilton, S. C., McInerney, J. O. and Pisani, D. (2012). Metazoan opsin evolution reveals a simple route to animal vision. *Proceedings of the National Academy of Sciences* 109, 18868-18872.
17. Foster, T. and Gilmour, J. P. (2016). Seeing red: Coral larvae are attracted to healthy-looking reefs. *Marine Ecology Progress Series* 559, 65-71.
18. Fox, H. M. (1932). Lunar periodicity in reproduction. *Nature* 130, 23-23.
19. Fritzenwanker, J. H. and Technau, U. (2002). Induction of gametogenesis in the basal cnidarian *Nematostella vectensis* (Anthozoa). *Development Genes Evolution*. 212.
20. Fukushiro, M., Takeuchi, T., Takeuchi, Y., Hur, S.-P., Sugama, N., Takemura, A., Kubo, Y., Okano, K. and Okano, T. (2011). Lunar phase-dependent expression of cryptochrome and a photoperiodic mechanism for lunar phase-recognition in a reef fish, goldlined spinefoot. *PLoS ONE* 6.
21. Garm, A., Bielecki, J., Petie, R. and Nilsson, D. E. (2016). Hunting in bioluminescent light: Vision in the nocturnal box jellyfish *Copula sivickisi*. *Frontiers in Physiology* 7.
22. Garm, A., Coates, M. M., Gad, R., Seymour, J. and Nilsson, D. E. (2007a). The lens eyes of the box jellyfish *Tripedalia cystophora* and *Chiropsalmus sp.* are slow and color-blind. *Journal of Comparative Physiology a-Neuroethology Sensory Neural and Behavioral Physiology* 193, 547-557.
23. Garm, A., Heddal, I., Islin, M. and Gurska, D. (2013). Pattern- and contrast-dependent visual response in the box jellyfish *Tripedalia cystophora*. *Journal of Experimental Biology* 216, 4520-4529.

24. Garm, A. and Mori, S. (2009). Multiple photoreceptor systems control the swim pacemaker activity in box jellyfish. *Journal of Experimental Biology* 212, 3951-3960.
25. Garm, A., O'Connor, M., Parkefelt, L. and Nilsson, D. E. (2007b). Visually guided obstacle avoidance in the box jellyfish *Tripedalia cystophora* and *Chiropsella bronzie*. *Journal of Experimental Biology* 210, 3616-3623.
26. Genikhovich, G. and Technau, U. (2009). Induction of spawning in the starlet sea anemone *Nematostella vectensis*, in vitro fertilization of gametes, and dejellying of zygotes. *Cold Spring Harbor protocols* 2009, pdb.prot5281-pdb.prot5281.
27. Gershwin, L.-A. and Dawes, P. (2008). Preliminary observations on the response of *Chironex fleckeri* (Cnidaria : Cubozoa : Chirodropida) to different colors of light. *Biological Bulletin* 215, 57-62.
28. Giese, A. C. (1959). Comparative physiology - Annual reproductive cycles of marine invertebrates. *Annual Review of Physiology* 21, 547-576.
29. Gladfelter, W. B. (1975). Sea-anemone with zooxanthellae - simultaneous contraction and expansion in response to changing light-intensity. *Science* 189, 570-571.
30. Gleason, D. F., Edmunds, P. J. and Gates, R. D. (2006). Ultraviolet radiation effects on the behavior and recruitment of larvae from the reef coral *Porites astreoides*. *Marine Biology* 148, 503-512.
31. Grant, R., Halliday, T. and Chadwick, E. (2013). Amphibians' response to the lunar synodic cycle-a review of current knowledge, recommendations, and implications for conservation. *Behavioral Ecology* 24, 53-62.

32. Grawunder, D., Hambleton, E. A., Bucher, M., Wolfowicz, I., Bechtoldt, N. and Guse, A. (2015). Induction of gametogenesis in the cnidarian endosymbiosis model *Aiptasia sp.* *Scientific Reports* 5.
33. Griffin, E., Staknis, A. and Weitz, C. J. (1999). Light-independent role of CRY1 and CRY2 in the mammalian circadian clock. *Science* 286, 768-771.
34. Hamner, W. M., Jones, M. S. and Hamner, P. P. (1995). Swimming, feeding, circulation and vision in the Australian box jellyfish, *Chiroaex fleckeri* (Cnidaria: Cubozoa). *Marine and Freshwater Research* 46, 985-990.
35. Hand, C. and Uhlinger, K. R. (1992). The culture, sexual and asexual reproduction, and growth of the sea anemone *Nematostella vectensis*. *Biological Bulletin* 182, 169-176.
36. Harrison, P. L., Babcock, R. C., Bull, G. D., Oliver, J. K., Wallace, C. C. and Willis, B. L. (1984). Mass spawning in tropical reef corals. *Science* 223, 1186-1189.
37. Hastings, M. H., Herbert, J., Martensz, N. D. and Roberts, A. C. (1985). Annual reproductive rhythms in mammals - mechanisms of light synchronization. *Annals of the New York Academy of Sciences* 453, 182-204.
38. Haug, M. F., Gesemann, M., Lazovic, V. and Neuhauss, S. C. F. (2015). Eumetazoan cryptochrome phylogeny and evolution. *Genome Biology and Evolution* 7, 601-619.
39. Hendricks, W. D., Byrum, C. A. and Meyer-Bernstein, E. L. (2012). Characterization of circadian behavior in the starlet sea anemone, *Nematostella vectensis*. *PLoS ONE* 7, e46843.

40. Hoadley, K. D., Szmant, A. M. and Pyott, S. J. (2011). Circadian clock gene expression in the coral *Favia fragum* over diel and lunar reproductive cycles. *PLoS ONE* 6, e19755.
41. Hoadley, K. D., Vize, P. D. and Pyott, S. J. (2016). Current understanding of the circadian clock within Cnidaria. In *The Cnidaria, Past, Present and Future: The world of Medusa and her sisters*, eds. S. Goffredo and Z. Dubinsky), pp. 511-520. Cham: Springer International Publishing.
42. Imamoto, Y. and Shichida, Y. (2014). Cone visual pigments. *Biochimica Et Biophysica Acta-Bioenergetics* 1837, 664-673.
43. Johnsen, S., Kelber, A., Warrant, E., Sweeney, A. M., Widder, E. A., Lee, R. L. and Hernandez-Andres, J. (2006). Crepuscular and nocturnal illumination and its effects on color perception by the nocturnal hawkmoth *Deilephila elpenor*. *Journal of Experimental Biology* 209, 789-800.
44. Kaartvedt, S., Klevjer, T. A., Torgersen, T., Sornes, T. A. and Rostad, A. (2007). Diel vertical migration of individual jellyfish (*Periphylla periphylla*). *Limnology and Oceanography* 52, 975-983.
45. Kanaya, H. J., Kobayakawa, Y. and Itoh, T. Q. (2019). *Hydra vulgaris* exhibits day-night variation in behavior and gene expression levels. *Zoological Letters* 5.
46. Kaniewska, P., Alon, S., Karako-Lampert, S., Hoegh-Guldberg, O. and Levy, O. (2015). Signaling cascades and the importance of moonlight in coral broadcast mass spawning. *Elife* 4.

47. Kauffmann, A., Gentleman, R. and Huber, W. (2009). arrayQualityMetrics--a bioconductor package for quality assessment of microarray data. *Bioinformatics* (Oxford, England) 25, 415-6.
48. Kim, S., Lee, K., Yoon, W. D., Lee, H. and Hwang, K. (2016). Vertical distribution of giant jellyfish, *Nemopilema nomurai* using acoustics and optics. *Ocean Science Journal* 51, 59-65.
49. Kolde, R. (2018). Pretty Heatmaps. Comprehensive R Archive Network.
50. Koyanagi, M., Takano, K., Tsukamoto, H., Ohtsu, K., Tokunaga, F. and Terakita, A. (2008). Jellyfish vision starts with cAMP signaling mediated by opsin-Gs cascade. *Proceedings of the National Academy of Sciences, USA* 105, 15576-15580.
51. Kume, K., Zylka, M. J., Sriram, S., Shearman, L. P., Weaver, D. R., Jin, X., Maywood, E. S., Hastings, M. H. and Reppert, S. M. (1999). mCRY1 and mCRY2 are essential components of the negative limb of the circadian clock feedback loop. *Cell* 98, 193-205.
52. Langfelder, P. and Horvath, S. (2008). WGCNA: an R package for weighted correlation network analysis. *BMC Bioinformatics* 9, 13.
53. Langmead, B. and Salzberg, S. L. (2012). Fast gapped-read alignment with Bowtie 2. *Nature Methods* 9, 357-U54.
54. Lapan, S. W. and Reddien, P. W. (2011). dlx and sp6-9 control optic cup regeneration in a prototypic eye. *PLoS Genetics* 7.

55. Last, K. S., Bailhache, T., Kramer, C., Kyriacou, C. P., Rosato, E. and Olive, P. J. W. (2009). Tidal, daily, and lunar-day activity cycles in the marine polychaete *Nereis virens*. *Chronobiology International* 26, 167-183.
56. Leach, W. B., Macrander, J., Peres, R. and Reitzel, A. M. (2018). Transcriptome-wide analysis of differential gene expression in response to light:dark cycles in a model cnidarian. *Comparative Biochemistry and Physiology Part D: Genomics and Proteomics* 26, 40-49.
57. Leach, W. B. and Reitzel, A. M. (2019). Transcriptional remodeling upon light removal in a model cnidarian: losses and gains in gene expression. *Molecular Ecology*.
58. Levy, O., Appelbaum, L., Leggat, W., Gothliff, Y., Hayward, D. C., Miller, D. J. and Hoegh-Guldberg, O. (2007). Light-responsive cryptochromes from a simple multicellular animal, the coral *Acropora millepora*. *Science* 318, 467-470.
59. Levy, O., Dubinsky, Z. and Achetuv, Y. (2003). Photobehavior of stony corals: responses to light spectra and intensity. *Journal of Experimental Biology* 206, 4041-4049.
60. Levy, O., Mizrahi, L., Chadwick-Furman, N. E. and Achetuv, Y. (2001). Factors controlling the expansion behavior of *Favia favaus* (Cnidaria : Scleractinia): Effects of light, flow, and planktonic prey. *Biological Bulletin* 200, 118-126.
61. Lewis, J. B. and Price, W. S. (1975). Feeding mechanisms and feeding strategies of Atlantic reef corals. *Journal of Zoology* 176, 527-544.
62. Love, M. I., Huber, W. and Anders, S. (2014). Moderated estimation of fold change and dispersion for RNA-seq data with DESeq2. *Genome Biology* 15.

63. Maas, A. E., Jones, I. T., Reitzel, A. M. and Tarrant, A. M. (2016). Daily cycle in oxygen consumption by the sea anemone *Nematostella vectensis* Stephenson. *Biology Open* 5, 161.
64. Martin, V. J. (2002). Photoreceptors of cnidarians. *Canadian Journal of Zoology* 80, 1703-1722.
65. Martin, V. J. (2004). Photoreceptors of cubozoan jellyfish. *Hydrobiologia* 530, 135-144.
66. Mason, B., Beard, M. and Miller, M. W. (2011). Coral larvae settle at a higher frequency on red surfaces. *Coral Reefs* 30, 667-676.
67. Mason, B., Schmale, M., Gibbs, P., Miller, M. W., Wang, Q., Levay, K., Shestopalov, V. and Slepak, V. Z. (2012). Evidence for multiple phototransduction pathways in a reef-building coral. *PLoS ONE* 7, e50371.
68. Mason, B. M. and Cohen, J. H. (2012). Long-wavelength photosensitivity in coral planula larvae. *Biological Bulletin* 222, 88-92.
69. Mehra, A., Baker, C. L., Loros, J. J. and Dunlap, J. C. (2009). Post-translational modifications in circadian rhythms. *Trends in Biochemical Sciences* 34, 483-490.
70. Mei, Q. M. and Dvornyk, V. (2015). Evolutionary history of the photolyase/cryptochrome superfamily in eukaryotes. *PLoS ONE* 10.
71. Meyer, E., Aglyamova, G. V. and Matz, M. V. (2011). Profiling gene expression responses of coral larvae (*Acropora millepora*) to elevated temperature and settlement inducers using a novel RNA-Seq procedure. *Molecular Ecology* 20, 3599-3616.

72. Mills, C. E. (1983). Vertical migration and diel activity patterns of hydromedusae - studies in a large tank. *Journal of Plankton Research* 5, 619-635.
73. Mundy, C. N. and Babcock, R. C. (1998). Role of light intensity and spectral quality in coral settlement: Implications for depth-dependent settlement? *Journal of Experimental Marine Biology and Ecology* 223, 235-255.
74. Musio, C. (1997). Extraocular photosensitivity in invertebrates: A look into functional mechanisms and biophysical processes. *Biophysics of Photoreception: Molecular and Phototransductive Events* 1, 245-262.
75. Nilsson, D. E. (2009). The evolution of eyes and visually guided behaviour. *Philosophical Transactions of the Royal Society B-Biological Sciences* 364, 2833-2847.
76. Oldach, M. J., Workentine, M., Matz, M. V., Fan, T. Y. and Vize, P. D. (2017). Transcriptome dynamics over a lunar month in a broadcast spawning acroporid coral. *Molecular Ecology* 26, 2514-2526.
77. Oliveri, P., Fortunato, A. E., Petrone, L., Ishikawa-Fujiwara, T., Kobayashi, Y., Todo, T., Antonova, O., Arboleda, E., Zantke, J., Tessmar-Raible, K. et al. (2014). The cryptochrome/photolyase family in aquatic organisms. *Marine Genomics* 14, 23-37.
78. Oren, M., Tarrant, A. M., Alon, S., Simon-Blecher, N., Elbaz, I., Appelbaum, L. and Levy, O. (2015). Profiling molecular and behavioral circadian rhythms in the non-symbiotic sea anemone *Nematostella vectensis*. *Scientific Reports* 5, 11418.
79. Palmer, J. D. (2000). The clocks controlling the tide-associated rhythms of intertidal animals. *Bioessays* 22, 32-37.

80. Passano, L. M. and McCullough, C. B. (1963). Pacemaker hierarchies controlling behaviour of hydras. *Nature* 199, 1174-&.
81. Pearse, V. B. (1974). Modification of sea anemone behavior by symbiotic zooxanthellae: phototaxis. *Biological Bulletin* 147, 630-640.
82. Pearson, W. R., Wood, T., Zhang, Z. and Miller, W. (1997). Comparison of DNA sequences with protein sequences. *Genomics* 46, 24-36.
83. Peres, R., Reitzel, A. M., Passamaneck, Y., Afeche, S. C., Cipolla-Neto, J., Marques, A. C. and Martindale, M. Q. (2014). Developmental and light-entrained expression of melatonin and its relationship to the circadian clock in the sea anemone *Nematostella vectensis*. *EvoDevo* 5, 26.
84. Picciani, N., Kerlin, J. R., Sierra, N., Swafford, A. J. M., Ramirez, M. D., Roberts, N. G., Cannon, J. T., Daly, M. and Oakley, T. H. (2018). Prolific origination of eyes in cnidaria with co-option of non-visual opsins. *Current Biology* 28, 2413-+.
85. Plachetzki, D. C., Degnan, B. M. and Oakley, T. H. (2007). The origins of novel protein interactions during animal opsin evolution. *PLoS ONE* 2, e1054.
86. Plachetzki, D. C., Fong, C. R. and Oakley, T. H. (2010). The evolution of phototransduction from an ancestral cyclic nucleotide gated pathway. *Proceedings of the Royal Society B-Biological Sciences* 277, 1963-1969.
87. Plachetzki, D. C., Fong, C. R. and Oakley, T. H. (2012). Cnidocyte discharge is regulated by light and opsin-mediated phototransduction. *BMC Biology* 10.
88. Putnam, N. H., Srivastava, M., Hellsten, U., Dirks, B., Chapman, J., Salamov, A., Terry, A., Shapiro, H., Lindquist, E., Kapitonov, V. V. et al. (2007). Sea anemone

genome reveals ancestral eumetazoan gene repertoire and genomic organization. *Science* 317.

89. Ramirez, M. D., Pairett, A. N., Pankey, M. S., Serb, J. M., Speiser, D. I., Swafford, A. J. and Oakley, T. H. (2016). The last common ancestor of most bilaterian animals possessed at least nine opsins. *Genome Biology and Evolution* 8, 3640-3652.
90. Reitzel, A. M., Behrendt, L. and Tarrant, A. M. (2010). Light entrained rhythmic gene expression in the sea anemone *Nematostella vectensis*: the evolution of the animal circadian clock. *PLoS ONE* 5, e12805.
91. Reitzel, A. M., Tarrant, A. M. and Levy, O. (2013). Circadian clocks in the cnidaria: environmental entrainment, molecular regulation, and organismal outputs. *Integrative and Comparative Biology* 53, 118-30.
92. Rivera, A. S., Ozturk, N., Fahey, B., Plachetzki, D. C., Degnan, B. M., Sancar, A. and Oakley, T. H. (2012). Blue-light-receptive cryptochrome is expressed in a sponge eye lacking neurons and opsin. *The Journal of Experimental Biology* 215, 1278-1286.
93. Saunders, D. (2008). Photoperiodism in insects and other animals. *Photobiology: The Science of Life and Light*, Second Edition, 389-416.
94. Schnitzler, C. E., Pang, K., Powers, M. L., Reitzel, A. M., Ryan, J. F., Simmons, D., Tada, T., Park, M., Gupta, J., Brooks, S. Y. et al. (2012). Genomic organization, evolution, and expression of photoprotein and opsin genes in *Mnemiopsis leidyi*: a new view of ctenophore photocytes. *BMC Biology* 10, 107-107.

95. Schuyler, Q. and Sullivan, B. K. (1997). Light responses and diel migration of the scyphomedusa *Chrysaora quinquecirrha* in mesocosms. *Journal of Plankton Research* 19, 1417-1428.
96. Sebens, K. P. and DeRiemer, K. (1977). Diel cycles of expansion and contraction in coral reef anthozoans. *Marine Biology* 43, 247-256.
97. Shichida, Y. and Matsuyama, T. (2009). Evolution of opsins and phototransduction. *Philosophical Transactions of the Royal Society of London, Series B: Biological Sciences* 364, 2881-2895.
98. Shoguchi, E., Tanaka, M., Shinzato, C., Kawashima, T. and Satoh, N. (2013). A genome-wide survey of photoreceptor and circadian genes in the coral, *Acropora digitifera*. *Gene* 515, 426-31.
99. Sorek, M., Schnytzer, Y., Ben-Asher, H. W., Caspi, V. C., Chen, C. S., Miller, D. J. and Levy, O. (2018). Setting the pace: host rhythmic behaviour and gene expression patterns in the facultatively symbiotic cnidarian *Aiptasia* are determined largely by *Symbiodinium*. *Microbiome* 6, 12.
100. Stewart, S. E. (1996). Field behavior of *Tripedalia cystophora* (class Cubozoa). *Zooplankton: sensory ecology and physiology.*, 511-524.
101. Strader, M. E., Davies, S. W. and Matz, M. V. (2015). Differential responses of coral larvae to the colour of ambient light guide them to suitable settlement microhabitat. *Royal Society Open Science* 2.
102. Suga, H., Schmid, V. and Gehring, W. J. (2008). Evolution and functional diversity of jellyfish opsins. *Current Biology* 18, 51-5.

103. Takeuchi, Y., Kabutomori, R., Yamauchi, C., Miyagi, H., Takemura, A., Okano, K. and Okano, T. (2018). Moonlight controls lunar-phase-dependency and regular oscillation of clock gene expressions in a lunar-synchronized spawner fish, Goldlined spinefoot. *Scientific Reports* 8.
104. Thumann, G., Dou, G., Wang, Y. and Hinton, D. R. (2013). Cell biology of the retinal pigment epithelium.
105. Vigh, B., Manzano, M. J., Zadori, A., Frank, C. L., Lukats, A., Rohlich, P., Szel, A. and David, C. (2002). Nonvisual photoreceptors of the deep brain, pineal organs and retina. *Histology and Histopathology* 17, 555-590.
106. Wang, W. J., Geiger, J. H. and Borhan, B. (2014). The photochemical determinants of color vision. *Bioessays* 36, 65-74.
107. Warman, C. G. and Naylor, E. (1995). Evidence for multiple, cue-specific circatidal clocks in the shore crab *Carcinus maenas*. *Journal of Experimental Marine Biology and Ecology* 189, 93-101.
108. Wickham, H. (2009). ggplot2.
109. Wolken, J. J. and Mogus, M. A. (1981). Extraocular photoreception. *Photochemical and Photobiological Reviews* 6, 181-199.
110. Wolstenholme, J., Nozawa, Y., Byrne, M. and Burke, W. (2018). Timing of mass spawning in corals: potential influence of the coincidence of lunar factors and associated changes in atmospheric pressure from northern and southern hemisphere case studies. *Invertebrate Reproduction & Development* 62, 98-108.

111. Yoshitane, H., Takao, T., Satomi, Y., Du, N. H., Okano, T. and Fukada, Y. (2009). Roles of CLOCK phosphorylation in suppression of E-box-dependent transcription. *Molecular and Cellular Biology* 29, 3675-3686.
112. Yuan, Q., Metterville, D., Briscoe, A. D. and Reppert, S. M. (2007). Insect cryptochromes: gene duplication and loss define diverse ways to construct insect circadian clocks. *Molecular Biology and Evolution* 24, 948-955.
113. Zantke, J., Ishikawa-Fujiwara, T., Arboleda, E., Lohs, C., Schipany, K., Hallay, N., Straw, Andrew D., Todo, T. and Tessmar-Raible, K. (2013). Circadian and circalunar clock interactions in a marine annelid. *Cell Reports* 5, 99-113.
114. Zhang, L., Hastings, M. H., Green, E. W., Tauber, E., Sladek, M., Webster, S. G., Kyriacou, C. P. and Wilcockson, D. C. (2013). Dissociation of circadian and circatidal timekeeping in the marine crustacean *Eurydice pulchra*. *Current Biology* 23, 1863-1873.
115. Zhu, H., Sauman, I., Yuan, Q., Casselman, A., Emery-Le, M., Emery, P. and Reppert, S. M. (2008). Cryptochromes define a novel circadian clock mechanism in monarch butterflies that may underlie sun compass navigation. *PLoS Biology* 6, e4.
116. Zhu, H., Yuan, Q., Froy, O., Casselman, A. and Reppert, S. M. (2005). The two CRYs of the butterfly. *Current Biology* 15, R953-R954.

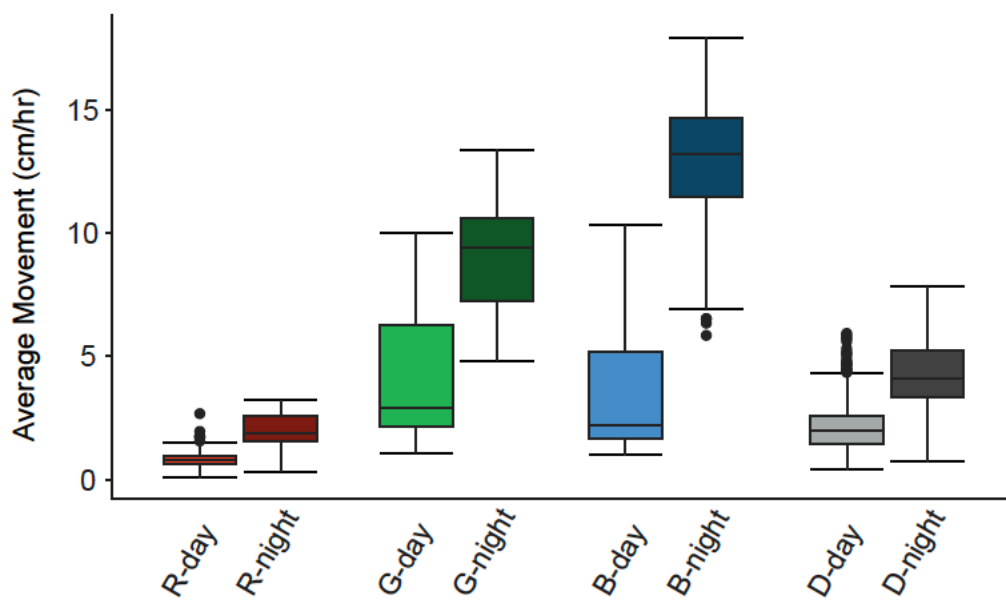


Figure 1. Average locomotive activity (cm/hr) of *Nematostella vectensis* during the photoperiod (light bars, left) versus scotoperiod (dark bars, right) over 48 hours in each light condition (R – red, G – green, B – blue, D – dark). All comparisons between photoperiod and scotoperiod of each color and within colors were significant (two-way ANOVA with Tukey post hoc tests). All statistical values for pairwise comparisons can be found in Table S1.

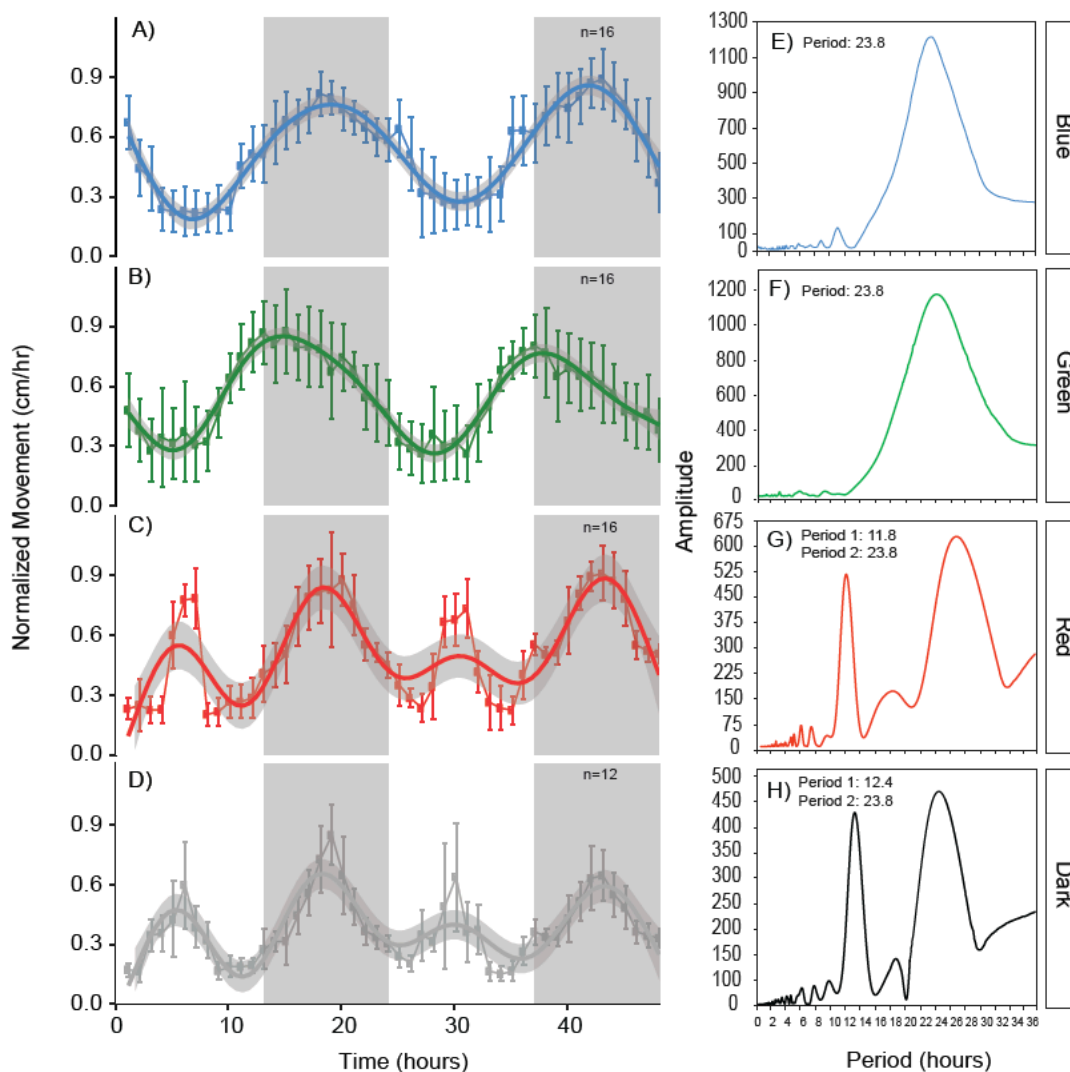


Figure 2. Normalized locomotive activity patterns of *Nematostella vectensis* over time (left panel) in A) blue light:dark conditions, B) green light:dark conditions, C) red light:dark conditions, and D) constant dark:dark conditions. The 48-hour time course is indicated by the x-axis, and normalized movement (cm/hr) on the y-axis of the left panel behavioral plots. White and grey boxes in the plot area indicate the light:dark cycle, or the photoperiod and scotoperiod of the time course, respectively. Each data point on the behavioral plots represent n replicates ($n_{\text{blue}} = 16$; $n_{\text{green}} = 16$, $n_{\text{red}} = 16$; $n_{\text{dark}} = 12$). The right panel (E-H) shows periodograms corresponding to each color (annotated in the far-right box) using Chi-square analysis from activity data for n individuals in each light condition (confidence interval < 0.01). Periodicity values are reported in the top left corner of each graph.

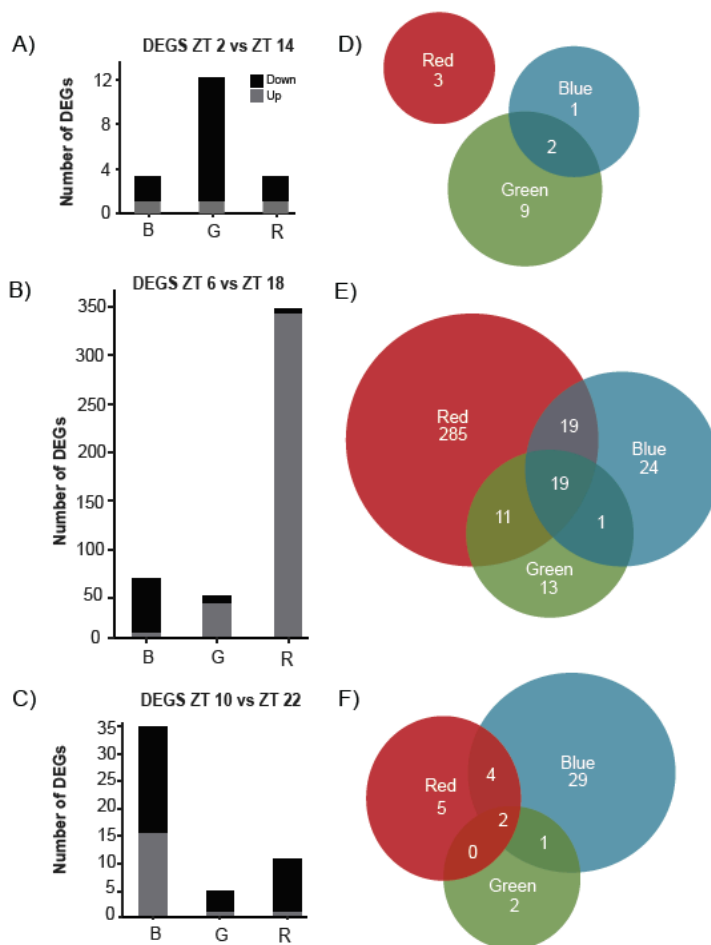


Figure 3. Time-of-day and wavelength-dependent differential gene expression analysis of *Nematostella vectensis*. A-C) Counts of differentially expressed (DE) genes between the day (ZT = 2, 6, 10) and night (ZT = 14, 18, 22) timepoints in each light treatment (B – blue, G – green, R – red). Up- and down-regulated genes with respect to the photoperiod are shown with black (down-regulated) and grey (up-regulated) bars (i.e., if up-regulated, genes are up during the photoperiod compared to the scotoperiod). D-F) Venn diagrams of DE genes shared between each light condition. No genes were differentially expressed between the different color light conditions and constant dark conditions; thus, they are not represented in this figure.

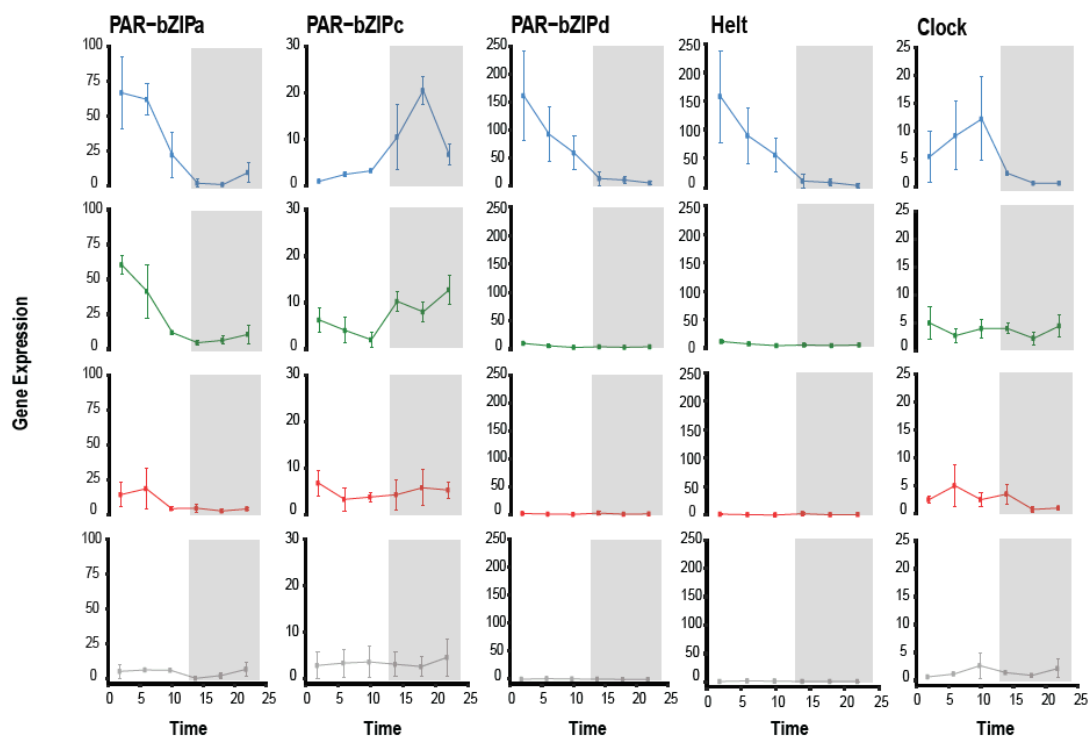


Figure 4. *Nematostella vectensis* candidate circadian gene profiles over the 24-hour sequencing time course, organized by gene and color. Each vertical set of plots represents a single gene's expression in each light condition in the following order: blue, green, red, dark. Data points on each plot represent four individually sequenced animals. Error bars are calculated from the standard error of the mean for each data point (n=4). The time course of the experiment is shown along the x-axis, and the normalized expression values are shown along the y-axis. Note the scale is the same for each light condition of a specific gene, but the scales differ across genes. White and grey boxes in the plot area indicate the light:dark cycle, or the photoperiod and scotoperiod of the time course, respectively. All statistical values for comparisons can be found in Table S5.

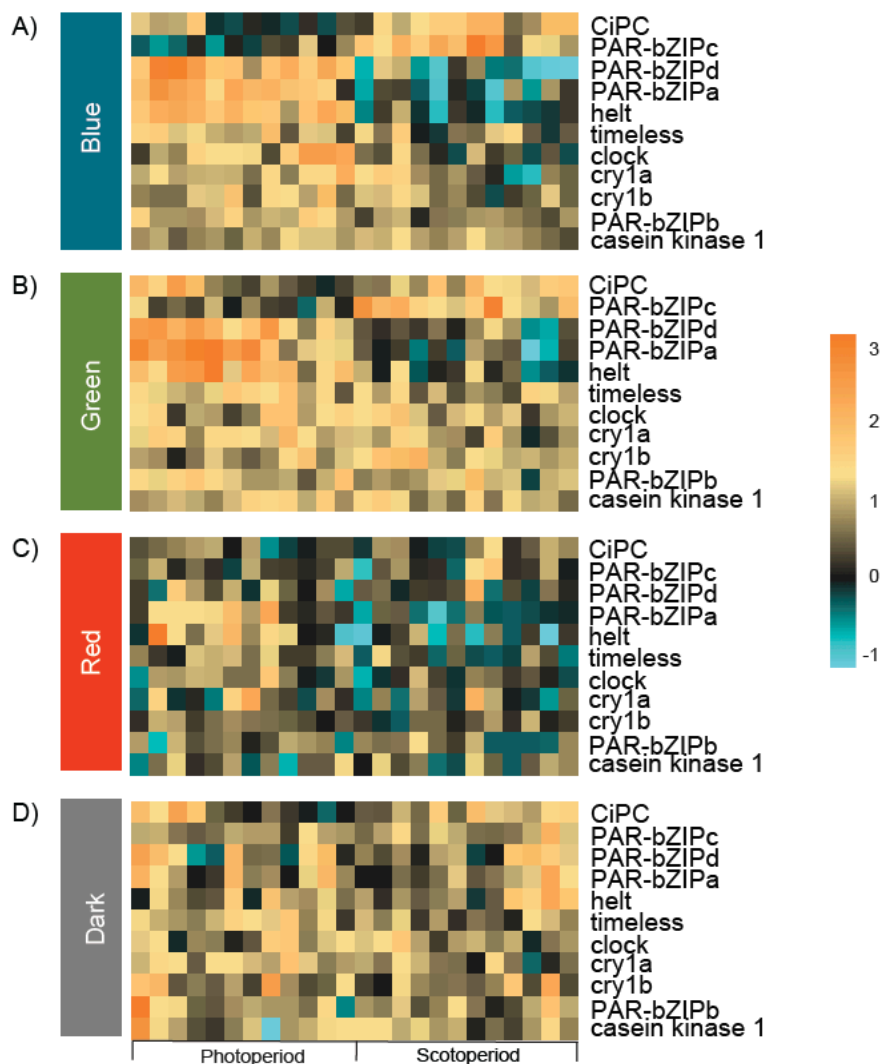


Figure 5. Heatmap of *Nematostella vectensis* candidate circadian genes across each light treatment A) blue, B) green, C) red, D) dark. The experiment key at the bottom of the lower heatmap identifies the ‘photoperiod’ and ‘scotoperiod’ sampling points of the 24-hour time course. Columns of each heatmap represent the replicate samples obtained every 4 hours during the time course. Each row of the heatmaps shows expression of a single annotated gene, labelled on the right. The color scale is log₂ fold change.

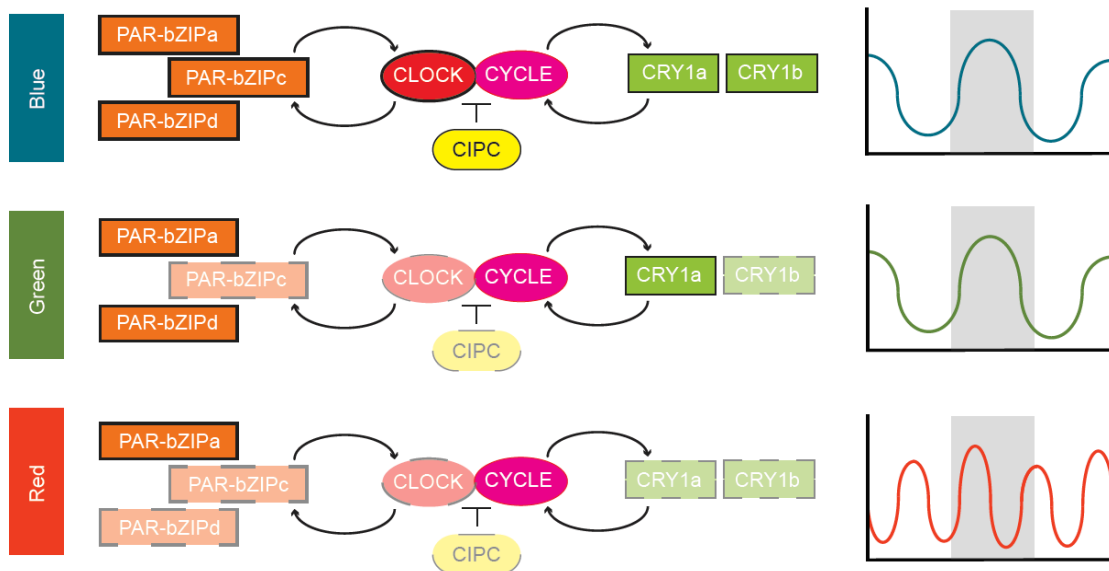
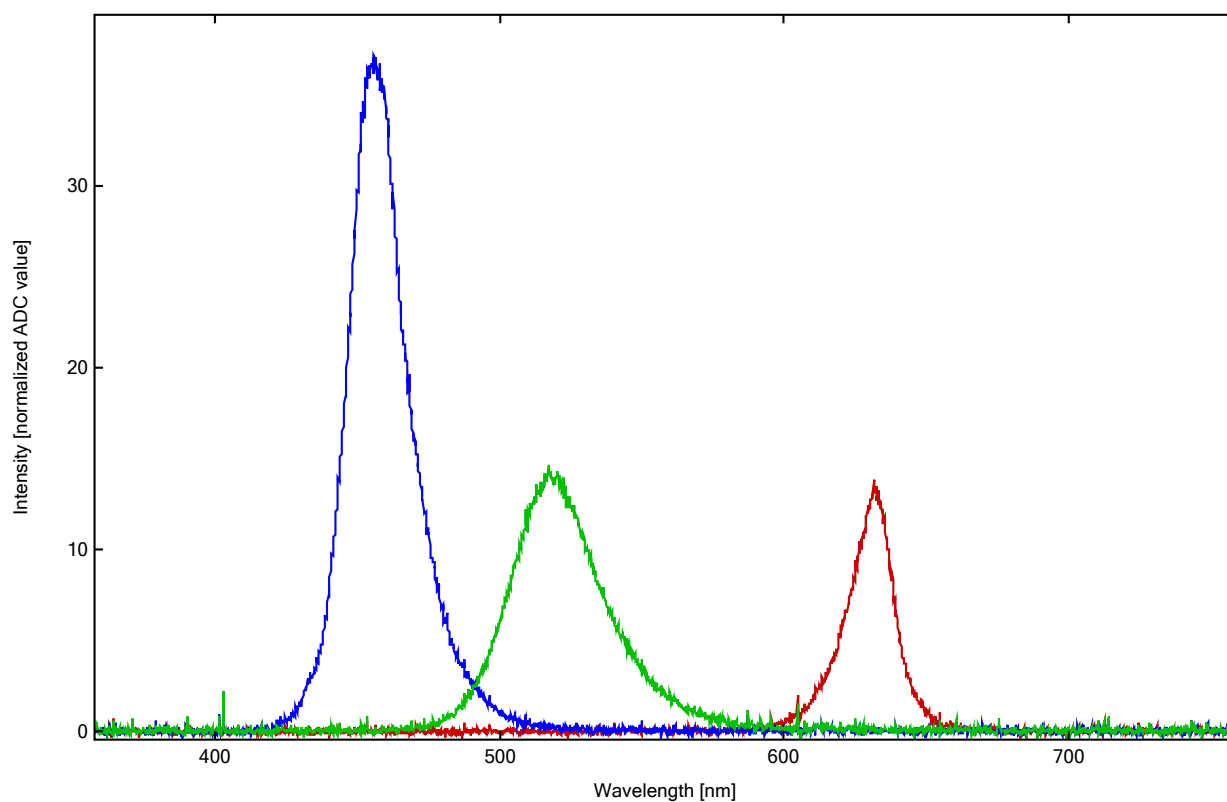
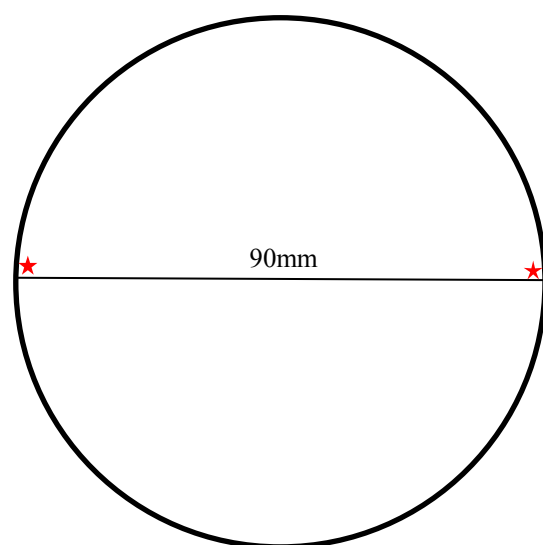


Figure 6. Proposed model for the cnidarian circadian clock composed of two loops adapted from Reitzel et al. (2013) and associated behavior. This proposed network combines the positive elements (center), the feed-forward loop (left), and the feedback loop (right). The positive elements, Clock and Cycle heterodimerize (CLOCK:CYCLE) and upregulate genes in the feed-forward and feedback loops (PAR-bZIPs and cryptochromes, respectively) where they act as transcriptional regulators for the positive elements. CIPIC is a predicted repressor of the CLOCK:CYCLE protein complex based on data from vertebrates. Differential expression (DE) of genes in this network are indicated with solid (DE) or dashed (not DE) lines for each color (key far left). Cycle is not outlined because this gene was not differentially expressed in any condition. Plots of behavioral responses to each wavelength are shown on the far right as cartoons.

A.



B.



	Outer	Inner
Blue	3.96-4.01	4.07-4.10
Green	2.47-2.55	2.54-2.58
Red	1.69-1.80	1.81-1.84

Figure S1. A. Light spectra intensity and energy values from the experimental treatments used in this study. Spectra were determined using a Qstick Subminiature Spectrometer (RGB Laser Systems). B. Energy values were determined using a radiometer (QSL 2100, Biospherical Instruments Inc.) at two positions in a 90mm petri dish, on the inner (left star) and outer (right star) edges. Measurements are in $\mu\text{mol}/\text{cm}^2/\text{sec}$ of photons.

CHAPTER 3

TEMPORAL SINGLE CELL GENE EXPRESSION OF *NEMATOSTELLA VECTENSIS*

Whitney B. Leach, Flora Plessier, Yann Loe-Mie, Heather Marlow, and Adam M. Reitzel

Abstract

Vertebrate and insect circadian clocks are driven by a master regulator in specialized brain neurons which coordinate timing of rhythms in peripheral tissues, which may have their own version of an oscillator. The extent of shared mechanisms for circadian clock regulation in these peripheral clocks for different animal tissues and their relationship to the central clock in the brain is an area of active investigation. In organisms without a cephalized nervous system, circulatory system or distinct organs, the molecular components for circadian coordination is even more poorly understood. Here, we report a comparative analysis of circadian transcript expression in three predominant cell types (neurons, gland cells, epithelial cells) in the cnidarian *Nematostella vectensis* in light:dark cycles. We find a total of 136 cycling transcripts overall all cell types, with overlap of only two genes, *nvClock* and *nvCIPC*, for all the three cell types. Circadian expression of cryptochromes was restricted to neural cells, and PAR-bZIP transcription factor expression was restricted to neural and gland cells.

Introduction

Circadian clocks in animals are composed of transcription-translation feedback loops that generate self-sustaining oscillations such that organisms can anticipate daily events (reviewed in Dunlap, 1999). In mammals, the central circadian pacemaker is

found within the suprachiasmatic nucleus (SCN) of the hypothalamus. Cells within the SCN are directly entrained by light input from the retina and can maintain a self-sustaining, free-running rhythm. In contrast, clocks in peripheral tissues, such as the liver, skeletal muscles, and adipose tissues (Zhang et al., 2014), exhibit rhythmic oscillations that peak at different times of day and typically degrade without entrainment by the SCN or environmental cues, which could be abiotic factors as well as microorganisms. The central pacemaker primarily functions to synchronize peripheral clocks located throughout the body by stimulating production of signaling molecules, particularly melatonin (Buijs et al., 2016; Mohawk et al., 2012). Similarly, in *Drosophila*, the pacemaker is composed of ~150 clock neurons within the brain (Helfrich-Förster, 2005) that coordinates rhythmic oscillations in peripheral tissues, such as the fat body (Xu et al., 2011). Thus, within diverse animal models, organs and tissues comprise a hierarchically structured circadian network where central regulators composed of a few cells, like the SCN, regulate the internal clock and signal peripheral clocks to synchronize outputs (Akhtar et al., 2001; Dibner et al., 2010). In addition, peripheral clocks may signal back to the central clock with information regarding tissue- or organ-specific information.

Tissue specificity in circadian regulation has been previously studied in both vertebrate and insect models (e.g., Agrawal et al., 2017; Meireles-Filho et al., 2014; Salgado-Delgado et al., 2013). Peripheral clocks vary both in their sensitivity to entraining cues as well as the downstream genes and processes that they regulate. Direct entrainment by light has been described in mammalian retina, zebrafish heart and kidney, and several *Drosophila* tissues (Agrawal et al., 2017; Tosini and Menaker, 1996; Whitmore et al., 2000). In mammals, the peripheral clocks of different tissues appear to utilize unique

combinations of about 20 transcriptional regulators in the central circadian clock with expression in different phases (Ukai and Ueda, 2010). Phase differences are explained, in part, by the contribution of particular activating and inhibitory components (the feedback loops) of each cell type's clock. The recruitment of different parts of the gene network for these individual clocks provide a mechanism how clock controlled genes (CCGs) can have different rhythmicity in particular tissues (Pett et al., 2018). Moreover, neuroendocrine and metabolic signals can impact the phase and amplitude of the clock in certain tissues in unique ways, which further complicates the relative roles for intracellular and extracellular factors in the entrainment of different tissues. For example, tissue-specific rhythms in both transcription factor activity and binding to distal enhancers are synchronized by periodic feeding in mouse liver and sodium homeostasis in the kidney (Yeung et al., 2018).

Beyond these traditional model animals, studies from an increasing number of invertebrate species (e.g., Kaiser et al., 2016; Perrigault and Tran, 2017; Zantke et al., 2013), including cnidarians (Hoadley et al., 2016; Reitzel et al., 2013b), have resulted in a deeper understanding of the conservation of the core mechanisms of the circadian circuitry in animals. These studies have also shown that organisms entrain to diverse environmental cues (e.g., tidal rhythm, temperature) that are hypothesized to utilize a similar gene network. *Nematostella vectensis*, an estuarine anemone, has emerged as a cnidarian model system for characterizing the evolution and expression of the circadian clock. To date, studies of rhythmic gene expression in light-entraining conditions have relied upon whole animal homogenates from different time points to identify genes with potential roles in diel behavior and physiology. This approach has identified a number of concordant gene expression patterns suggestive of a conserved role for particular

transcription factors and light-sensitive proteins in the cnidarian-bilaterian clockwork. However, studies from bilaterians have clearly shown tissue specificity of circadian clock rhythms and the genes involved (see above), which could be easily obscured when looking at all animal tissues and cell types in one sample. Here, we compared transcriptome-wide gene expression for three common cell types in *Nematostella* to determine how gene expression varies during a diel lighting environment for each cell type to identify similar and unique patterns. Because anemones have a tissue-grade level of organization, our results are particularly insightful for isolating the role of external cues on the entrainment of cell-specific clocks that will be informative to understand the complexities of the hierarchical signaling in mammalian and insect species.

Materials and Methods

Transgenesis for cell/tissue-specific markers

To facilitate isolation of specific cell and tissue types, we generated transgenic *Nematostella* expressing Kikume reporter under the control of the predicted promoters for a gland cell subpopulation specific gene (JGI v1g199428, Vienna NVE4653), referred to here as Gd2) and an ectodermal epithelium marker (Ep3K) (Vienna model ID NVE17842). The regions of the promoter were amplified from genomic DNA using locus specific primers (all primers provided in Supplemental Table 1.3) and then inserted in a construct (pNvT-MHC::mCH plasmid) reported in Renfer et al. (2010) where the mCherry reporter was replaced with the KikGR reporter (Nowotschin and Hadjantonakis, 2009), from the pCAG:KikGR plasmid, donated from Anna-Katerina Hadjantonakis (Addgene plasmid # 32608; <http://n2t.net/addgene:32608> ; RRID:Addgene_32608). The

constructs were injected into 1-cell stage embryos with the yeast meganuclease I-SceI (New England Biolabs) to facilitate genomic integration (Renfer et al., 2010). Following germline integration, stable transgenic animals were visualized under an Axio Imager Z1. Transgenic *Nematostella* expressing mOrange under the control of the ELAV promoter NvElav1::mOrange that labels a subset of neurons were reported in a previous publication (Nakanishi et al., 2012). These animals were generously donated by the Rentzsch lab (SARS, Norway).

Animal culturing and sampling

Juvenile transgenic *Nematostella* from each line were cultured in finger bowls under a 12 hour light : 12 hour dark (here after, LD) at 25°C in temperature controlled incubators (HerpNursery). Illumination was provided by full spectrum LED lights (Minger). Anemones were fed freshly hatched *Artemia* nauplii 5 times a week at ZT = 14 and cleaned weekly during their light period for 3weeks. Feeding ceased 2 days prior to experimental sampling. Single polyps from the Gd2 and Ep3K transgenic lines and two polyps from the ELAV transgenic line were dublicately sampled every four hours for 48 hours and immediately transferred to low-binding Eppendorf tubes containing fresh 13.5ppt Ca²⁺/Mg²⁺-free artificial seawater (CMFSW) for cell dissociation. A total of 48 individuals from the ELAV transgenic line were collected (n=2 pooled individuals * 12 time points * 2 biological replicates), and a total of 24 individuals each from the Gd2_v1g199428_KikGR and Ep3K transgenic lines were collected (n=1 individual * 12 timepoints * 2 biological replicates).

Tissue processing, cell sorting, and MARS-seq

Immediately following sampling, anemones were processed for cell sorting and sequence-library preparation as previously reported (Sebé-Pedrós et al., 2018). Briefly, cells were dissociated with gelatin-coated pipette tips for ~20 minutes using Liberase TM (Roche, 05401119001). Dissociation was halted by adding 1/10th volume of 500mM EDTA, and placed into fresh 13.5ppt CMFSW, followed by the addition of a 2X master mix solution of CMFSW, Calcein AM Violet (Life Technologies, C34858) final concentration, and SytoxRed (Thermo S34859). Final volume was approximately 1mL with 1uL/mL final of SytoxRed and 1µg/mL final of Calcein violet. Pools of single cells (Elav – 100 cells, Ep3k 20 cells and Gd2k – 20-50 cells) were prepared at each time point (i.e., every four hours). The dissociation suspension was filtered onto a 35µm nylon mesh FACS tube. A BD FACSAria III (FACS DIVA 8.0 software) cell sorter was used to sort for the fluorescent reporter in each line: mOrange for ELAV (Elav-mOr1) and Kikume Green-Red protein (Gd2-KikGR, Ep3K-KikGR) for Gd2 and Ep3K. The gating strategy was as follows: multiplets were excluded based on FSC-H vs FSC-W profile, then live singlets were selected as Calcein-violet (405nm excitation, 450/40 BP emission filter) positive and SytoxRed negative population (633nm excitation, 660/20 BP emission filter). Then KikGR-positive cells (from the Gd2_v1g199428_KikGR cell suspension) or mOrange-positive cells (from the Elav:mOr cell suspension) were selected based on their FITC-A (488excitation, 525/50 emission filter) vs PE-A (561nm excitation, 582/12 emission filter) signal: FITC-high/ PE-low for KikGR-positive cells and PE-high/FITC-low for mOrange-positive cells as there are strongly autofluorescent cells on the FITC-A (488-525/50) vs PE-A(561-582/12) diagonal. Then live KikGR+ or mOr+ singlets above

5um were selected based on FSC-A vs SSC-A profile. As there are additional endogenous FITC+ and PE-A-positive populations that overlap with the KikGR+ and mOr+ gates (respectively), it is expected that the sorted pools of cells are significantly enriched for the reporter-labelled populations but not pure. Pools of 100 live mOr+ singlets (Elav::mOr line), or 20-50 live KikGR+ cells for the (Gd2_v1g199428_KikGR line) were sorted in up to 64 separate wells (until sortable cells were exhausted for each sample tube) of a 384-well capture plate containing 2 μ l of lysis solution (0.2% Triton-X-100, RNase inhibitors (RNasin inhibitors, PROMEGA), and barcoded poly(T) reverse-transcription (RT) primers). Each plate contained 2 biological replicates (separate dissociations) for each line sorted per ZT timepoint and was then spun down and frozen at -80°C until processing.

Cell-type sequencing libraries were prepared on a Bravo automated liquid handling platform (Agilent), as described in Seb e-Pedr s et al. (2018). Subsequent Illumina-based sequencing was performed using the protocol reported in (Seb e-Pedr s et al., 2018) using the MARS-seq protocol (Jaitin et al., 2014). Libraries were sequenced using the Illumina NSQ® 500 hi- Output KT v2 (75 cycle) with an Illumina NextSeq 500 sequencer.

Cyclic transcript expression analyses

The R package MetaCycle 2D (Wu et al., 2016) was used to detect cyclic transcripts from the time series expression data of each cell type (Gd2K, Elav_mOrange, Ep3K). Transcripts with no counts or missing replicates were discarded. The meta-analysis uses three algorithms to detect significant ($p < 0.05$) rhythmic signals: JTK_CYCLE, Lomb-Scargle, and ARSER.

Results and Discussion

Using the MARS-seq protocol as previously described (Jaitin et al., 2014), we identified transcripts with circadian expression in three cell types of *Nematostella*. A total of 136 significantly rhythmic genes ($p < 0.05$) were detected by MetaCycle 2D (Wu et al., 2016). In gland cells 34 transcripts were cycling, 61 transcripts were cycling in neural cells, and 41 transcripts were cycling in epithelial cells (Figure 1). It should be noted that data from the ectodermal reporter (Gd2) is currently being reviewed, as the expression of this reporter in adults was problematic during sorting due to low expression.

In each of the three cell types, the circadian-related genes *clock* and *clock-interacting pacemaker complex protein*, or *CIPC*, were significantly cycling with 24-hour periodicity (Figure 2). These were the only genes with cyclical expression for all three cell types. A microarray study in *Drosophila* suggested tissue-specific mRNA cycling when comparing transcripts from heads and bodies, where little overlap was seen in cyclic mRNAs between the two tissues except in core clock genes (Ceriani et al., 2002), as we see in this study of cell type cyclic expression in *Nematostella*. Consistent with prior studies that quantified gene expression of whole anemone homogenates, *nvClock* was significantly up-regulated during the photoperiod, with peak expression occurring just before the light-dark transition (Leach and Reitzel, 2019; Oren et al., 2015; Peres et al., 2014; Reitzel et al., 2010) in each cell type of this study. Similarly, *nvCycle* did not exhibit cyclic expression, similar to the pattern of *Clock* and *Cycle* expression in *Drosophila* (Cyran et al., 2003). *nvCIPC* expression was out of phase with *nvClock* showing up-regulation during the scotoperiod (Figure 2), consistent with previous reports

of this transcript in *Nematostella* and *Acropora* (Leach and Reitzel, 2019; Oren et al., 2015). The typical description of the central "animal" circadian clock requires a pair of E-box binding transcriptional activators, typically *clock* and *cycle*, to drive rhythmicity in tissue specific gene expression of clock-controlled genes (CCGs). In this pairing, oscillating expression of CLOCK or CYCLE (BMAL in mammals) promotes coordinated regulation of cyclic physiological and metabolic functions in various tissues (Hardin and Panda, 2013; Mohawk et al., 2012; Storch et al., 2002). Like other CLOCK:CYCLE targets, mouse and human CIPC has an E-box binding site suggesting circadian regulation and is also robustly expressed in a cyclic manner in peripheral tissues. The role, if any, of the cnidarian CIPC ortholog in circadian regulation is unknown, but we have identified canonical E-box motifs in the promoter region ~1000 bp upstream of this gene in *Nematostella*. Together, the 24-hour rhythmic, out of phase expression pattern to *nvCLOCK* and presence of E-box reporters in of *nvCIPC* correlatively suggests involvement of this gene in cnidarian clocks. Further, the circadian expression of *nvClock* and *nvCIPC* in multiple cell types suggests that these bHLH-PAS transcription factors have a similar circadian function in each cell type.

Four genes were shared between gland and neural cell lines: *cytochrome b-c1 complex subunit 7*, *nuclear receptor TLX*, *DEAD box polypeptide 41*, and a transcription factor in the proline- and acid-rich (PAR) subfamily of the basic leucine zipper proteins, or *PAR-bZIP*. The expression of each of the four shared genes exhibited the same general peak and trough in both cell types. The circadian network of animals involves feedback mechanisms via transcriptional regulators or direct repressors to the core clock components, either *Clock* or *Cycle*. In *Drosophila*, members of the PAR-bZIP family are

involved in this regulation and bind to the promoter region of *Clock* inhibiting or activating its transcription (Cyran et al., 2003). The proposed mechanism for this feedback in cnidarian circadian clocks is analogous, where it is hypothesized that PAR-bZIP transcription factors A, C, and D heterodimerize to regulate *nvClock* activity (Reitzel et al., 2013a). Further analysis of these genes in *Nematostella* have revealed expression patterns consistent with circadian expression when measured under diel light conditions (Peres et al., 2014; Reitzel et al., 2010); however their rhythmic expression is not maintained in the absence of a regular light cue (Leach and Reitzel, 2019; Peres et al., 2014). In the present study, significant rhythmic *nvPAR-bZIPC* expression was only detected in gland and neural cells. Our present data did not detect *nvPAR-bZIP A, B, or D* with significant 24-hour rhythmic expression in any cell of the three types, which suggests they may not be uniquely expressed in specific cell types. Because *nvPAR-bZIPC* does not appear to be co-expressed with two of its potential PAR-bZIP heterodimeric partners, these data may also suggest that this transcription factor acts as a homodimer or monomer. Alternatively, detection of other PAR-bZIPs in this dataset may be due to the stringent filtering criteria applied in MetaCycle (see Methods).

One gene, *hairy and enhancer or split-related protein (HELT)*, was shared between the epithelial cells and neural cells and one unannotated gene, NVE7446, was shared between epithelial cells and gland cells. Recent investigation of diel transcriptomic responses in *Nematostella* have suggested *nvHELT* expression is largely light dependent (Leach and Reitzel, 2019), with peak expression occurring mid-photoperiod (Leach and Reitzel, 2019; Oren et al., 2015) consistent with our findings in this study in both neural and epithelial cells.

Of the 55 genes unique to the neural cells, three cryptochromes and a *cAMP responsive element binding protein-like, CREB-like*, transcription factor were rhythmically oscillating. Of the cryptochromes, peak *nvCry1a* expression occurred right after the light-dark transition. Two *nvCry1b* transcripts were identified with cyclic expression (JGI genome: v1g106062 and v1g106211), however both of these transcripts map to the same position for the Vienna transcriptome (NVE2424). It is unclear if these are unique genes based on the first-generation annotation of the genome (Putnam et al., 2007). The slightly different expression patterns of v1g106062 and v1g106211 suggests that they could be different genes but without better gene models we are unable to resolve this discrepancy. Both *nvCry1b* transcripts exhibited expression peaks just before the light-dark transition and are identical to previous literature using whole animal homogenates (Leach and Reitzel, 2019; Oren et al., 2015; Peres et al., 2014; Reitzel et al., 2010). In vertebrate and non-drosophilid insect clock networks, Type II cryptochromes dimerize with *period* or *timeless* (insects) genes to directly repress action of CLOCK:CYCLE/BMAL heterodimers (Dunlap, 1999; Harmer et al., 2001; Yuan et al., 2007). In the atypical *Drosophila* clock, Type I cryptochromes act to indirectly repress CLOCK:CYCLE function in a light-dependent manner (Zhu et al., 2008; Zhu et al., 2005). Because cnidarians lack both *period* and *timeless* genes (Reitzel et al., 2010; Shoguchi et al., 2013), which, as discussed above, are typically circadian clock repressors, Reitzel et al. (2010) hypothesized that cryptochromes, particularly *nvCry1a* and *nvCry1b* are involved in the feedback arm of cnidarian circadian clocks, providing light-dependent repression of the core components *nvClock* and *nvCycle*. In this study,

circadian expression of cryptochromes was restricted to neural cells, suggesting the time setting through light entrainment may be specific to only neurons.

Our study is the first investigation of cell type specific expression of circadian-related genes in any cnidarian. Previous research has provided evidence supporting cyclic expression of core clock components in cnidarians, however collectively there is an inconsistency between reports of true circadian expression of these genes, or their light-dependency. This discrepancy may be due, in part, to experimental design and temporal differences between studies, but a conceivable explanation could be that the molecular mechanisms responsible for cyclic phenotypes are spatially restricted to a subset of cells. Because using whole animal homogenates does not allow for identification of spatial transcriptomic signatures, and likely dampens expression signals from genes that have restricted expression, characterizing transcriptome profiles of different cell types could help mitigate conflicting observations in *Nematostella*. Traditionally, the use of in-situ hybridization (ISH) has been used to look at cell type specific expression patterns of particular genes to hypothesize a mechanism, which would sometimes be followed up by knockdowns or transgenics. While these methods are complementary, they certainly do not allow for a complete picture. In order to understand a network, one clearly needs to know all of the components within a cell that could be interacting. By using a cell type transcriptomic approach, we can more accurately explore mechanisms responsible for the generation of circadian behavior and physiology in cnidarians that are not clear when looking at the whole organism level. The data presented here suggest that in *Nematostella*, neural cells have the components of what could be a complete clock, with the potential for light entrainment.

References

1. Agrawal, P., Houl, J. H., Gunawardhana, K. L., Liu, T., Zhou, J., Zoran, M. J. and Hardin, P. E. (2017). *Drosophila* CRY entrains clocks in body tissues to light and maintains passive membrane properties in a non-clock body tissue independent of light. *Current Biology* 27, 2431-2441. e3.
2. Akhtar, R. A., Reddy, A. B., Maywood, E. S., Clayton, J. D., King, V. M., Smith, A. G., Gant, T. W., Hastings, M. H. and Kyriacou, C. P. (2001). Circadian cycling of the mouse liver transcriptome, as revealed by cDNA microarray, is driven by the suprachiasmatic nucleus. *Current Biology* 12, 540-550.
3. Buijs, F. N., León-Mercado, L., Guzmán-Ruiz, M., Guerrero-Vargas, N. N., Romo-Nava, F. and Buijs, R. M. (2016). The circadian system: A regulatory feedback network of periphery and brain. *Physiology* 31, 170-181.
4. Ceriani, M. F., Hogenesch, J. B., Yanovsky, M., Panda, S., Straume, M. and Kay, S. A. (2002). Genome-wide expression analysis in *Drosophila* reveals genes controlling circadian behavior. *Journal of Neuroscience* 22, 9305-9319.
5. Cyran, S. A., Buchsbaum, A. M., Reddy, K. L., Lin, M.-C., Glossop, N. R. J., Hardin, P. E., Young, M. W., Storti, R. V. and Blau, J. (2003). Vrille, Pdp1, and dClock form a second feedback loop in the *Drosophila* circadian clock. *Cell* 112, 329-341.
6. Dibner, C., Schibler, U. and Albrecht, U. (2010). The mammalian circadian timing system: organization and coordination of central and peripheral clocks. *Annual review of physiology* 72, 517-549.
7. Dunlap, J. C. (1999). Molecular bases for circadian clocks. *Cell* 96, 271-290.

8. Hardin, P. E. and Panda, S. (2013). Circadian timekeeping and output mechanisms in animals. *Current Opinion in Neurobiology* 23, 724-731.
9. Harmer, S. L., Panda, S. and Kay, S. A. (2001). Molecular bases of circadian rhythms. *Annual Review of Cell and Development Biology* 17, 215-253.
10. Helfrich-Förster, C. (2005). Neurobiology of the fruit fly's circadian clock. *Genes, Brain and Behavior* 4, 65-76.
11. Hoadley, K. D., Vize, P. D. and Pyott, S. J. (2016). Current understanding of the circadian clock within Cnidaria. In the cnidaria, past, present and future: The world of medusa and her sisters, eds. S. Goffredo and Z. Dubinsky, pp. 511-520. Cham: Springer International Publishing.
12. Jaitin, D. A., Kenigsberg, E., Keren-Shaul, H., Elefant, N., Paul, F., Zaretsky, I., Mildner, A., Cohen, N., Jung, S., Tanay, A. et al. (2014). Massively parallel single-cell RNA-seq for marker-free decomposition of tissues into cell types. *Science* 343, 776.
13. Kaiser, T. S., Poehn, B., Szkiba, D., Preussner, M., Sedlazeck, F. J., Zrim, A., Neumann, T., Nguyen, L.-T., Betancourt, A. J., Hummel, T. et al. (2016). The genomic basis of circadian and circalunar timing adaptations in a midge. *Nature* 540, 69.
14. Langmead, B. and Salzberg, S. L. (2012). Fast gapped-read alignment with Bowtie 2. *Nature Methods* 9, 357-U54.
15. Leach, W. B. and Reitzel, A. M. (2019). Transcriptional remodeling upon light removal in a model cnidarian: losses and gains in gene expression. *Molecular Ecology*.

16. Meireles-Filho, A. C., Bardet, A. F., Yáñez-Cuna, J. O., Stampfel, G. and Stark, A. J. C. B. (2014). Cis-regulatory requirements for tissue-specific programs of the circadian clock. *Current Biology* 24, 1-10.
17. Mohawk, J. A., Green, C. B. and Takahashi, J. S. (2012). Central and peripheral circadian clocks in mammals. *Annual Review of Neuroscience* 35, 445-462.
18. Nakanishi, N., Renfer, E., Technau, U. and Rentzsch, F. (2012). Nervous systems of the sea anemone *Nematostella vectensis* are generated by ectoderm and endoderm and shaped by distinct mechanisms. *Development* 139, 347.
19. Nowotschin, S. and Hadjantonakis, A. K. (2009). Use of KikGR a photoconvertible green-to-red fluorescent protein for cell labeling and lineage analysis in ES cells and mouse embryos. *BMC Developmental Biology* 9.
20. Oren, M., Tarrant, A. M., Alon, S., Simon-Blecher, N., Elbaz, I., Appelbaum, L. and Levy, O. (2015). Profiling molecular and behavioral circadian rhythms in the non-symbiotic sea anemone *Nematostella vectensis*. *Scientific Reports* 5, 11418.
21. Peres, R., Reitzel, A. M., Passamaneck, Y., Afeche, S. C., Cipolla-Neto, J., Marques, A. C. and Martindale, M. Q. (2014). Developmental and light-entrained expression of melatonin and its relationship to the circadian clock in the sea anemone *Nematostella vectensis*. *EvoDevo* 5, 26.
22. Perrigault, M. and Tran, D. (2017). Identification of the molecular clockwork of the oyster *Crassostrea gigas*. *PLoS ONE* 12, e0169790.
23. Pett, J. P., Kondoff, M., Bordyugov, G., Kramer, A. and Herzog, H. (2018). Co-existing feedback loops generate tissue-specific circadian rhythms. *Life Science Alliance* 1.

24. Putnam, N. H., Srivastava, M., Hellsten, U., Dirks, B., Chapman, J., Salamov, A., Terry, A., Shapiro, H., Lindquist, E., Kapitonov, V. V. et al. (2007). Sea anemone genome reveals ancestral eumetazoan gene repertoire and genomic organization. *Science* 317.
25. Reitzel, A. M., Behrendt, L. and Tarrant, A. M. (2010). Light entrained rhythmic gene expression in the sea anemone *Nematostella vectensis*: the evolution of the animal circadian clock. *PLoS ONE* 5, e12805.
26. Reitzel, A. M., Tarrant, A. M. and Levy, O. (2013a). Circadian clocks in the cnidaria: environmental entrainment, molecular regulation, and organismal outputs. *Integrative and Comparative Biology* 53, 118-30.
27. Renfer, E., Amon-Hassenzahl, A., Steinmetz, P. R. H. and Technau, U. (2010). A muscle-specific transgenic reporter line of the sea anemone, *Nematostella vectensis*. *Proceedings of the National Academy of Sciences USA* 107.
28. Salgado-Delgado, R. C., Saderi, N., Basualdo Mdel, C., Guerra-Vargas, N. N., Escobar, C. and Buijs, R. M. (2013). Shift work or food intake during the rest phase promotes metabolic disruption and desynchrony of liver genes in male rats. *PLoS ONE* 8, e60052.
29. Seb e-Pedr os, A., Saudemont, B., Chomsky, E., Plessier, F., Mailh e, M.-P., Renno, J., Loe-Mie, Y., Lifshitz, A., Mukamel, Z., Schmutz, S. et al. (2018). Cnidarian cell type diversity and regulation revealed by whole-organism single-cell RNA-seq. *Cell* 173, 1520-1534.e20.

30. Shoguchi, E., Tanaka, M., Shinzato, C., Kawashima, T. and Satoh, N. (2013). A genome-wide survey of photoreceptor and circadian genes in the coral, *Acropora digitifera*. *Gene* 515, 426-31.
31. Storch, K. F., Lipan, O., Leykin, I., Viswanathan, N., Davis, F. C., Wong, W. H. and Weitz, C. J. (2002). Extensive and divergent circadian gene expression in liver and heart. *Nature* 417, 78-83.
32. Tosini, G. and Menaker, M. (1996). Circadian rhythms in cultured mammalian retina. *Science* 272, 419-421.
33. Ukai, H. and Ueda, H. R. (2010). Systems biology of mammalian circadian clocks. *Annual Review of Physiology* 72, 579-603.
34. Whitmore, D., Foulkes, N. S. and Sassone-Corsi, P. (2000). Light acts directly on organs and cells in culture to set the vertebrate circadian clock. *Nature* 404, 87.
35. Wu, G., Anafi, R. C., Hughes, M. E., Kornacker, K. and Hogenesch, J. B. (2016). MetaCycle: an integrated R package to evaluate periodicity in large scale data. *Bioinformatics* 32, 3351-3353.
36. Xu, K., DiAngelo, J. R., Hughes, M. E., Hogenesch, J. B. and Sehgal, A. (2011). The circadian clock interacts with metabolic physiology to influence reproductive fitness. *Cell Metabolism* 13, 639-654.
37. Yeung, J., Mermet, J., Jouffe, C., Marquis, J., Charpagne, A., Gachon, F. and Naef, F. (2018). Transcription factor activity rhythms and tissue-specific chromatin interactions explain circadian gene expression across organs. *Genome Research* 28, 182-191.

38. Yuan, Q., Metterville, D., Briscoe, A. D. and Reppert, S. M. (2007). Insect cryptochromes: gene duplication and loss define diverse ways to construct insect circadian clocks. *Molecular Biology Evolution* 24, 948-955.
39. Zantke, J., Ishikawa-Fujiwara, T., Arboleda, E., Lohs, C., Schipany, K., Hallay, N., Straw, Andrew D., Todo, T. and Tessmar-Raible, K. (2013). Circadian and circalunar clock interactions in a marine annelid. *Cell Reports* 5, 99-113.
40. Zhang, R., Lahens, N. F., Ballance, H. I., Hughes, M. E. and Hogenesch, J. B. (2014). A circadian gene expression atlas in mammals: Implications for biology and medicine. *Proceedings of the National Academy of Sciences USA* 111, 16219.
41. Zhu, H., Sauman, I., Yuan, Q., Casselman, A., Emery-Le, M., Emery, P. and Reppert, S. M. (2008). Cryptochromes define a novel circadian clock mechanism in monarch butterflies that may underlie sun compass navigation. *PLoS Biology* 6, e4.
42. Zhu, H., Yuan, Q., Froy, O., Casselman, A. and Reppert, S. M. (2005). The two CRYs of the butterfly. *Current Biology* 15, R953-R954.

Figures

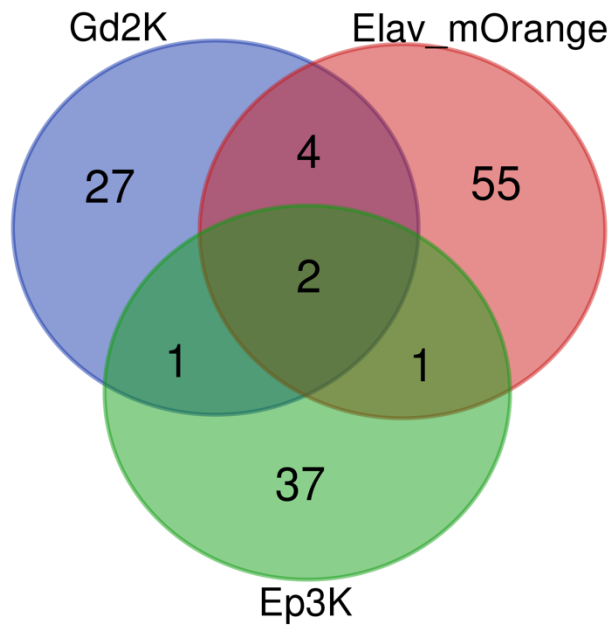


Figure 1. Venn diagram of significant 24-hour cycling genes in the three lines: gland cells (Gd2K), neural cells (Elav_mOrange), and epithelial cells (Ep3K).

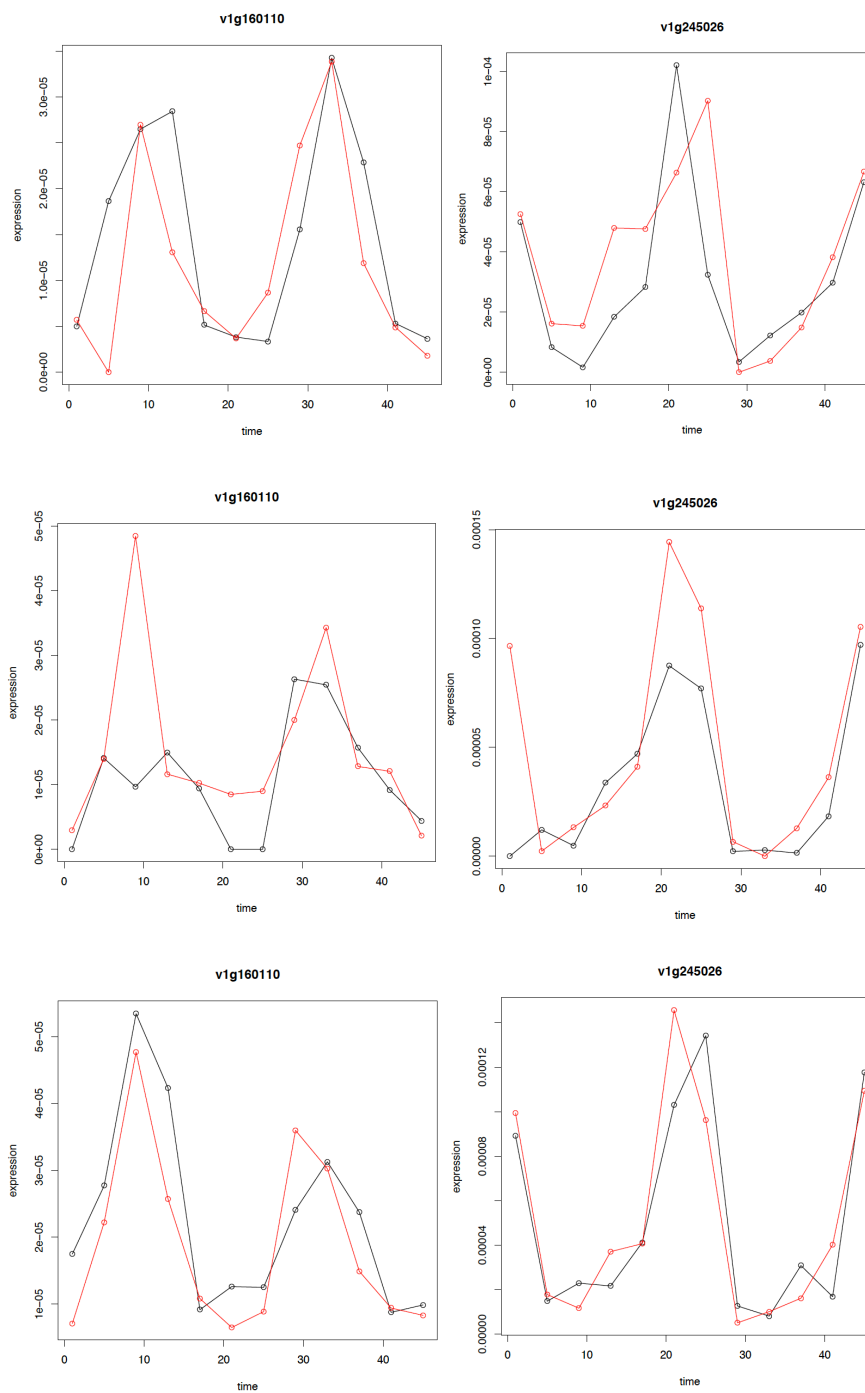


Figure 2. Time series transcript expression of *nvClock* (left) and *nvCIPC* (right) in the Gd2K (A), Ep3K (B), and Elav_mOrange (C) lines from two technical replicates (black and red lines).

Supplemental Note 1

Primers

Fwd1_pV1g199428_NVE4653 (5'=> 3')

ATCTGATTAATTAACAGCGTGCAACATGCAATTACAG

Rev1_pV1g199428_NVE4653

ATCTGAGGCGCGCCCTTCCCCTATGAACGTCTCC

Fwd1_pNVE17842

ATCTGATTAATTAATGTTGGACCCATAGTCCTTG

Rev1_pNVE17842

ATCTGAGGCGCGCCCTTGTACCTTAATCGTAAAT

Primers include restriction sites (AscI for the reverse primer, PacI for the Fwd, and a 6bp additional sequence for restriction digestion)

CHAPTER 4

BACTERIAL RHYTHMS IN *NEMATOSTELLA VECTENSIS*

Whitney B. Leach, Tyler J. Carrier, and Adam M. Reitzel

Citation

Leach WB, Carrier TJ, Reitzel AM. 2019. Diel patterning in the bacterial community associated with the sea anemone *Nematostella vectensis*. Ecology and Evolution **9.17**: 9935-9947.

Abstract

Microbes can play an important role in the physiology of animals by providing essential nutrients, inducing immune pathways, and influencing the specific species that compose the microbiome through competitive or facilitatory interactions. The community of microbes associated with animals can be dynamic depending on the local environment, and factors that influence the composition of the microbiome are essential to our understanding of how microbes may influence the biology of their animal hosts. Regularly repeated changes in the environment, such as diel lighting, can result in two different organismal responses: a direct response to the presence and absence of exogenous light and endogenous rhythms resulting from a molecular circadian clock, both of which can influence the associated microbiota. Here, we report how diel lighting and a potential circadian clock impacts the diversity and relative abundance of bacteria in the model cnidarian *Nematostella vectensis* using an amplicon-based sequencing approach. Comparisons of bacterial communities associated with anemones cultured in constant darkness and in light:dark conditions revealed that individuals entrained in the dark had a

more diverse microbiota. Overall community composition showed little variation over a 24-hour period in either treatment; however, abundances of individual bacterial OTUs showed significant cycling in each treatment. A comparative analysis of genes involved in the innate immune system of cnidarians showed differential expression between lighting conditions in *N. vectensis*, with significant up-regulation during long-term darkness for a subset of genes. Together, our studies support a hypothesis that the bacterial community associated with this species is relatively stable under diel light conditions when compared with static conditions and that particular bacterial members may have time-dependent abundance that coincides with the diel photoperiod in an otherwise stable community.

Introduction

Animals and other eukaryotes associate with diverse microbial communities that are known to have distinct and sometimes essential roles in the development, physiology, and life history of various species (Fraune & Bosch, 2010; Kohl & Dearing, 2012; Macke, Tasiemski, Massol, Callens, & Decaestecker, 2017; McFall-Ngai & Ruby, 2000; Sommer & Backhed, 2013). The members that compose host-associated microbial communities often shift depending on the local environmental conditions (Carrier & Reitzel, 2017), the presence of particular species that may facilitate or limit the colonization by other microbes (Vega & Gore, 2017), and the expression of the immune system by the host (Nyholm & Graf, 2012; Christoph A. Thaiss, Zmora, Levy, & Elinav, 2016). Over the past few decades, sequence-based approaches have broadened our understanding of diverse interactions between hosts and associated microbial communities (O'Brien, Webster, Miller, & Bourne, 2019). Specifically, these studies have provided insight into the relative proportions of

microbes that are stably symbiotic or transient with a host when experiencing variable environmental conditions (Shade & Handelsman, 2012), including external factors (e.g., temperature, nutrients) or host-regulation (e.g., immune system). Determining how these factors impact the host-associated microbial communities in general, and how they affect specific OTUs (operational taxonomic units), would provide a better understanding of how complex microbial communities vary for eukaryotes.

Light is an environmental factor that influences many organisms through a combination of two principal responses. First, light can significantly impact the physiology and survival of an organism following direct exposure, and photosynthetically active wavelengths may impact the function of microbial partners. The result can be positive for increasing growth of certain microbes (e.g., cyanobacteria), where photons are harvested for production of photosynthates. Light can also have negative effects by causing damage that can inhibit growth, particularly for short wavelength portions of the light spectrum (Dai et al., 2012). Secondly, animal-associated bacterial communities can, in turn, shift following responses by the host due to an entrained endogenous pathway (the circadian clock). Circadian rhythms are critical internal regulatory systems that allow organisms to anticipate daily changes in their environment and adjust biological processes appropriately. Using an endogenous centralized clock, cycles of about 24 hours are entrained and maintained by exogenous cues (Zeitgebers) that modulate temporal rhythms through a series of transcription-translation feedback loops (Dunlap, 1999). Previous work with vertebrates suggests that the circadian clock is an important regulator of the immune system, which can impact portions of the bacterial community throughout a day. In humans (Huang, Ramsey, Marcheva, & Bass, 2011) and mice (Leone et al., 2015), the gut

microbiota is time-of-day–dependent and is hypothesized to modulate the regulation of host metabolism and immunity (Keller et al., 2009; Liang, Bushman, & FitzGerald, 2015; C. A. Thaiss et al., 2014). However, the interaction between light-dependent responses that influence the host's behavior and an endogenous circadian clock remains unknown.

Our knowledge of the connections between diel lighting, circadian rhythms, and symbiotic microbiota remain limited in invertebrates, notably in aquatic habitats. One of the best studied examples is the mutualism between the squid *Euprymna scolopes* and bacterium *Aliivibrio fischeri* (formally *Vibrio fischeri*; Boettcher, Ruby, & McFall-Ngai, 1996; Heath-Heckman et al., 2013; Wier et al., 2010), where the expression of a light-sensitive cryptochrome (*escry1*) in the host has been linked to the presence of *A. fischeri*. While the *Euprymna-Aliivibrio* system provides a host-focused view of circadian-related symbioses, decades of work on the coral microbiome has provided additional context for the evolutionary ecology of daily cycles exhibited by both the holobiont and by each partner (Hoadley, Vize, & Pyott, 2016). *Symbiodiniaceae*, a eukaryotic endosymbiotic mutualist of corals and other invertebrates, demonstrates diel periodicity of photosynthetic processes in the free-living and mutualistic states, suggesting that symbiotic partners maintain their own circadian clocks and, perhaps, contribute to that of the holobiont (Roopin, Yacobi, & Levy, 2013; Michal Sorek, Díaz-Almeyda, Medina, & Levy, 2014; M. Sorek, Yacobi, Roopin, Berman-Frank, & Levy, 2013). Aside from these systems, oscillations of individual members or communities of host-associated microbiota in marine invertebrates are poorly understood. Further, how much of the holobiont rhythmicity is due to a direct response to environmental cues (e.g., light) or is driven by endogenous

mechanisms remains an active area of research (Brady, Willis, Harder, & Vize, 2016; W. B. Leach, Macrander, Peres, & Reitzel, 2018; Oren et al., 2015; Vize, 2009).

Nematostella vectensis, an infaunal sea anemone that lives in shallow estuaries, is an emerging model for studying the host-associated microbial communities and circadian biology of cnidarians. Similar to corals, *N. vectensis* exhibits nocturnal patterns in behavior [e.g., circadian locomotion and body expansion (Hendricks, Byrum, & Meyer-Bernstein, 2012; Oren et al., 2015)], gene expression [e.g., immunity and stress tolerance (W. B. Leach et al., 2018)], and metabolism (Maas, Jones, Reitzel, & Tarrant, 2016). Unlike corals, *N. vectensis* does not associate with zooxanthellate and thus, exhibits rhythmicity independent of the eukaryotic mutualist of corals and other cnidarians. Previous studies have shown that the bacterial community associated with *N. vectensis* is diverse in natural habitats (Har et al., 2015), variable across development (Mortzfeld et al., 2016), and significantly dissimilar for individuals from different geographic locations (Mortzfeld et al., 2016), which together support this species as a system to study animal and bacterial interactions (Fraune, Foret, & Reitzel, 2016).

The innate immune system is a combination of molecular mechanisms that may explain the variation in bacteria associated with cnidarians (Bosch et al., 2009). Genomic and transcriptomic resources for a number of anthozoan and hydrozoan species have identified numerous genes predicted to be involved in cnidarian immunity (Miller et al., 2007; A. M. Reitzel, Sullivan, Traylor-Knowles, & Finnerty, 2008). Based on sequence similarity and experimental characterization, cnidarians have many components of a traditionally defined innate immune system, including the Toll-like and NOD-like receptors for microbial recognition (Bosch et al., 2009; J. J. Brennan et al., 2017), at least

three complement families [e.g., C3, Bf, and MASP (Kimura, Sakaguchi, & Nonaka, 2009), MyD88 and other proteins for intracellular signal transduction (Franzenburg et al., 2012), and Nf- κ B along with other Rel-related proteins for transcriptional regulation of effector genes (Sullivan et al., 2009; Wolenski et al., 2011)]. These studies support the hypothesis that the cnidarian-bilaterian ancestor had a rich and complex innate immune system. The regulation of the cnidarian system and how environmental changes may modulate the expression of components of this pathway remain unstudied.

Using high throughput sequencing of 16S amplicons representing the bacterial communities associated with *N. vectensis*, we tested two hypotheses regarding if and how diel lighting influences the anemone-associated bacterial community. First, we tested whether the bacterial community of *N. vectensis* exhibits diel oscillations synchronous with light:dark cycling, and second, whether individual OTUs were differentially abundant after host exposure to light:dark cycles. Here, we identify compositional differences between anemones exposed to light:dark cycles or constant darkness. Further, these data reveal specific bacterial OTUs that exhibit diel patterns of abundance in either light regime. By assessing bacterial abundance across diel and constant conditions, our research sheds light on the potential of microbial interactions in the regulation of host anemone cyclic behavior and physiology measured in other studies (Hendricks et al., 2012; Maas et al., 2016; Oren et al., 2015).

Materials and Methods

Animal culturing and experimental conditions

Adult *Nematostella vectensis* derived from the original "Maryland strain" (Putnam et al., 2007) were used for these experiments. Individuals were reared in a single dish at room temperature (~20-25°C) and ambient lighting conditions (as described in Hand & Uhlinger, 1994). In preparation for the experiment, adults from the common garden conditions were split into two glass dishes and transferred to an incubator at 25°C. Individuals were fed freshly hatched brine shrimp (*Artemia sp.*) haphazardly three times weekly and water was replaced following feeding using 200 mL of 15 ppt artificial saltwater.

To simulate diel light conditions, full spectrum LED lights (MINGER) were set to 12-hour light:12-hour dark (LD) cycles, with lights on at 11:30 AM (ZT = 0) and lights-off (ZT = 12) at 11:30 PM. Each dish of individuals was assigned to LD or DD (constant darkness) and were subsequently kept in their respective conditions for 30 days (Figure 1). During this entrainment period, individuals were kept on the same feeding and water change schedule as previous. Feeding and water changes occurred during 'daytime' hours (between ZT = 0 and ZT = 12). To eliminate the potential for light contamination in DD animals, dishes were wrapped in tin foil during the entrainment and sampling periods; however, dishes were briefly removed from the incubator and were handled in a dark room for feeding and water changes.

Two days prior to sampling, individuals from each light regime were split into four glass dishes per condition (LD 1-4; DD 1-4) with 200 mL of fresh, 15 ppt artificial seawater and were starved. Beginning at 9:30 AM (ZT = 22), individuals from each dish were sampled at four-hour intervals for a total of 11 time points (Figure 1). Four biological

replicates per time point (A-D, one per bowl) per condition (LD and DD) were collected for a total 88 samples. Samples were preserved in RNAlater at -20°C until processing.

Assaying microbial communities

Total DNA was extracted from *N. vectensis* samples using the Qiagen All Prep Kit (Thermo Scientific), quantified using the NanoDrop 2000 UV-Vis Spectrophotometer (Thermo Scientific), and standardized to 5 ng μL^{-1} using RNase/DNase-free water.

Bacterial sequences were amplified using universal primers for the V3/V4 regions of the 16S rDNA gene (Forward: 5' CCTACGGGNGGCWGCAG, Reverse: 5' GACTACHVGGGTATCTAATCC; (Klindworth et al., 2013); (see Dryad for Table S1). Products were purified using the Axygen AxyPrep Mag PCR Clean-up Kit (Axygen Scientific), indexed via PCR using the Nextera XT Index Kit V2 (Illumina Inc.), and then purified again. At each of these three clean up steps, fluorometric quantification was performed using a Qubit (Life Technologies), and libraries were validated using a Bioanalyzer High Sensitivity DNA chip (Agilent Technologies). Illumina MiSeq sequencing (v3, 2x300 bp paired-end reads) was performed at the University of North Carolina at Charlotte.

Forward and reverse sequences were paired and trimmed using PEAR (Zhang, Kobert, Flouri, & Stamatakis, 2014) and Trimmomatic (Bolger, Lohse, & Usadel, 2014), respectively, converted from fastq to fasta using a custom script (see Dryad for Supplemental Note), and, prior to analysis of bacterial 16S rDNA sequences, chimeric sequences were detected using USEARCH (Edgar, Haas, Clemente, Quince, & Knight, 2011) and removed using filter_fasta.py. Using QIIME 1.9.1 (Caporaso et al., 2010) and SILVA (Quast et al., 2013), bacterial 16S rDNA sequences were grouped into operational

taxonomic units (OTUs) based on a minimum 99% similarity. The biom table generated by `pick_open_reference_otus.py` was filtered of OTUs with less than ten reads, as well as ‘unassigned’ sequences.

Using the filtered biom table and “`biom summarize-table`” function to count total sequences per sample, the rarefaction depth of 1,080 (see Dryad for Figure S1) was determined and applied to all subsequent analyses. Alpha diversity (i.e., McIntosh dominance index, McIntosh evenness index, Menhinick richness index, Faith’s phylogenetic distance, and observed OTUs) was calculated using `alpha_diversity.py` and compared statistically using Student’s t-test in JMP. Beta diversity was calculated using unweighted and weighted UniFrac (Lozupone & Knight, 2005), compared using principal coordinate analyses (PCoA) with `jackknifed_beta_diversity.py`, visualized using `make_2d_plots.py`, and stylized for presentation in Adobe Illustrator CS6. UniFrac distances were then compared statistically using an analysis of similarity (ANOSIM) in QIIME as part of `compare_categories.py`. Community composition was generated using `summarize_taxa_through_plots.py` and stylized using Prism 7 (GraphPad Software) and Adobe Illustrator CS6. Differential abundance of OTUs between light regimes was tested using the `DESeq2_nbinom` algorithm as part of `differential_abundance.py`. Lastly, the shared or ‘core’ community was determined using `compute_core_microbiome.py` and `shared_phylotypes.py`. Venn diagrams showing shared and unique OTUs were generated by comparing taxa between treatments.

A step-by-step listing of the informatic pipeline, including QIIME scripts, used to convert and process raw reads are available on Dryad in file “Supplemental Note.”

Identification of oscillating OTUs

Using the filtered biom table, we identified oscillating OTUs using the R statistical package JTK_Cycle (version 3.1; Hughes, Hogenesch, & Kornacker, 2010). Specifically, we used the script described by Hughes et al. (2010), setting the parameters to select significantly cycling OTUs between 20-28 hours (JTK_Cycle, $p < 0.05$; 'per' = 24) and shifts in peak expression (JTK_Cycle, 'lag') between LD and DD samples were compared (Zeitgeber Time: ZT). JTK_Cycle does not classify units into rhythmic categories, therefore we compared read counts for OTUs based on their periodicity values ('per') and significance (p-value). ANOVA and post hoc Tukey tests were performed with GraphPad Prism between timepoints and within treatments.

Results

To characterize the variation in the bacterial community associated with *N. vectensis* when cultured in two treatments, light:dark (LD) and constant dark (DD), we used 16S rDNA sequencing to compare microbial diversity and abundance in each light regime.

Community-level dynamics

Differences in the bacterial communities associated with *N. vectensis* were best explained by the presence of a diel photoperiod (Figure 2A; ANOSIM, unweighted UniFrac: $p < 0.001$; ANOSIM, weighted UniFrac: $p = 0.056$). When comparing alpha diversity between LD and DD, communities were similar in dominance (t-test, McIntosh dominance index: $p = 0.580$), evenness (t-test, McIntosh evenness index: $p = 0.520$), richness (t-test, Menhinick richness index: $p = 0.297$), and observed OTUs (t-test; $p = 0.078$) (see Dryad for Table S2). Anemones cultured in constant darkness however,

associated with a bacterial community that was 13% more phylogenetically diverse than anemones cultured under light:dark conditions (t-test, Faith's phylogenetic distance: $p = 0.047$; see Dryad for Table S2).

There was no difference in the bacterial taxa (membership; ANOSIM, unweighted UniFrac: $p < 0.418$) or their relative abundance (composition; ANOSIM, weighted UniFrac: $p = 0.798$) between day and night periods in LD. However, there was dissimilarity in membership (ANOSIM, unweighted UniFrac: $p = 0.046$), but not composition (ANOSIM, weighted UniFrac: $p = 0.329$) for DD individuals. Moreover, when comparing bacterial communities across all sampled time points, we observed no differences in LD membership or composition (ANOSIM, unweighted UniFrac: $p = 0.280$; ANOSIM, weighted UniFrac: $p = 0.309$), but time-dependent differences were observed in membership for DD entrained individuals (ANOSIM, unweighted UniFrac: $p = 0.016$; ANOSIM, weighted UniFrac: $p = 0.329$).

Lastly, the community-level pattern observed for LD or DD was not confounded by differences between biological replicates ("bowl effects"). Specifically, there was no significant variation in the taxonomy and composition of *N. vectensis* associated bacterial communities under LD (ANOSIM, unweighted UniFrac: $p = 0.082$; ANOSIM, weighted UniFrac: $p = 0.170$) and DD (ANOSIM, unweighted UniFrac: $p = 0.892$; ANOSIM, weighted UniFrac: $p = 0.925$) conditions.

Composition of the bacterial community

The bacterial communities associated with *N. vectensis* were best explained by the presence/absence of a diel photoperiod, so we next compared the taxonomic profiles of bacteria in each lighting treatment. The bacterial communities of anemones in LD consisted

primarily of seven bacterial classes: Gammaproteobacteria (Proteobacteria; 55.70%), Mollicutes (Tenericutes; 13.40%), Betaproteobacteria (Proteobacteria; 10.70%), Flavobacteriia (Bacteroidetes; 5.90%), Alphaproteobacteria (Proteobacteria; 5.70%), Deltaproteobacteria (Proteobacteria; 1.80%), and Phycisphaerae (Planctomycetes; 1.20%) (Figure 2B). The bacterial communities of anemones in DD primarily associated with the same seven bacterial classes but at different relative proportions: Gammaproteobacteria (Proteobacteria; 49.20%), Betaproteobacteria (Proteobacteria; 13.30%), Mollicutes (Tenericutes; 13.10%), Flavobacteriia (Bacteroidetes; 8.70%), Alphaproteobacteria (Proteobacteria; 6.80%), Deltaproteobacteria (Proteobacteria; 2.30%), and Phycisphaerae (Planctomycetes; 1.00%) (Figure 2B). Although we did observe treatment-specific OTUs (Figure 2C), total OTUs within these abundant bacterial classes varied little between LD and DD as well as across time (Figure 2D; see Dryad for Table S3).

Differences in the bacterial communities of LD and DD entrained anemones were due, in part, to the differential abundance of 37 bacterial OTUs (Table 1.4). Of those 37 differentially abundant OTUs, 17 (45.9%) were over-abundant in LD while 20 (54.1%) were under-abundant (Table 1.4). Relative to DD, the bacterial classes with over-abundant OTUs that were in significantly higher proportions in LD included: Saprospirae and Flavobacteriia (Bacteroidetes), Chlamydiia (Chlamydiae), Lentisphaeria (Lentisphaerae), OM190 (Planctomycetes), and Alphaproteobacteria and Gammaproteobacteria (Proteobacteria) (Table 1.4). The bacterial classes with under-abundant OTUs included: Flavobacteriia, Phycisphaerae and Planctomycetia (Planctomycetes), Alphaproteobacteria and Gammaproteobacteria, and Opitutae and Verrucomicrobiae (Verrucomicrobia) (Table 1.4).

Shared taxa between LD and DD

A shared (or ‘core’) bacterial community for *N. vectensis* in LD and DD was determined for different proportions of shared OTUs. At a core level of 60%, 70%, 80%, 90%, and 100% (i.e., bacterial phylotypes found in at least ‘N’% of samples), we observed that 141, 93, 63, 38, and nine phylotypes (see Dryad for Figure S2), respectively, were shared between LD and DD conditions. At core levels 60% and 70%, we observed that the taxonomic representation (but not composition) of these communities were distinct but converged at a core level of 80% (see Dryad for Figure S3).

The taxonomic composition of the ‘core’ community was dominated by three bacterial classes that were also common in the full communities: Gammaproteobacteria (Proteobacteria), Mollicutes (Tenericutes), and Betaproteobacteria (Proteobacteria) (see Dryad for Figure S4). In these core communities, we also observed Actinobacteria (Actinobacteria), Flavobacteriia (Bacteroidetes), Lentisphaeria (Lentisphaerae), OM190 and Phycisphaerae (Planctomycetes), Alphaproteobacteria and Deltaproteobacteria (Proteobacteria), Spirochaetes (Spirochaetes), and Opitutae (Verrucomicrobia) (see Dryad for Figure S4).

Patterns of abundance in LD and DD

Using JTK_cycle (Hughes et al., 2010), we identified 26 bacterial OTUs in LD that showed rhythmic cycling ($p < 0.05$), five of which exhibited a 24-hour periodicity with peak abundance at either $ZT = 20$ or $ZT = 22$ ($per = 24$; Figure 3; Table 2.4). Of these five OTUs, four were from the bacterial order Rhodobacterales and the other was from Alteromonadales (Table 2.4). In DD, 16 bacterial OTUs showed rhythmic cycling ($p < 0.05$), and five of these exhibited 24-hour periodicity with peak abundance ranging

between ZT = 2 and ZT = 20 (per = 24; Figure 3; Table 2.4). Unlike the cycling OTUs in LD, OTUs in DD with 24-hour cycling were from four disparate bacterial orders: Chlamydiales, Spirochaetales, Oceanospirillales, and CL500-15 (Table 2.4). When comparing the ten bacterial OTUs that exhibited a 24-hour periodicity to the core community, we observed that OTUs 'LD 1,' 'LD 2,' and 'LD 5' were specific to LD while OTU 'DD 2' was specific to DD. Moreover, OTUs 'LD 2,' and 'LD 5' were observed at the 80% core level while the OTU 'DD 2' was only detected at the 60% core level.

Discussion

Photoperiods and circadian clocks are an integral part of diverse biological processes for animals, ranging from immune performance to metabolism to host-microbe associations (Heath-Heckman, 2016; Hubbard et al., 2018; Liang et al., 2015; Zarrinpar, Chaix, Yooseph, & Panda, 2014). In traditional mammalian systems, such as mice and humans, the composition of the gut microbiota of individuals entrained to light:dark or constant darkness differ for particular taxonomic groups of bacteria (Deaver, Eum, & Toborek, 2018; Wu et al., 2018). Thus, the photoperiod may influence compositional dynamics of host-associated bacterial communities in other animals, and the responses may also involve an endogenous circadian clock. While *N. vectensis*, like other cnidarians, has well described rhythmic behavior, physiology and gene expression under light entrainment (Hendricks et al., 2012; Maas et al., 2016; Oren et al., 2015; Adam M. Reitzel, Behrendt, & Tarrant, 2010), this is the first investigation of potential rhythmicity in their associated bacterial community. Here, we show that *N. vectensis* entrained to constant darkness associate with a phylogenetically more diverse bacterial community than anemones

entrained to light:dark. Moreover, we find support that the relative abundance of a limited number of OTUs oscillate over the course of a day (Figure 3). Of those OTUs specific to light:dark conditions, four were within the bacterial order Rhodobacterales, while those oscillating in constant conditions were phylogenetically disparate (Table 2.4).

The research we report here suggests that diel lighting may impact a fraction of the microbial community, but this effect appears to be relatively small compared with differences in the associated microbiota over developmental stages or in natural populations (Har et al., 2015; Mortzfeld et al., 2016). For *N. vectensis* and other animals, the role of the animal host, the environment, and the resident microbiota may play in shaping host-microbe interactions remains fragmentary. One hypothesis for the observed shift in community level composition reported here is that the lack of a photoperiod drives ecological (or stochastic) drift in the microbes associated with *N. vectensis*. Generally, in ecological systems, species diversity is expected to increase as environmental heterogeneity increases up to a point as described in Curd et al. (2018). Our results do not show a positive relationship between environmental variation (i.e., diel lighting) and community diversity; rather, we measured greater community level variability in constant conditions (Table 2.4).

A second hypothesis for community-level shifts over a diel light period is that changes in bacteria are attributed to physiological differences between individuals in light:dark and constant darkness (i.e., gene expression, behavior, metabolism; W. B. Leach et al., 2018; Maas et al., 2016; Peres et al., 2014; Adam M. Reitzel et al., 2010; Roopin & Levy, 2012). The photoperiod may influence compositional dynamics of host-associated bacterial communities through differential regulation of the immune system, potentially

through an endogenous circadian clock. Studies in *Hydra* have shown that immune factors and bacteria-bacteria interactions are critical for function in restricting membership of the microbiome (Augustin et al., 2017; Bosch et al., 2009; Franzenburg et al., 2012; Fraune et al., 2015). While previous research has shown that *N. vectensis* has a circadian clock based on behavioral, physiology, and molecular measurements (see Introduction), genes likely to be involved in innate immunity have little differential expression over a 24-hour period, at least when measured in whole animal homogenates. As a preliminary investigation using previously published transcriptomic data (W.B. Leach & Reitzel, 2019), we compared expression of candidate cnidarian immune genes from anemones sampled in LD and DD conditions. The genes selected include the hypothesized principal innate immune genes (e.g., Toll-like receptors, Nf- κ B) from Miller et al. (2007) and Brennan et al. (2017), the NOD-like receptors from Lange et al. (2011) and Yuen et al. (2014), and the complement genes identified by Kimura et al. (2009) (see Table 3.4). These transcriptomic comparisons showed only a small portion of the genes predicted to be involved in the cnidarian innate immune system (7 out of the 34 surveyed) to be differently expressed between LD and DD (Table 3.4). Of these seven, four genes were up-regulated in constant dark conditions (compared to LD) and included predicted members of the cnidarian multi-complement pathway (e.g., *NvC3-1*, *NvBF1*, and *NvBF2*) and NOD-like receptors. The function of any of these genes in *N. vectensis* is unknown, but the complement genes have spatially restrictive expression in the endoderm (Kimura et al., 2009). Overall similarity in the expression of immune genes may explain the consistency of the microbial community between lighting treatments. The small number of OTUs showing 24-hour oscillating

abundance could be a result of the subset of differentially expressed immune genes which could be tissue specific.

Complementary to photoperiod-related shifts in cnidarian-associated microbiota we report here, a number of studies have shown that additional rhythmic abiotic factors may affect compositional changes in these symbiont communities (Cai et al., 2018; Sharp, Pratte, Kerwin, Rotjan, & Stewart, 2017; Silveira et al., 2017; Sweet, Brown, Dunne, Singleton, & Bulling, 2017). At present, we have a rudimentary understanding of what drives the observed specificity between a host and their associated species-specific microbial communities. When comparing the bacterial communities of *N. vectensis* across development, environmental conditions, and geographic locations, Mortzfeld et al. (2016) and Domin et al. (2018) both detected Rhodobacterales and Alteromonadales. Additionally, studies in several reef building corals find both of these bacterial groups to be part of the associated microbiota (Kelly et al., 2014; Taniguchi, Yoshida, Hibino, & Eguchi, 2015). Consistent detection of these two bacterial groups in select anthozoan cnidarians may imply non-random associations and conserved taxa, together suggesting some biological importance. However, while differences between the animal-associated bacteria and those in the surrounding environment suggests selection, neutral and stochastic factors may explain how these bacterial communities shift over time and between individuals (Sieber et al., 2018). For example, it is unclear if the OTUs we identified as cycling may be a result of the anemone, inter-bacterial interactions independent of the host, or a combination of both factors. Future research with these OTUs to determine spatial localization and competition would be of interest.

Our comparisons of the bacterial communities associated with *N. vectensis* suggest a correlation between presence of a circadian photoperiod and that individual OTUs exhibit a 24-hour periodicity. To determine if community-level shifts are biologically important to the anemone, future research will compare individuals cultured microbe-free to determine if anemones have different physiology, behavior, or gene expression. At the OTU-level, isolation of the identified Rhodobacterales and Alteromonadales would be useful to determine their genomic function and physiology. This set of experiments, alongside the continued development of diverse cnidarian systems, would position this clade as a comparative model for the evolution and ecology animal-bacterial symbioses across circadian and diel photoperiods.

Acknowledgements

We thank the Reitzel Laboratory for continual support, Jason Macrander informatic assistance, Daniel Janies (UNC Charlotte) for sequencing resources, and Karen Lopez (UNC Charlotte) for technical assistance with sequencing. Funding for this project was provided by an NIH grant R15GM114740 (WBL, AMR), the Human Frontier Science Program Award RGY0079/2016 (AMR), and a NSF Graduate Research Fellowship (TJC).

References

1. Augustin, R., Schroder, K., Rincon, A. P. M., Fraune, S., Anton-Erxleben, F., Herbst, E. M., . . . Bosch, T. C. G. (2017). A secreted antibacterial neuropeptide shapes the microbiome of *Hydra*. *Nature Communications*, 8. doi:10.1038/s41467-017-00625-1
2. Boettcher, K. J., Ruby, E. G., & McFall-Ngai, M. J. (1996). Bioluminescence in the symbiotic squid *Euprymna scolopes* is controlled by a daily biological rhythm. *Journal of Comparative Physiology a-Sensory Neural and Behavioral Physiology*, 179(1), 65-73.
3. Bolger, A. M., Lohse, M., & Usadel, B. (2014). Trimmomatic: A flexible trimmer for Illumina sequence data. *Bioinformatics*, 30(15), 2114-2120.
4. Bosch, T. C. G., Augustin, R., Anton-Erxleben, F., Fraune, S., Hemmrich, G., Zill, H., . . . Schroder, J. M. (2009). Uncovering the evolutionary history of innate immunity: The simple metazoan *Hydra* uses epithelial cells for host defense. *Developmental and Comparative Immunology*, 33(4), 559-569.
doi:10.1016/j.dci.2008.10.004
5. Brady, A. K., Willis, B. L., Harder, L. D., & Vize, P. D. (2016). Lunar phase modulates circadian gene expression cycles in the broadcast spawning coral *Acropora millepora*. *Biological Bulletin*, 230(2), 130-142. doi:10.1086/BBLv230n2p130
6. Brennan, J. J., Messerschmidt, J. L., Williams, L. M., Matthews, B. J., Reynoso, M., & Gilmore, T. D. (2017). Sea anemone model has a single Toll-like receptor that can function in pathogen detection, NF-kappaB signal transduction, and development. *Proceedings of the National Academy of Sciences USA*, 114(47), E10122-e10131.
doi:10.1073/pnas.1711530114

7. Brennan, J. J., Messerschmidt, J. L., Williams, L. M., Matthews, B. J., Reynoso, M., & Gilmore, T. D. (2017). Sea anemone model has a single Toll-like receptor that can function in pathogen detection, NF- κ B signal transduction, and development. *Proceedings of the National Academy of Sciences*, 114(47), E10122-E10131. doi:10.1073/pnas.1711530114
8. Cai, L., Zhou, G., Tong, H., Tian, R.-M., Zhang, W., Ding, W., . . . Qian, P.-Y. (2018). Season structures prokaryotic partners but not algal symbionts in subtropical hard corals. *Applied Microbiology and Biotechnology*, 102(11), 4963-4973. doi:10.1007/s00253-018-8909-5
9. Caporaso, J. G., Kuczynski, J., Stombaugh, J., Bittinger, K., Bushman, F. D., Costello, E. K., . . . Knight, R. (2010). QIIME allows analysis of high-throughput community sequencing data. *Nature Methods*, 7(5), 335-336.
10. Carrier, T. J., & Reitzel, A. M. (2017). The hologenime across environments and the implications of a host-associated microbial repertoire. *Frontiers in Microbiology*, 8. doi:10.3389/fmicb.2017.00802
11. Curd, E. E., Martiny, J. B. H., Li, H. Y., & Smith, T. B. (2018). Bacterial diversity is positively correlated with soil heterogeneity. *Ecosphere*, 9(1). doi:10.1002/ecs2.2079
12. Dai, T., Gupta, A., Murray, C. K., Vrahas, M. S., Tegos, G. P., & Hamblin, M. R. (2012). Blue light for infectious diseases: *Propionibacterium acnes*, *Helicobacter pylori*, and beyond? *Drug Resistance Updates*, 15(4), 223-236. doi:10.1016/j.drug.2012.07.001

13. Deaver, J. A., Eum, S. Y., & Toborek, M. (2018). Circadian disruption changes gut microbiome taxa and functional gene composition. *Frontiers in Microbiology*, 9. doi:10.3389/fmicb.2018.00737
14. Domin, H., Zurita-Gutierrez, Y. H., Scotti, M., Buttlar, J., Humeida, U. H., & Fraune, S. (2018). Predicted bacterial interactions affect in vivo microbial colonization dynamics in *Nematostella*. *Frontiers in Microbiology*, 9. doi:10.3389/fmicb.2018.00728
15. Dunlap, J. C. (1999). Molecular bases for circadian clocks. *Cell*, 96(2), 271-290.
16. Edgar, R. C., Haas, B. J., Clemente, J. C., Quince, C., & Knight, R. (2011). UCHIME improves sensitivity and speed of chimera detection. *Bioinformatics*, 27(16), 2194-2200.
17. Franzenburg, S., Fraune, S., Kunzel, S., Baines, J. F., Domazet-Loso, T., & Bosch, T. C. G. (2012). MyD88-deficient *Hydra* reveal an ancient function of TLR signaling in sensing bacterial colonizers. *Proceedings of the National Academy of Sciences of the United States of America*, 109(47), 19374-19379. doi:10.1073/pnas.1213110109
18. Fraune, S., Anton-Erxleben, F., Augustin, R., Franzenburg, S., Knop, M., Schroder, K., . . . Bosch, T. C. G. (2015). Bacteria-bacteria interactions within the microbiota of the ancestral metazoan *Hydra* contribute to fungal resistance. *ISME Journal*, 9(7), 1543-1556. doi:10.1038/ismej.2014.239
19. Fraune, S., & Bosch, T. C. G. (2010). Why bacteria matter in animal development and evolution. *Bioessays*, 32(7), 571-580. doi:10.1002/bies.200900192

20. Fraune, S., Foret, S., & Reitzel, A. M. (2016). Using *Nematostella vectensis* to study the interactions between genome, epigenome, and bacteria in a changing environment. *Frontiers in Marine Science*, 3. doi:10.3389/fmars.2016.00148
21. Hand, C., & Uhlinger, K. R. (1994). The unique, widely distributed, estuarine sea anemone, *Nematostella vectensis* Stephenson: a review, new facts, and questions. *Estuaries*, 17. doi:10.2307/1352679
22. Har, J. Y., Helbig, T., Lim, J. H., Fernando, S. C., Reitzel, A. M., Penn, K., & Thompson, J. R. (2015). Microbial diversity and activity in the *Nematostella vectensis* holobiont: insights from 16S rRNA gene sequencing, isolate genomes, and a pilot-scale survey of gene expression. *Frontiers in Microbiology*, 6. doi:10.3389/fmicb.2015.00818
23. Heath-Heckman, E. A. C. (2016). The metronome of symbiosis: interactions between microbes and the host circadian clock. *Integrative and Comparative Biology*, 56(5), 776-783. doi:10.1093/icb/icw067
24. Heath-Heckman, E. A. C., Peyer, S. M., Whistler, C. A., Apicella, M. A., Goldman, W. E., & McFall-Ngai, M. J. (2013). Bacterial bioluminescence regulates expression of a host cryptochrome gene in the squid-vibrio symbiosis. *mBio*, 4(2). doi:10.1128/mBio.00167-13
25. Hendricks, W. D., Byrum, C. A., & Meyer-Bernstein, E. L. (2012). Characterization of circadian behavior in the starlet sea anemone, *Nematostella vectensis*. *PLoS ONE*, 7(10), e46843. doi:10.1371/journal.pone.0046843
26. Hoadley, K. D., Vize, P. D., & Pyott, S. J. (2016). Current understanding of the circadian clock within Cnidaria. In S. Goffredo & Z. Dubinsky (Eds.), *The Cnidaria*,

- Past, Present and Future: The world of Medusa and her sisters (pp. 511-520). Cham: Springer International Publishing.
27. Huang, W., Ramsey, K. M., Marcheva, B., & Bass, J. (2011). Circadian rhythms, sleep, and metabolism. *Journal of Clinical Investigation*, 121(6), 2133-2141. doi:10.1172/jci46043
 28. Hubbard, C. J., Brock, M. T., van Diepen, L. T., Maignien, L., Ewers, B. E., & Weinig, C. (2018). The plant circadian clock influences rhizosphere community structure and function. *ISME Journal*, 12(2), 400-410. doi:10.1038/ismej.2017.172
 29. Hughes, M. E., Hogenesch, J. B., & Kornacker, K. (2010). JTK_CYCLE: An efficient nonparametric algorithm for detecting rhythmic components in genome-scale data sets. *Journal of Biological Rhythms*, 25(5), 372-380. doi:10.1177/0748730410379711
 30. Keller, M., Mazuch, J., Abraham, U., Eom, G. D., Herzog, E. D., Volk, H.-D., . . . Maier, B. (2009). A circadian clock in macrophages controls inflammatory immune responses. *Proceedings of the National Academy of Sciences*, 106(50), 21407-21412. doi:10.1073/pnas.0906361106
 31. Kelly, L. W., Williams, G. J., Barott, K. L., Carlson, C. A., Dinsdale, E. A., Edwards, R. A., . . . Rohwer, F. (2014). Local genomic adaptation of coral reef-associated microbiomes to gradients of natural variability and anthropogenic stressors. *Proceedings of the National Academy of Sciences of the United States of America*, 111(28), 10227-10232. doi:10.1073/pnas.1403319111
 32. Kimura, A., Sakaguchi, E., & Nonaka, M. (2009). Multi-component complement system of Cnidaria: C3, Bf, and MASP genes expressed in the endodermal tissues of

- a sea anemone, *Nematostella vectensis*. *Immunobiology*, 214(3), 165-178.
doi:10.1016/j.imbio.2009.01.003
33. Klindworth, A., Pruesse, E., Schweer, T., Peplies, J., Quast, C., Horn, M., & Glockner, F. O. (2013). Evaluation of general 16S ribosomal RNA gene PCR primers for classical and next-generation sequencing-based diversity studies. *Nucleic Acids Research*, 41(1), e1.
34. Kohl, K. D., & Dearing, M. D. (2012). Experience matters: prior exposure to plant toxins enhances diversity of gut microbes in herbivores. *Ecology Letters*, 15(9), 1008-1015. doi:10.1111/j.1461-0248.2012.01822.x
35. Lange, C., Hemmrich, G., Klostermeier, U. C., Lopez-Quintero, J. A., Miller, D. J., Rahn, T., . . . Rosenstiel, P. (2011). Defining the origins of the NOD-like receptor system at the base of animal evolution. *Molecular Biology and Evolution*, 28(5), 1687-1702. doi:10.1093/molbev/msq349
36. Leach, W. B., Macrander, J., Peres, R., & Reitzel, A. M. (2018). Transcriptome-wide analysis of differential gene expression in response to light:dark cycles in a model cnidarian. *Comparative Biochemistry and Physiology Part D: Genomics and Proteomics*, 26, 40-49. doi:org/10.1016/j.cbd.2018.03.004
37. Leach, W. B., & Reitzel, A. M. (2019). Transcriptional remodeling upon light removal in a model cnidarian: losses and gains in gene expression. *Molecular Ecology*, 28(14), 3414-3426. doi.org/10.1111/mec.15163
38. Leone, V., Gibbons, S. M., Martinez, K., Hutchison, A. L., Huang, E. Y., Cham, C. M., . . . Chang, E. B. (2015). Effects of diurnal variation of gut microbes and high-fat

- feeding on host circadian clock function and metabolism. *Cell Host & Microbe*, 17(5), 681-689. doi:10.1016/j.chom.2015.03.006
39. Liang, X., Bushman, F. D., & FitzGerald, G. A. (2015). Rhythmicity of the intestinal microbiota is regulated by gender and the host circadian clock. *Proceedings of the National Academy of Sciences of the United States of America*, 112(33), 10479-10484. doi:10.1073/pnas.1501305112
40. Lozupone, C., & Knight, R. (2005). UniFrac: a new phylogenetic method for comparing microbial communities. *Applied and Environmental Microbiology*, 71(12), 8228-8235.
41. Maas, A. E., Jones, I. T., Reitzel, A. M., & Tarrant, A. M. (2016). Daily cycle in oxygen consumption by the sea anemone *Nematostella vectensis* Stephenson. *Biology Open*, 5(2), 161.
42. Macke, E., Tasiemski, A., Massol, F., Callens, M., & Decaestecker, E. (2017). Life history and eco-evolutionary dynamics in light of the gut microbiota. *Oikos*, 126(4), 508-531. doi:10.1111/oik.03900
43. McFall-Ngai, M. J., & Ruby, E. G. (2000). Developmental biology in marine invertebrate symbioses. *Current Opinion in Microbiology*, 3(6), 603-607. doi:10.1016/s1369-5274(00)00147-8
44. Miller, D. J., Hemmrich, G., Ball, E. E., Hayward, D. C., Khalturin, K., Funayama, N., . . . Bosch, T. C. (2007). The innate immune repertoire in Cnidaria - ancestral complexity and stochastic gene loss. *Genome Biology*, 8(4), R59. doi:10.1186/gb-2007-8-4-r59

45. Mortzfeld, B. M., Urbanski, S., Reitzel, A. M., Kunzel, S., Technau, U., & Fraune, S. (2016). Response of bacterial colonization in *Nematostella vectensis* to development, environment and biogeography. *Environmental Microbiology*, 18(6), 1764-1781. doi:10.1111/1462-2920.12926
46. Nyholm, S. V., & Graf, J. (2012). Knowing your friends: invertebrate innate immunity fosters beneficial bacterial symbioses. *Nature Reviews Microbiology*, 10(12), 815-827. doi:10.1038/nrmicro2894
47. O'Brien, P. A., Webster, N. S., Miller, D. J., & Bourne, D. G. (2019). Host-microbe coevolution: applying evidence from model systems to complex marine invertebrate holobionts. *mBio*, 10(1). doi:10.1128/mBio.02241-18
48. Oren, M., Tarrant, A. M., Alon, S., Simon-Blecher, N., Elbaz, I., Appelbaum, L., & Levy, O. (2015). Profiling molecular and behavioral circadian rhythms in the non-symbiotic sea anemone *Nematostella vectensis*. *Scientific Reports*, 5, 11418. doi:10.1038/srep11418
49. Peres, R., Reitzel, A. M., Passamanek, Y., Afeche, S. C., Cipolla-Neto, J., Marques, A. C., & Martindale, M. Q. (2014). Developmental and light-entrained expression of melatonin and its relationship to the circadian clock in the sea anemone *Nematostella vectensis*. *EvoDevo*, 5, 26. doi:10.1186/2041-9139-5-26
50. Putnam, N. H., Srivastava, M., Hellsten, U., Dirks, B., Chapman, J., Salamov, A., . . . Rokhsar, D. S. (2007). Sea anemone genome reveals ancestral eumetazoan gene repertoire and genomic organization. *Science*, 317. doi:10.1126/science.1139158

51. Quast, C., Pruesse, E., Yilmaz, P., Gerken, J., Schweer, T., Yarza, P., . . . Glockner, F. O. (2013). The SILVA ribosomal RNA gene database project: improved data processing and web-based tools. *Nucleic Acids Research*, 41, 590-596.
52. Reitzel, A. M., Behrendt, L., & Tarrant, A. M. (2010). Light entrained rhythmic gene expression in the sea anemone *Nematostella vectensis*: the evolution of the animal circadian clock. *PLoS ONE*, 5(9), e12805.
53. Reitzel, A. M., Sullivan, J. C., Traylor-Knowles, N., & Finnerty, J. R. (2008). Genomic survey of candidate stress-response genes in the estuarine anemone *Nematostella vectensis*. *Biological Bulletin*, 214. doi:10.2307/25470666
54. Roopin, M., & Levy, O. (2012). Temporal and histological evaluation of melatonin patterns in a 'basal' metazoan. *Journal of Pineal Research*, 53(3), 259-269. doi:10.1111/j.1600-079X.2012.00994
55. Roopin, M., Yacobi, Y. Z., & Levy, O. (2013). Occurrence, diel patterns, and the influence of melatonin on the photosynthetic performance of cultured *Symbiodinium*. *Journal of Pineal Research*, 55(1), 89-100. doi:10.1111/jpi.12046
56. Shade, A., & Handelsman, J. (2012). Beyond the Venn diagram: the hunt for a core microbiome. *Environmental Microbiology*, 14(1), 4-12. doi:10.1111/j.1462-2920.2011.02585
57. Sharp, K. H., Pratte, Z. A., Kerwin, A. H., Rotjan, R. D., & Stewart, F. J. (2017). Season, but not symbiont state, drives microbiome structure in the temperate coral *Astrangia poculata*. *Microbiome*, 5. doi:10.1186/s40168-017-0329-8

58. Sieber, M., Pita, L., Weiland-Bräuer, N., Dirksen, P., Wang, J., Mortzfeld, B., . . . Traulsen, A. (2018). *The Neutral Metaorganism*. bioRxiv, 367243.
doi:10.1101/367243
59. Silveira, C. B., Gregoracci, G. B., Coutinho, F. H., Silva, G. G. Z., Haggerty, J. M., de Oliveira, L. S., . . . Thompson, F. L. (2017). Bacterial community associated with the reef coral *Mussismilia braziliensis*'s momentum boundary layer over a diel cycle. *Frontiers in Microbiology*, 8. doi:10.3389/fmicb.2017.00784
60. Sommer, F., & Backhed, F. (2013). The gut microbiota - masters of host development and physiology. *Nature Reviews Microbiology*, 11(4), 227-238.
doi:10.1038/nrmicro2974
61. Sorek, M., Díaz-Almeyda, E. M., Medina, M., & Levy, O. (2014). Circadian clocks in symbiotic corals: The duet between *Symbiodinium* algae and their coral host. *Marine Genomics*, 14, 47-57. doi:10.1016/j.margen.2014.01.003
62. Sorek, M., Yacobi, Y. Z., Roopin, M., Berman-Frank, I., & Levy, O. (2013). Photosynthetic circadian rhythmicity patterns of *Symbiodinium*, the coral endosymbiotic algae. *Proceedings of the Royal Society B-Biological Sciences*, 280(1762). doi:10.1098/rspb.2013.1012
63. Sullivan, J. C., Wolenski, F. S., Reitzel, A. M., French, C. E., Traylor-Knowles, N., Gilmore, T. D., & Finnerty, J. R. (2009). Two alleles of NF- κ B in the sea anemone *Nematostella vectensis* are widely dispersed in nature and encode proteins with distinct activities. *PLoS ONE*, 4(10), e7311.

64. Sweet, M. J., Brown, B. E., Dunne, R. P., Singleton, I., & Bulling, M. (2017). Evidence for rapid, tide-related shifts in the microbiome of the coral *Coelastrea aspera*. *Coral Reefs*, 36(3), 815-828. doi:10.1007/s00338-017-1572-y
65. Taniguchi, A., Yoshida, T., Hibino, K., & Eguchi, M. (2015). Community structures of actively growing bacteria stimulated by coral mucus. *Journal of Experimental Marine Biology and Ecology*, 469, 105-112. doi:10.1016/j.jembe.2015.04.020
66. Thaiss, C. A., Zeevi, D., Levy, M., Zilberman-Schapira, G., Suez, J., Tengeler, A. C., . . . Elinav, E. (2014). Transkingdom control of microbiota diurnal oscillations promotes metabolic homeostasis. *Cell*, 159(3), 514-529. doi:10.1016/j.cell.2014.09.048
67. Thaiss, C. A., Zmora, N., Levy, M., & Elinav, E. (2016). The microbiome and innate immunity. *Nature*, 535(7610), 65-74. doi:10.1038/nature18847
68. Vega, N. M., & Gore, J. (2017). Stochastic assembly produces heterogeneous communities in the *Caenorhabditis elegans* intestine. *PLoS Biology*, 15(3). doi:10.1371/journal.pbio.2000633
69. Vize, P. D. (2009). Transcriptome analysis of the circadian regulatory network in the coral *Acropora millepora*. *Biological Bulletin*, 216(2), 131-137.
70. Wier, A. M., Nyholm, S. V., Mandel, M. J., Massengo-Tiasse, R. P., Schaefer, A. L., Koroleva, I., . . . McFall-Ngai, M. J. (2010). Transcriptional patterns in both host and bacterium underlie a daily rhythm of anatomical and metabolic change in a beneficial symbiosis. *Proceedings of the National Academy of Sciences of the United States of America*, 107(5), 2259-2264. doi:10.1073/pnas.0909712107

71. Wolenski, F. S., Garbati, M. R., Lubinski, T. J., Traylor-Knowles, N., Dresselhaus, E., Stefanik, D. J., . . . Gilmore, T. D. (2011). Characterization of the core elements of the NF- κ B signaling pathway of the sea anemone *Nematostella vectensis*. *Molecular and Cellular Biology*, 31(5), 1076-1087. doi:10.1128/mcb.00927-10
72. Wu, G., Tang, W., He, Y., Hu, J., Gong, S., He, Z., . . . Chen, P. (2018). Light exposure influences the diurnal oscillation of gut microbiota in mice. *Biochemical and Biophysical Research Communications*, 501(1), 16-23. doi:10.1016/j.bbrc.2018.04.095
73. Yuen, B., Bayes, J. M., & Degnan, S. M. (2014). The characterization of sponge NLRs provides insight into the origin and evolution of this innate immune gene family in animals. *Molecular Biology and Evolution*, 31(1), 106-120. doi:10.1093/molbev/mst174
74. Zarrinpar, A., Chaix, A., Yooseph, S., & Panda, S. (2014). Diet and feeding pattern affect the diurnal dynamics of the gut microbiome. *Cell Metabolism*, 20(6), 1006-1017. doi:10.1016/j.cmet.2014.11.008
75. Zhang, J., Kobert, K., Flouri, T., & Stamatakis, A. (2014). PEAR: A fast and accurate Illumina Paired-End reAd mergeR. *Bioinformatics*, 30(5), 614-620

Table 1.4. Taxonomic classification for differentially abundant OTUs associated with *Nematostella vectensis* in light:dark (LD) relative to constant darkness (DD) conditions.

Phylum	Class	Order	Family	Genus	Log ₂ fold change	p-value	Adjusted p-value
Overabundant							
Bacteroidetes	Saprosiriae	Saprosirales	Chitinophagaceae	-	0.813	2.30E-06	3.30E-05
	Flavobacteria	Flavobacteriales	Flavobacteriaceae	Aequorivita	0.442	8.20E-03	5.40E-02
				Flavobacterium	0.73	3.40E-05	4.20E-04
				Polaribacter	0.959	7.50E-08	1.60E-06
				Tenacibaculum	0.658	7.40E-05	8.50E-04
Chlamydiae	Chlamydia	Chlamydiales	-	-	1.502	1.90E-18	1.60E-16
Lentisphaerae	Lentisphaeria	Lentisphaerales	Lentisphaeraceae	-	0.471	7.30E-03	5.20E-02
Planctomycetes	OM190	CL500-15	-	-	0.611	4.10E-04	3.90E-03
Proteobacteria	Alphaproteobacteria	Kiloniellales	-	-	0.429	1.30E-02	7.10E-02
			Kiloniellaceae	-	0.852	2.90E-07	5.00E-06
			Alteromonadaceae	Alteromonas	0.445	1.20E-02	6.70E-02
			Colwelliaceae	Thalassomonas	1.239	2.70E-13	1.60E-11
			Shewanellaceae	Shewanella	1.229	6.70E-12	2.90E-10
				-	0.467	6.50E-03	4.80E-02
				-	0.411	1.60E-02	8.20E-02
			Oceanospirillaceae	Oleibacter	0.467	8.20E-03	5.40E-02
			Pseudomonadaceae	Pseudomonas	1.024	8.80E-09	2.20E-07
Underabundant							
Bacteroidetes	Flavobacteria	Flavobacteriales	Cryomorphaceae	Fluviicola	-0.416	1.80E-02	8.50E-02
			Flavobacteriaceae	-	-0.44	1.00E-02	6.20E-02
				Polaribacter	-0.849	1.00E-06	1.60E-05
				Sediminicola	-0.515	1.90E-03	1.60E-02
				-	-0.937	8.30E-08	1.60E-06
Cyanobacteria ^a	Chloroplast	Stramenopiles	-	-	-1.71	1.30E-21	2.20E-19
				-	-1.085	7.70E-10	2.20E-08
Planctomycetes	Phycisphaerae	Phycisphaerales	Phycisphaeraceae	-	-0.599	1.90E-04	2.00E-03
				-	-0.512	1.60E-03	1.50E-02
			Pirellulaceae	-	-0.44	1.20E-02	6.90E-02
Proteobacteria	Alphaproteobacteria	Rhizobiales	Bradyrhizobiaceae	-	-0.418	1.50E-02	8.00E-02
		Rhodobacterales	Rhodobacteraceae	-	-0.408	1.70E-02	8.30E-02
		Sphingomonadales	-	-	-0.479	5.30E-03	4.10E-02

(Continues)

Table 1.4 Continued.

Phylum	Class	Order	Family	Genus	Log2 fold change	p-value	Adjusted p-value
	Gammaproteobacteria	Alteromonadales	Alteromonadaceae	-	-0.811	4.90E-06	6.50E-05
		Oceanospirillales	Oceanospirillaceae	Neptunomonas	-0.538	2.40E-03	2.00E-02
		Vibrionales	Pseudoalteromonadaceae	-	-0.447	9.20E-03	5.80E-02
			Vibrionaceae	Photobacterium	-0.422	1.80E-02	8.50E-02
				Vibrio	-0.464	9.50E-03	5.80E-02
Verrucomicrobia	Opitutae	Punicococcales	Punicococcaceae	Coraliomargarita	-0.648	2.50E-04	2.50E-03
	Verrucomicrobiae	Verrucomicrobiales	Verrucomicrobiaceae	Persicirhabdus	-1.1	4.10E-10	1.40E-08

^aPotential algal contaminant.

Table 2.4. Taxonomy of OTUs with significant 24-hour periodicity associated with adult *Nematostella vectensis* in light:dark (LD) and constant darkness (DD) conditions, as determined by JTK_Cycle.

	Operational Taxonomic Unit	Phylum	Class	Order	Family	Genus
LD						
OTU LD 1	New.ReferenceOTU9413	Proteobacteria	Alphaproteobacteria	Rhodobacterales	Rhodobacteraceae	-
OTU LD 2	DQ234245.1.1495	Proteobacteria	Alphaproteobacteria	Rhodobacterales	Rhodobacteraceae	-
OTU LD 3	DQ234200.1.1520	Proteobacteria	Alphaproteobacteria	Rhodobacterales	Rhodobacteraceae	-
OTU LD 4	KX874549.1.1479	Proteobacteria	Alphaproteobacteria	Rhodobacterales	Rhodobacteraceae	-
OTU LD 5	CP010912.3828314.3829852	Proteobacteria	Gammaproteobacteria	Alteromonadales	Alteromonadaceae	Alteromonas
DD						
OTU DD 1	New.ReferenceOTU22615	Chlamydiae	Chlamydia	Chlamydiales	-	-
OTU DD 2	JN713484.1.1490	Spirochaetes	Spirochaetes	Spirochaetales	Spirochaetaceae	-
OTU DD 3	JQ999980.1.1535	Proteobacteria	Gammaproteobacteria	Oceanospirillales	Alcanivoracaceae	Alcanivorax
OTU DD 4	FPLL01004330.9.1533	Chlamydiae	Chlamydia	Chlamydiales	-	-
OTU DD 5	New.ReferenceOTU16126	Planctomycetes	OM190	CL500-15	-	-

Table 3.4. Differential gene expression of candidate cnidarian innate immune genes between light:dark (LD) and constant darkness (DD) determined by DESeq2. NOD genes were arbitrarily given numbers and the order matches the order in Supplemental Table 1 from Lange et al. (2011).

Annotation	JGI	log2 fold change ^a	p-value ^b
BF1	41116	-0.7869	0.0084
BF2	204186	-0.3549	0.0393
C3-1	18	-1.1465	0.0002
IκB	-	NA	NA
IKK	163386	0.0700	0.4012
LBP	170435	-0.0743	0.5176
MASP	138799	NA	NA
Myd88	82163	0.1660	0.1944
NFκB	174238	NA	NA
RIGIa	87071	0.3639	0.0051
TAB2	233007	0.1264	0.1200
TAK1 (MAP3K7)	87118	-0.0534	0.7785
TLR1	16780	NA	NA
TLR2	201237	NA	NA
TLR3	196737	NA	NA
TLR4	204009	NA	NA
TRAF6	178259	0.1389	0.3813
Nod_2	160179	-0.1109	0.4910
Nod_23	220102	-0.4177	0.0077
Nod_29	248679	0.0308	0.9093
Nod_30	242728	0.0705	0.7583
Nod_31	247590	0.2500	0.0210
Nod_35	240600	0.4993	0.1402
Nod_36	240601	0.2482	0.0486
Nod_51	94204	0.0571	0.7559
Nod_53	87696	-0.1262	0.3731
Nod_54	60625	0.1746	0.2458
Nod_55	138346	0.0657	0.7723
Nod_61	247717	0.1617	0.1242
Nod_62	215101	0.1173	0.2788
Nod_63	246451	-0.1069	0.4213
Nod_66	244932	-0.0894	0.4993
Nod_68	239890	0.1620	0.2123

Note: NA genes did not meet the mean count cutoff for DESeq2.

Bold text indicates significant up- or down-regulation.

^aPairwise comparisons using Wald tests in DESeq2.

^bBenjamini-Hochberg FDR corrected p-value.

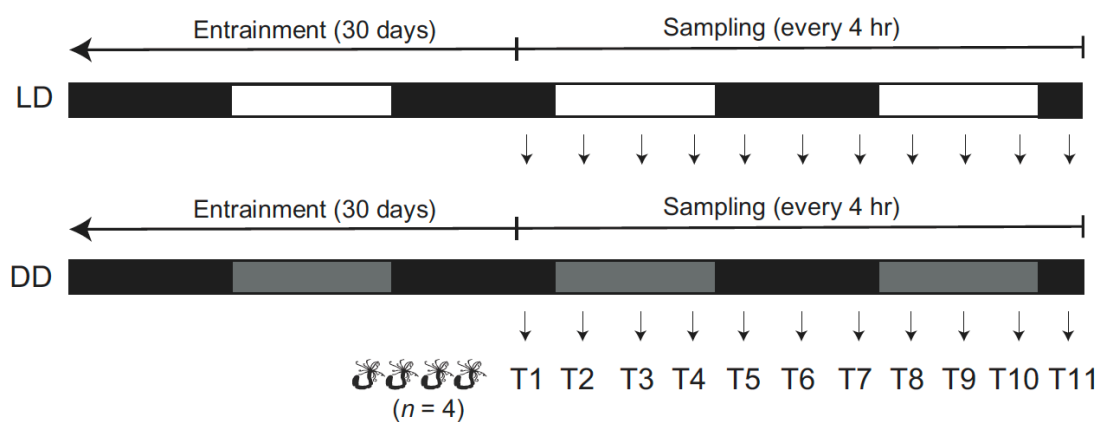


Figure 1. Experimental design for light:dark (LD) and constant dark conditions (DD) and corresponding sampling.

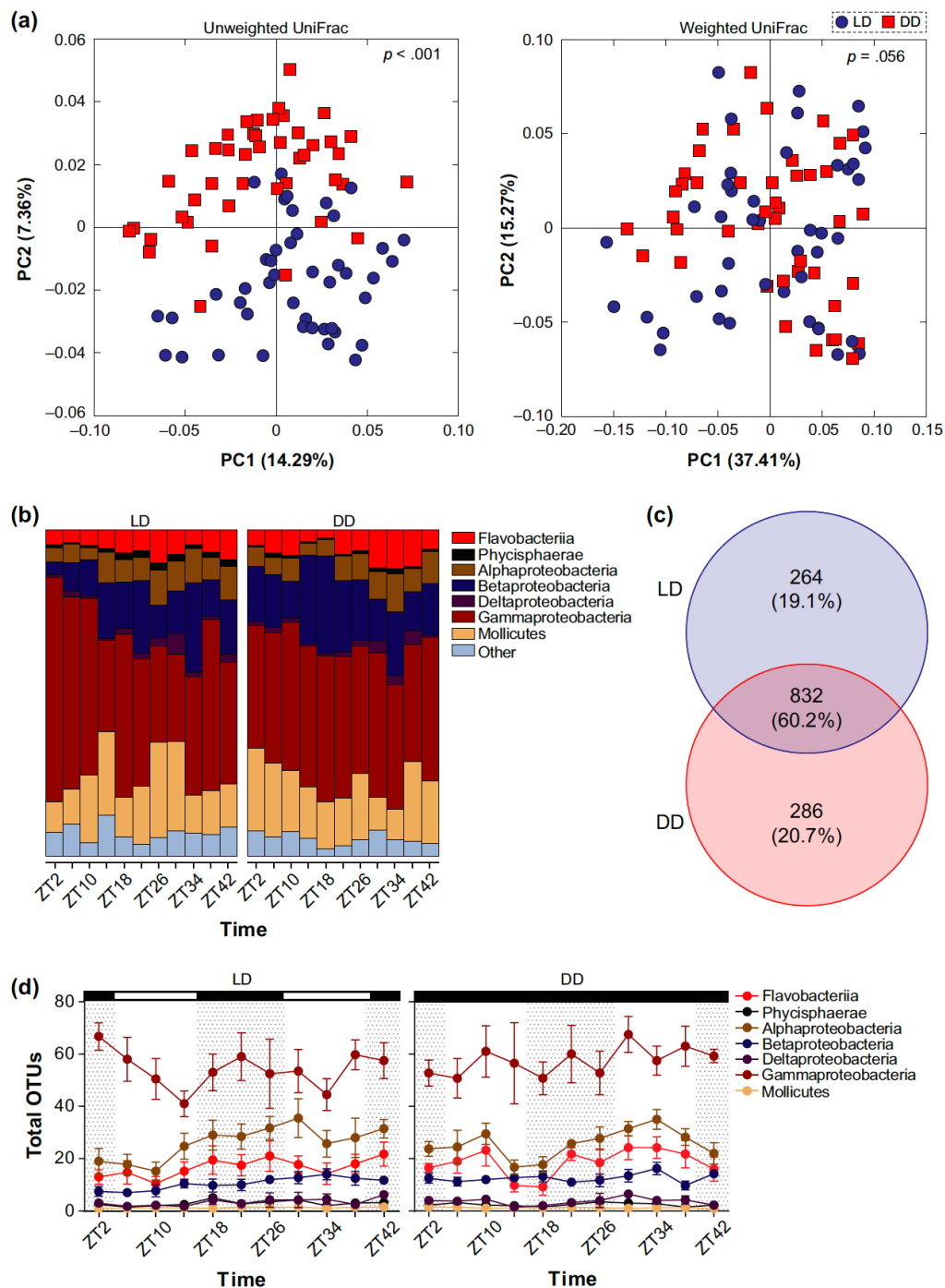


Figure 2. Similarity amongst the bacterial community associated with light:dark (LD) and constant darkness (DD) entrained *Nematostella vectensis*. (A) Community similarity for *N. vectensis* entrained to a diel photoperiod and constant conditions based on unweighted and weighted UniFrac metric. (B) Bacterial classes associated with *N. vectensis* when entrained to LD or DD that represent at least 1% of the community (with classes representing less than 1% of the community grouped under ‘other’). (C) Bacterial OTUs that were either LD-specific, DD-specific, or shared between the two conditions. (D) Total OTUs for each bacterial class (that represents at least 1% of the community).

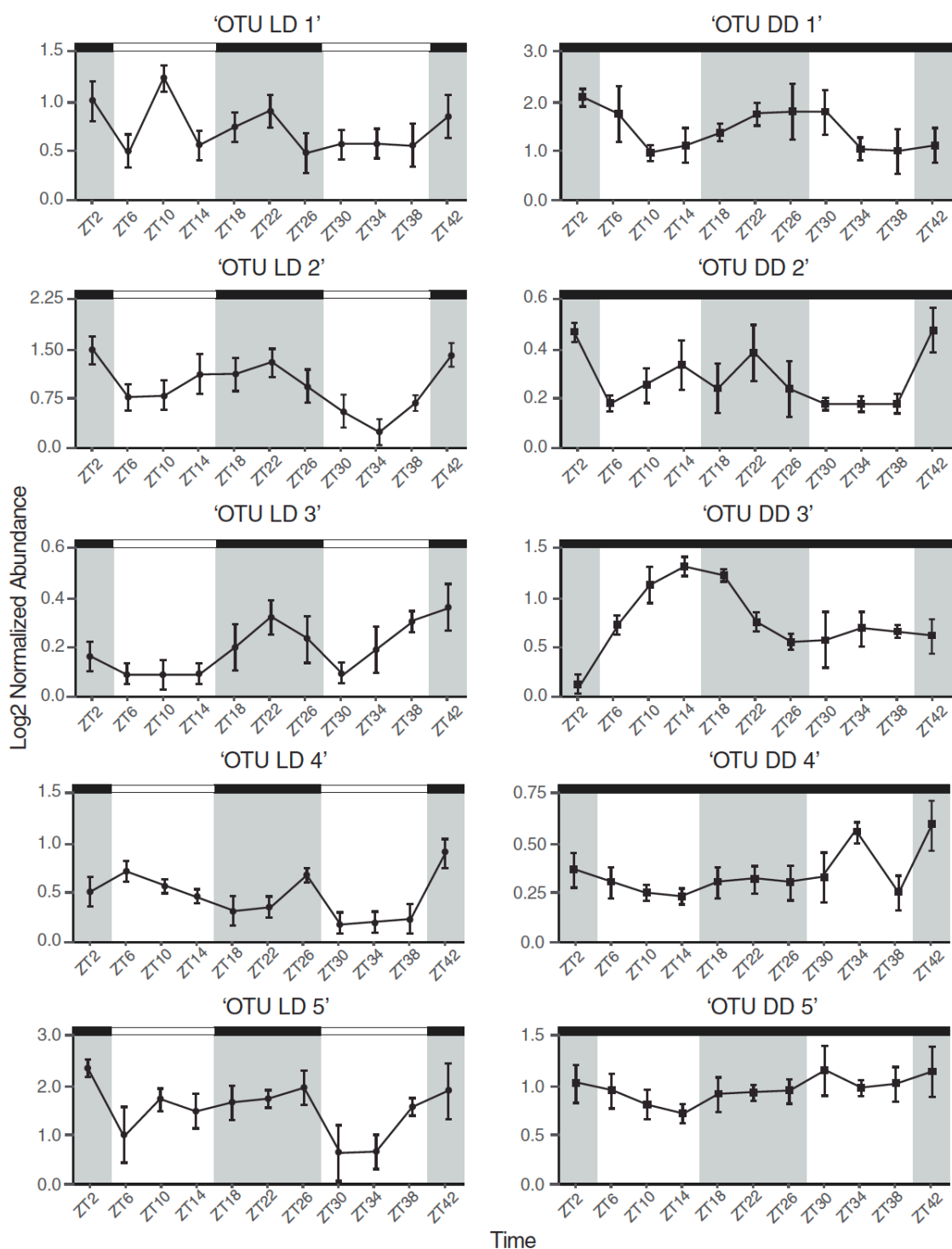


Figure 3. Abundance plots of 24-hour cycling bacterial OTUs during light:dark (left panel; black and white boxes) and constant darkness (right panel; solid black boxes) over the time course. Grey shaded areas indicate night and white areas indicate day. OTU names have been simplified, and full names can be found in Table 2.

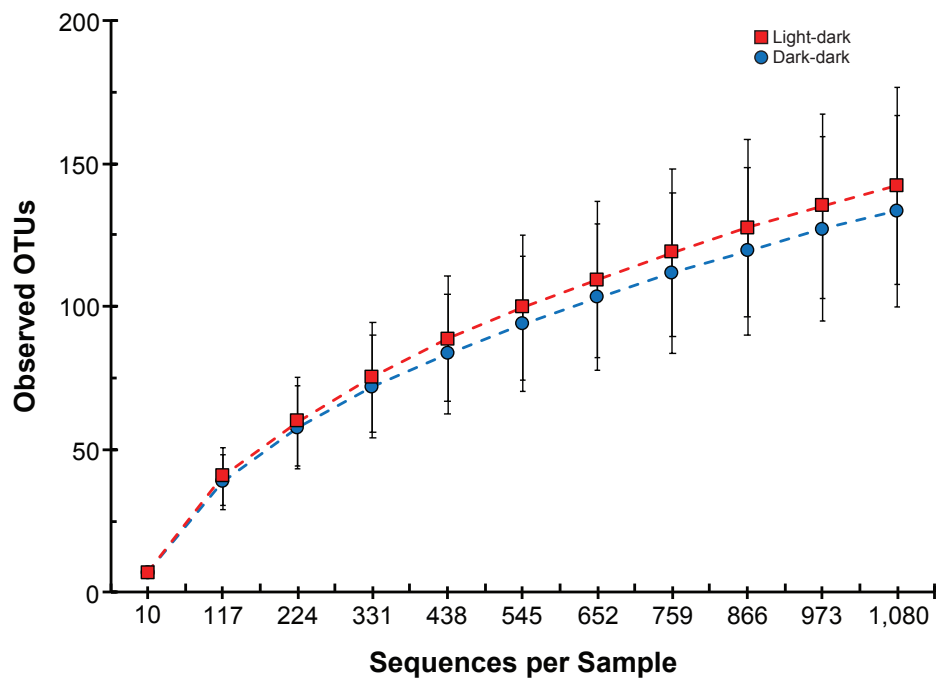


Figure S1. Alpha rarefaction curves for LD and DD entrained *Nematostella vectensis*. Alpha rarefaction curves for the associated microbiota for *N. vectensis* that were entrained to either a 12-hour light: 12-hour dark light cycle (red squares) or 24 hours of darkness (blue circles) based on the rarefaction depth (1,080 sequences) used for all PCoA plots.

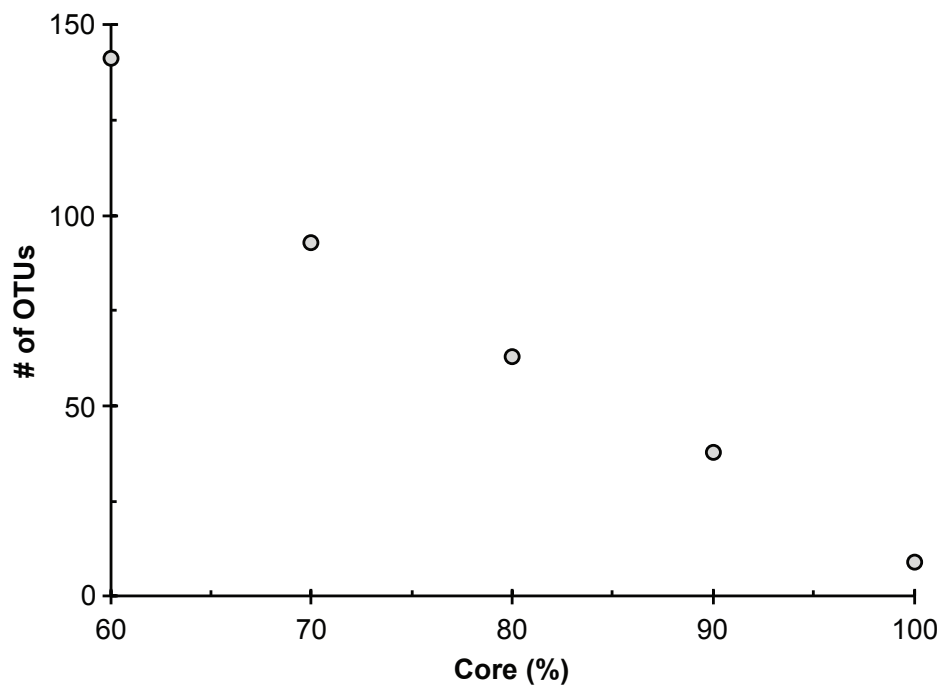


Figure S2. Number of OTUs for the 'core' bacterial community. Enumeration of the bacterial phylotypes of the 'core' bacterial community associated with *Nematostella vectensis* for LD and DD entrained individuals for 60%, 70%, 80%, 90%, and 100% of sampled anemones.

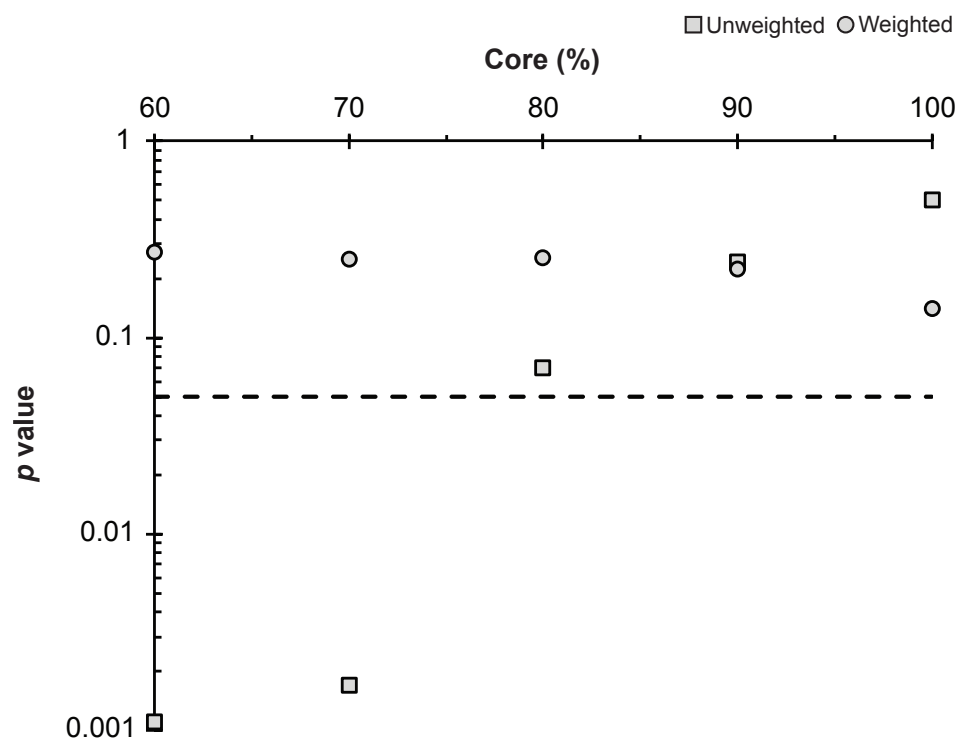


Figure S3. Beta-diversity statistics for 'core' diversity analyses. Representation of statistical comparisons (ANOSIM) between the 'core' (at 60%, 70%, 80%, 90%, and 100%) bacterial communities associated with LD and DD entrained *Nematostella vectensis*.

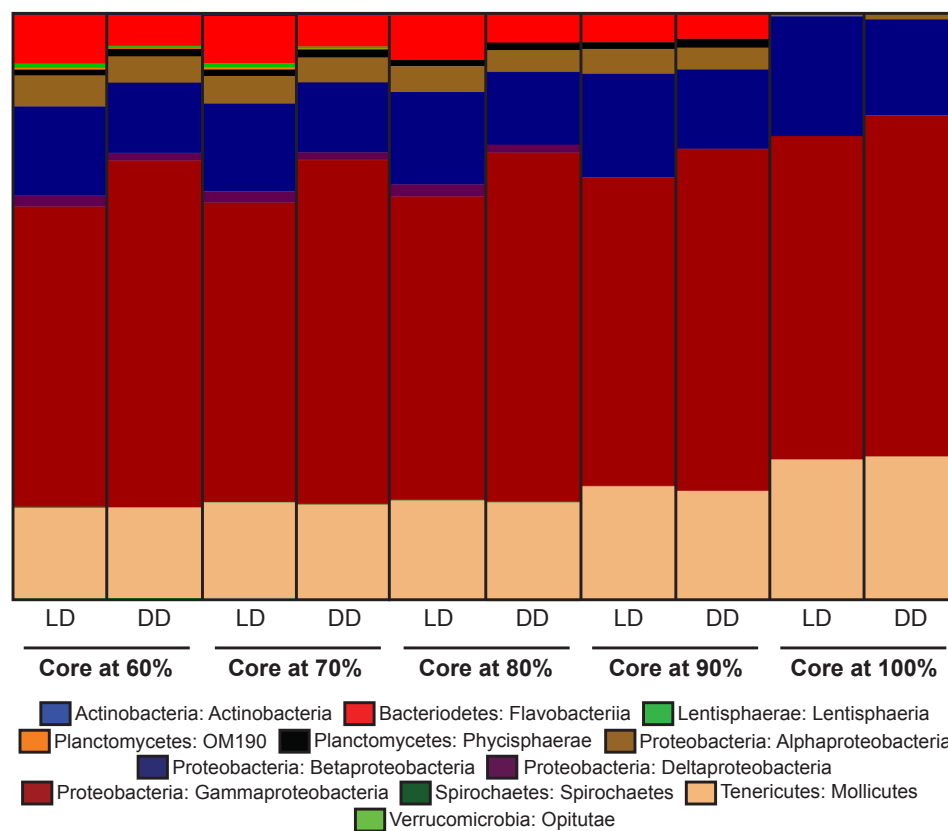


Figure S4. ‘Core’ bacterial taxa associated with adult *Nematostella vectensis* across treatments. Classes of bacteria associated with LD and DD entrained *N. vectensis* for the ‘core’ community at the 60%, 70%, 80%, 90%, and 100% level.

Supplemental Note 1

Quality control and preparation for analyses in QIIME:

- 1) Pair forward and reverse files using PEAR (pear-0.9.10-bin-64)
- 2) Trim paired files using Trimmomatic (trimmomatic-0.36.jar)
- 3) Convert paired and trimmed .fastq to .fasta using the custom code: `cat [input .fastq] | paste - - - | cut -f 1,2 | sed 's/^/>/' | tr "\t" "\n" >[output .fasta]`
- 4) Validate tab-delimited mapping file using 'validate_mapping_file.py'
- 5) Generate meta-.fasta files using 'add_qiime_labels.py'
- 6) Detect chimeras using usearch and the 'rdp_gold.fa' database from the meta-.fasta (called, 'combined_seqs.fna').
- 7) Filter chimeras using 'filter_fasta.py'
- 8) Pick OTUs with a 99% clustering using 'pick_open_reference_otus.py' and the 'silva_132_99_16S.fna' database
- 9) Filter OTUs with <10 reads and 'unassigned' using 'filter_otus_from_otu_table.py'
- 10) Determine rarefaction depth using 'biom summarize-table'
- 11) Rarefaction depth was visualized using 'alpha_rarefaction.py'

Community-level dynamics:

- 12) All beta diversity via PCoA were calculated using 'jackknifed_beta_diversity.py'
- 13) Two-dimensional PCoA were created from the 'pcoa' sub-directory of the 'jackknifed_beta_diversity.py' output using 'make_2d_plots.py'
- 14) Alpha diversity estimates were calculated using 'alpha_diversity.py'
- 15) Filtered .biom tables for beta diversity analyses using sub-sets of samples were split using 'split_otu_table.py'

Composition of the bacterial community

- 16) Community composition plots were generated using 'summarize_taxa_through_plots.py'
- 17) Differentially abundant OTUs were determined using 'differential_abundance.py' using 'DESeq2_nbinom' and dark-dark as 'x' and light-dark as 'y'

Shared taxa between LD and DD

- 18) Core bacterial communities were determined using 'compute_core_microbiome.py'
- 19) Beta diversity comparisons were performed using 'jackknifed_beta_diversity.py' and statistics were completed using 'compare_categories.py'
- 20) Community composition plots of the 'core' bacterial community were generated using 'summarize_taxa_through_plots.py'

CHAPTER 5

GLOBAL TEMPORAL GENE EXPRESSION OF *NEMATOSTELLA VECTENSIS* IN-SITU

Whitney B. Leach, Ann M. Tarrant, and Adam M. Reitzel

Abstract

Aquatic organisms in their natural environments are continuously subjected to several fluctuating environmental factors at once, including temperature, salinity, and resource availability. Comparative transcriptomics provides robust gene expression datasets without being cost prohibitive to characterize how individuals respond to complex environments and are increasingly more common in the field of ecological and environmental biology. We assessed genome-wide temporal transcript expression patterns in the sea anemone, *Nematostella vectensis*, in Great Sippewissett Marsh in Massachusetts, where anemones experienced a natural light cycle with intensity varying from 0-200 lum/ft², daily temperature fluctuations of ~9°C. We measured 'in situ' gene expression from recaptured anemones every hour from 0800 to 1700 and identified six time-dependent gene clusters, represented by several genes involved in metabolism, stress, and transcription-translation related functions. Of the six clusters, three were composed of genes up-regulated in the afternoon, and three were composed of genes up-regulated in the morning. A total of 2,311 transcripts were differentially expressed between morning and afternoon samples, including genes related to G-protein-coupled receptors and heat shock binding proteins. By sampling *Nematostella* in the field, we have a greater understanding of the transcriptional responses that vary in natural conditions when exposed to multiple environmental factors simultaneously.

Introduction

In the field of molecular ecology, recent advances in sequencing technologies have greatly increased our ability to relate transcription-level responses of organisms to environmental and ecosystem level factors. Next generation transcriptomic approaches that use high throughput sequencing have allowed researchers to screen thousands of genes simultaneously in order to identify those that impact ecologically relevant traits, particularly environmental stress tolerance (Chen et al., 2015; Li et al., 2014; Lu et al., 2016; Smith et al., 2013). Application of transcriptomics has led to a rich understanding of how complex traits are shaped by genes in controlled laboratory settings; however, utilization of these techniques in ecological, field-based studies remain quite rare and nascent (Todd et al., 2016). When organisms are sampled from natural habitats, most studies sample just once during the day and we know of no studies that have looked at organismal responses over shorter time scales.

An organism's response to environmental stressors, or even standard daily oscillations in conditions, typically involves many genes and could have complex responses involving synergism, antagonisms, and additivity when these environmental signals are in combination (Schaefer and Piggott, 2018). It is rare for an organism to experience an isolated single stress event that typifies a majority of lab-based studies because important contextual elements of real world ecosystems are removed (Gunderson et al., 2016; Hofmann et al., 2005; Jackson et al., 2002; Purugganan and Gibson, 2003). Gene expression is also temporally variable affected by light:dark cycles, life history stage, or developmental stage (Aubin-Horth and Renn, 2009). This interaction between

an organism and its environment provides opportunity for measuring responses to dynamic conditions simultaneously, where transcriptional response to complex signals and/or challenges would otherwise not be observed (Chapman et al., 2011; Li and Brouwer, 2013; Mishra et al., 2012; Muller et al., 1998; Overgaard et al., 2010; Satake et al., 2019; Vanin et al., 2012). Meta-analyses on the interaction between multiple stressors in marine ecosystems found that most multi-stressor events are synergistic (Crain et al., 2008; Harvey et al., 2013; McBryan et al., 2013; Przeslawski et al., 2015), but only 10% of evaluated studies were conducted in a field setting (Crain et al., 2008).

The physiological or molecular response to any environmental variable is complicated by the presence of both individual and population level genetic variation. In order to define the context-specific biological importance of differential transcriptomic responses, it may be critical to understand the existing level of variation in gene expression within individuals or populations that potentially reflect adaptations (Crawford and Oleksiak, 2007; Dalziel et al., 2009; Oleksiak et al., 2002). Further, inter-individual variation in gene expression is rarely reported and is often assumed to be minimal between genetically related individuals. In order to adequately define biological significance of a gene or gene set in transcriptomic studies and if mRNA expression drives organismal phenotypes, it is important to evaluate how gene expression varies within individuals (Crawford and Oleksiak, 2007; Oleksiak et al., 2002). Previous studies of transcriptomic responses have not explicitly included genetic variation in the analyses of differences in gene expression. One study by Reitzel et al. (2013a) suggested that different clonal genotypes vary in their responses to temperature, but a genetic connection was not explicitly performed. Therefore, while there is some evidence that

different genotypes vary in their response to abiotic variation, specific responses and the genetic correlations have not been studied. Small changes in the environment are reported to have significant effects on gene expression studies done in natural populations, particularly in genes related to stress response (Richards et al., 2012). Expression variation may also reflect differential regulatory elements or epigenetic modifications independent of genotypic variation within individuals or populations (Oleksiak et al., 2002).

Estuaries play a key role in coastal biodiversity as a nursery used by several aquatic and terrestrial species as well as resident habitat for estuarine specialists (Beck et al., 2001). These brackish environments are areas with high nutrient content that experience a complete salinity gradient, significant fluctuations in temperature and salinity, and daily pH oscillations. Because of these conditions, estuarine specialists must be adapted to a broad range of abiotic perturbations, particularly aquatic benthic species. *Nematostella vectensis* is a euryhaline, sessile sea anemone with a broad geographical range (Hand and Uhlinger, 1994; Williams, 1983). The distribution of *Nematostella* reflects their ability to survive extreme, with respect to typical open ocean conditions, daily and seasonal temperature and salinity gradients, unpredictable food availability, pollutants, and variation in oxygen. This exposure to large shifts in abiotic factors positions *Nematostella* as an experimental model for investigating the molecular basis of environmental stress response (Reitzel et al., 2013a).

A number of studies have taken traditional approaches to characterizing *Nematostella* gene expression in normal and variable laboratory conditions (Elran et al., 2014; Helm et al., 2013; Leach and Reitzel, 2019; Oren et al., 2015; Warner et al., 2018).

While straightforward and valuable for understanding transcriptional changes in response to environmental variables, transcript response profiles of animals exposed to simulated stressors likely only reveal a subset of the behavioral and physiological responses exhibited in natural ecological conditions. The position of this species in the thixotropic sediments of tidally restricted estuarine pools makes it possible to study them ‘*in-situ*’.

We present here the first study to quantify temporal shifts in the transcriptome for a cnidarian in the field over a high-density time series (hourly). Combining our knowledge of molecular and organismal biology, these data contribute to our understanding of how daily abiotic fluctuations drive specific molecular responses in this species, and how gene expression among individuals varies in a natural population. We collected anemones hourly for 10 hours from a tidal pool in Great Sippewissett Marsh on Cape Cod in Massachusetts. This approach allowed us to identify genes that significantly vary in expression over a fine time scale in a dynamic habitat, revealing that time-of-day and sampling strategy impact the interpretation of gene expression analyses.

Methods

Animal culture: in the laboratory and in the field

Adult *Nematostella* originally collected from Great Sippewissett Marsh, Massachusetts were maintained in the laboratory for several generations as described in Hand and Uhlinger (1992). In preparation for the study, salinity was adjusted to mimic field conditions (30 parts per thousand), and 200 anemones were transferred to marsh sediments of a tidally restricted pool in Sippewissett, MA (41°58' N, 70°63' W), where a native population of *Nematostella* is routinely collected (Hand and Uhlinger, 1994;

Reitzel et al., 2013b) (Figure 1). To ensure recapture, anemones were housed in 10 small pens constructed from mesh netting and open plastic cages designed for rearing aquarium fish. Each pen was anchored into the sediment using steel tent stakes to ensure the pens would remain fully submerged at each tidal stage (Figure S1). On June 18, 2018, the pens were recovered hourly beginning at 0800, ZT = 3 and ending at 1700, ZT = 12. At each time point, 10 individuals from each pen were removed from the pens with a transfer pipette while still in the field and immediately placed in RNAlater. Four animals were prepared for sequencing as individuals (A, B, C, D) and the remaining six were pooled in groups of two (E, F, G) for each time point. Environmental conditions were monitored using a HOBO logger which measured temperature and light (Onset Computer Corporation, Borne MA) from 5/23/18 through 6/29/18 in 10-minute intervals.

TagSeq: library preparation, sequencing, and processing

Total RNA was isolated from 70 samples: single individuals ($n = 4$) and pools of two anemones ($n = 3$) for 10 time points, using the RNAqueous kit (Ambion) according to the manufacturer's protocol followed by DNase treatment with a DNA-free kit (Invitrogen). RNA quantity was assessed using a NanoDrop 2000 spectrophotometer (Thermo Fisher Scientific) and after normalization, RNA was sent to the University of Texas at Austin's Genomic Sequencing and Analysis Facility (GSAF) for tag-based library preparation and sequencing with Illumina HiSeq 2500. Four of 70 samples were lost due to poor RNA quality prior to sequencing: three samples from time point 2 (T2A, T2B, T2G) and one sample from time point 4 (T4E). Raw sequence data from the remaining 66 libraries were delivered from the UT Austin GSAF (100 bp, SE).

An average of 3,780,445 million raw reads were generated from TagSeq ranging from 2,253,661 to 5,472,173 per sample resulting in a total of 255,449,390 raw reads. Reads were trimmed of the 5' Illumina leader sequence and reads without it were discarded. Reads were then quality-filtered and trimmed immediately following the adapter sequence or the degenerate tag using FastX-toolkit (Pearson et al., 1997) to retain sequences with at least 20 bases. Trimmed and filtered reads were mapped to the Vienna *Nematostella* transcriptome using Bowtie2 (Langmead and Salzberg, 2012). Reads mapping to the reference at the same start position with 100% alignment identify of the transcript were regarded as PCR duplicates and discarded from the dataset. Only reads mapping to a single gene in the reference transcriptome were sorted into a read-counts-per-gene table before import into the R environment for all downstream statistical analysis (R3.5.0, R Core Team 2015).

Expression variation between individual and pooled samples

The raw count data were transformed and statistically compared using a Levene's test in order to test the homogeneity of variance between pooled and individual samples (Levene, 1960). At each of the 10 time points, to calculate the dispersion statistic, one replicate was removed from the individual samples (replicate D) to have an equal number of samples in each group. An unequal sample size due to the loss of three samples excluded time point 2 from this analysis. Transformed counts were rounded to the nearest integer and arranged into a read-counts-per-gene table (Table S1). The Levene transformed counts table was reduced to genes with at least three counts. DESeq2 (Love et al., 2014) was then used to identify genes with significant differences in variation of expression between each sampling strategy. The variance between replicates of pooled

and individual samples was compared for each differentially variable gene at each of the 9 time points.

Gene expression analyses

The raw read-counts-per-gene table was filtered to contain only genes with at least three counts. The filtered counts table was used to perform outlier detection with the `arrayQualityMetrics` package (Kauffmann et al., 2009). Using the distance between arrays method within `arrayQualityMetrics`, the distribution of all values was calculated and a threshold of 25.8 was determined. All values exceeding this value ($n=3$) were discarded from future analyses. The remaining 63 libraries' count data were analyzed using the R package `DESeq2` (Love et al., 2014), which produced a normalized counts-per-gene table, to be used in subsequent analyses. For principal component analyses (PCA), gene ontology analyses (GO), and cluster analyses (WGCNA) the normalized count data was regularized-logarithm transformed (`rlog`) using `DESeq2` as in Leach & Reitzel (2019).

Transcriptional profiles in this field-based study were compared with a previous laboratory-based study by Leach and Reitzel (2019) for similarities and differences in gene expression over a similar period of daylight. In the laboratory study, a time series experiment was performed by sequencing transcript profiles of anemones entrained to 12-hour light: 12-hour dark cycles (LD) were in 4-hour intervals for a period of one day, whereupon sampling continued for two additional days after the exogenous light cue was removed. The light cycle was set to mimic natural light conditions, where Zeitgeber time, or $ZT = 0$ / "lights on" was at 7:00 AM and $ZT = 12$ / "lights off" was at 7:00 PM. The first sampling occurred at $ZT = 2$, or 9:00 AM and the second sampling point was collected at $ZT = 6$, or 1:00 PM. In the current field-based study, the first sampling time

point was at ZT = 3 or 8:00 AM (ZT = 0, or sunrise, was at 5:08 AM, with 15 hours and 11 minutes of daylight hours). In order to make the most accurate (*potential section of discussion*) comparison, differential gene expression between ZT = 2 and ZT = 6 of the laboratory-based study was compared to ZT = 3 and ZT = 6 of the field-based study.

Results

Differentially variable genes between pooled and individual samples

Applying a Levene-test to transformed count data and subsequently analyzing differently variable genes between single individual or pooled (two individuals per sample) samples per time point revealed a total of 1,219 significantly differently variable genes across all time points (excluding ZT = 4, see methods) after correction for multiple testing (FDR 10%). Comparison of mean variances of individual and pooled samples at each time point did not indicate a consistent direction of variance between the two groups. Instead, larger variance was observed in either individual or pooled samples, depending on the time point. At ZT = 3, ZT = 5, ZT = 6, and ZT = 12, the variance in individual samples was greater, at ZT = 7, ZT = 8, ZT = 9, the variation was greater in pooled samples, and at ZT = 10 and ZT = 11 the variance was equal between the two groups; therefore, individual and pooled samples were treated as biological replicates for gene expression analyses in later analyses. Broadly, the variation for samples early in the day was greater than samples later in the afternoon. At ZT = 3, 222 genes were differently variable between groups and of these, 80% were more variable among individual samples. At ZT = 9, 105 genes were differently variable between groups but

79% were more variable in pooled samples. No genes were consistently variable between groups at every time point.

Nematostella 'in-situ' gene expression is correlated with time-of-day

Of the ~12,000 genes remaining after outlier removal and filtering, 2,311 significantly differentially expressed genes (DEGs) between morning and afternoon time points were identified (10% FDR correction, padj in DESeq2). Of these DEGs, 1,099 were up-regulated in the afternoon and 1,212 were up-regulated in the morning. Principle component analysis of all significant DEGs (padj < 0.1) revealed that PC1 explains 24% of the variation and PC2 explains 8% of the variation between morning (blue) and afternoon samples (yellow) (Figure 2). Heat shock proteins (HSPs) are often up-regulated in cnidarians as a thermal stress response, particularly HSP70s (Waller et al., 2018). Interestingly, we measured up-regulation of several HSP40s (also referred to as DNAJ) in the afternoon, with the highest expression at ZT = 9, approximately one hour after the daily high temperature. These genes have been linked to protein folding in the coral *Stylophora pistillata* during early heat stress (Maor-Landaw et al., 2014).

Functional enrichment of genes that differed between morning and afternoon sampled *Nematostella* indicated temporal regulation of gene expression *in-situ*. Gene ontology analysis (GO) for DEGs (2,311 genes; 10% FDR) found genes up-regulated in the morning to be enriched for 'G protein-coupled receptor' (GO:0001664), 'DNA-binding transcription activator' (GO:0001228; GO:0001216), and 'signaling receptor' (GO:0004888; GO:0038023) of the Molecular Function category (Figure S2). Genes up-regulated in the afternoon were enriched for the Molecular Functions 'HSP70 protein binding' (GO:0030544), 'methylated histone binding' (GO:0035064; GO:0140034),

'transcription factor binding' (GO:0008134), and *'modification-dependent protein binding'* (GO:0140030). In the Biological Processes category, genes of the GO terms *'oxidation-reduction process'* (GO:0055114), *'respiratory electron transport chain'* (GO:0022900; GO:0022904; GO:0006119), and *'generation of precursor metabolites and energy'* (GO:0006091; GO:0015980) were up-regulated in the morning, while genes of the GO terms *'DNA metabolic process'* (GO:0006259), and *'histone modification'* (GO:0016570; GO:0016569) were up-regulated in the afternoon (Figure S3).

Of the 2,311 transcripts DESeq2 identified as differentially expressed, 1,883 were partitioned into six co-expression cluster eigengene, or modules. Each cluster was assigned an arbitrary color name (Figure 3) and correlates with samples from either morning or afternoon collected samples. The brown gene cluster (381 genes), blue gene cluster (393 genes), and red gene clusters (93 genes) were significantly negatively correlated with morning expression (Figure 3). The black gene cluster (68 genes), along with the pink gene cluster (217 genes) and the turquoise gene cluster (731 genes) were significantly positively correlated with morning expression at several time points (Figure 3). No clusters were significantly different between replicates (A-G, Figure 3). These relationships were validated by calculating the absolute value of the correlation of each gene within a cluster, or the gene significance, and the correlation of each gene's expression in the cluster to the entire clusters' expression pattern, or module membership (i.e., of all of the genes in a single cluster, the proportion with the same expression pattern is significant). The strongest relationship was observed for genes in the turquoise cluster at ZT = 5 (Pearson's $R^2 = 0.61$, $p\text{-value} = 1e-75$; Figure S4A) and at 2PM (Pearson's $R^2 = 0.66$, $p\text{-value} = 1.3e-92$; Figure S4B). Genes in this cluster were

significantly up-regulated in the morning (ZT = 5, p -value = 8e-04) and significantly down-regulated in the afternoon (ZT = 9, p -value = 3e-05) (Figure 3).

Functional analysis of gene clusters with up-regulation in the afternoon revealed enrichment (blue, brown, red; Figure 4) for chromatin modifications [i.e., '*chromatin binding*' (GO:0003682), '*helicase*' (GO:0004386; GO:0008026; GO:0070035), '*histone acetyltransferase*' (GO:0000123; GO:0031248; GO:1902493), '*regulation of chromosome organization*' (GO:0033044), '*N-methyltransferase*' (GO:0008170; GO:0008276)]; RNA modifications [i.e., '*translation regulator*' (GO:0045182), '*RNA splicing*' (GO:0006397), '*RNA processing*' (GO:0006396), '*DNA-directed RNA polymerase complex*' (GO:0000428)]; and protein regulation [i.e., '*protein domain specific binding*' (GO:0019904), '*protein binding*' (GO:0030674), '*positive regulation of protein modification process*' (GO:0001934)].

Clusters with up-regulation in the morning (black, pink, turquoise; Figure 4) were enriched for functions involving metabolism [i.e., '*oxidation-reduction process*' (GO:0055114), '*oxidative phosphorylation*' (GO:0006119), '*ATP metabolic process*' (GO:0046034), '*steroid metabolic process*' (GO:0008202), '*glucose metabolic process*' (*glucose metabolic process*), '*carbohydrate metabolic process*' (GO:0005975), '*cellular response to oxygen-containing compound*' (GO:1901701)]; immune function ('*regulation of immune system process*' (GO:0002682), '*innate immune response*' (GO:0045087), '*regulation of defense response*' (GO:0031347), '*immune effector process*' (GO:0002252)]; and photo-response [i.e., '*G protein-coupled receptor*' (*G protein-coupled receptor*), '*signaling receptor*' (GO:0004888), '*molecular transducer*' (GO:0004871), '*regulation of response to external stimulus*' (GO:0032101),

'photoreceptor cell differentiation' (GO:0046530), *'sensory organ development'* (GO:0007423)].

Environmental conditions

Temperature and light monitoring of the pool where anemones were collected was monitored before and after sampling occurred for > 1 month. The salinity was not monitored continuously but was recorded at 31 PPT on the day of sampling. Light intensity ranged from 0-200 lum/ft², with peak intensity at ZT = 6 (11:10AM) on the day of sampling. The temperature of the pool during the sampling period ranged from 18.9°C – 30.55°C, however the pool experienced temperature fluctuations of +/- 24.6°C between 5/23/18 and 6/29/18. The lowest temperature during monitoring was recorded as 12.4°C on 6/5/18 at 4:30AM and the hottest temperature was recorded at 37°C on 6/17/18 (the day prior to sampling) at 2:40 PM. During the sampling period, peak water temperature occurred at ZT = 8 (1:00 PM).

Nematostella gene expression *in-situ* and in laboratory conditions

Differences in transcript expression between this field-based study and a laboratory-based study by Leach and Reitzel (2019) revealed there were no genes commonly differentially expressed when comparing morning vs afternoon samples from each experiment. Six genes were significantly differentially expressed between ZT = 2 and ZT = 6 of the laboratory-based study ($p_{adj} < 0.1$). In the field-based study, 57 genes were significantly differentially expressed between ZT = 3 and ZT = 8 ($p_{adj} < 0.1$) and were enriched for metabolism- and energy-related GO terms [i.e., *'glutathione peroxidase'* (GO:0004602), *'antioxidant'* (GO:0016209), *'NADH dehydrogenase'* (GO:0003954), *'electron transport chain'* (GO:0022900), and *'oxidation-reduction*

process' (GO:0055114)]. In addition to evaluating gene expression between groupings of early time points (ZT = 3, ZT = 4, ZT = 5, ZT = 6, ZT = 7) and late time points (ZT = 8, ZT = 9, ZT = 10, ZT = 11, ZT = 12), pairwise comparisons between ZT = 3 (time point one; 0800) and later time points revealed that some genes are uniquely differentially expressed at very specific times of the day *in-situ*. *nvHSP70D* was only up-regulated at ZT = 9 (1400; compared to ZT = 3) and *nvHSP70E* was only up-regulated at ZT = 9 and ZT = 10 (1400 and 1500; compared to ZT = 3). Other genes, for example a universal stress protein (NVE2579) was upregulated for a distinct period of time (ZT = 7, 8, 9, 10, and 11 compared to ZT = 3). Together, considering these results, it is not surprising that gene expression differs between lab- and field-based studies, but understanding the multi-factors contribution to these disparities may help shed light on the underlying mechanisms that drive organism-level phenotypic responses.

Discussion

Studies in molecular ecology often experimentally test the relationship between gene expression and physiological or behavioral phenotypes in controlled laboratory settings, but few studies are conducted in the field, where multiple stressors contribute to organismal output despite being regarded as one of the most important questions in marine ecology (Breitburg et al., 1998). Marine systems, particularly coastal habitats, experience a range of environmental stressors that do not act in isolation (Crain et al., 2008) and the response to numerous intrinsic and extrinsic factors may vary depending on individual species, interacting communities or species, and/or the frequency and duration of stress(ors) (Griffen et al., 2016). The study presented here is the first to

provide insight into the transcriptomic response to combinatorial environmental factors over a tight temporal time series for a marine invertebrate in the field. By using genomic tools, these data highlight genes that have a potential ecological relevance under fluctuating environmental conditions. Our results indicate that the response of this species ‘*in-situ*’ varied significantly over the course of our 10-hour sampling period, with detection of temporal differences in gene expression, a response that could be missed if the sampling strategy was to only collect at a single time point and would complicate biological interpretation of results.

The transcriptomic responses of *Nematostella* can be broadly grouped into two major categories: up-regulated in the morning and up-regulated in the afternoon. Individual genes in each group exhibit significantly similar patterns of expression despite the complexity of abiotic fluctuations during sampling. Temperature measurements obtained every 10-minutes on the day of sampling appear to correlate with gene expression patterns. While it should be noted that these observations are limited to a single 10-hour period and likely do not provide the entire story because gene expression is a complex response to multiple interacting factors that were not quantitatively measured here, these data suggest that there was little overlap in gene expression between lab- and field-based studies. Despite these limitations, our data do support the role of certain genes or gene sets of cnidarians in response to environmental fluctuations, including heat shock genes (Black et al., 1995; Brown et al., 2002; Waller et al., 2018) and redox regulatory genes (Helm et al., 2018; Maor-Landaw and Levy, 2016).

Our study on estuarine sea anemones demonstrates the effectiveness and utility of this species to investigate environmental gene expression responses using genomic tools.

We cannot speculate on the synergy of unmeasured effects, such as oxygen availability, predator-prey interactions, or nutrient and food abundance in this system but gene expression clearly reflects environmental changes over the course of a day. The efficacy of future studies investigating variation in gene expression in response to environmental or ecosystem level changes would be significantly strengthened by an experimental design that carefully considers time-of-day, particularly in studies that only collect a few samples. In the lab or in the field, a proper approach to studies of molecular ecology will offer a better understanding of the underlying molecular basis allowing organisms to adapt to variable environments.

References

1. Aubin-Horth, N. and Renn, S. C. P. (2009). Genomic reaction norms: using integrative biology to understand molecular mechanisms of phenotypic plasticity. *Molecular Ecology* 18, 3763-3780.
2. Beck, M. W., Heck, K. L., Able, K. W., Childers, D. L., Eggleston, D. B., Gillanders, B. M., Halpern, B., Hays, C. G., Hoshino, K., Minello, T. J. et al. (2001). The identification, conservation, and management of estuarine and marine nurseries for fish and invertebrates. *Bioscience* 51, 633-641.
3. Black, N. A., Voellmy, R. and Szmant, A. M. (1995). Heat shock protein induction in *Montastraea faveolata* and *Aiptasia pallida* exposed to elevated temperatures. *Biological Bulletin* 188, 234-240.
4. Breitburg, D. L., Baxter, J. W., Hatfield, C. A., Howarth, R. W., Jones, C. G., Lovett, G. M. and Wigand, C. (1998). Understanding effects of multiple stressors: Ideas and challenges. *Successes, Limitations, and Frontiers in Ecosystem Science*, 416-431.
5. Brown, B. E., Downs, C. A., Dunne, R. P. and Gibb, S. W. (2002). Exploring the basis of thermotolerance in the reef coral *Goniastrea aspera*. *Marine Ecology Progress Series* 242, 119-129.
6. Chapman, R. W., Mancina, A., Beal, M., Veloso, A., Rathburn, C., Blair, A., Holland, A. F., Warr, G. W., Didinato, G., Sokolova, I. M. et al. (2011). The transcriptomic responses of the eastern oyster, *Crassostrea virginica*, to environmental conditions. *Molecular Ecology* 20, 1431-1449.

7. Chen, K., Li, E. C., Li, T. Y., Xu, C., Wang, X. D., Lin, H. Z., Qin, J. G. and Chen, L. Q. (2015). Transcriptome and molecular pathway analysis of the hepatopancreas in the Pacific white shrimp *Litopenaeus vannamei* under chronic low-salinity stress. *PLoS ONE* 10.
8. Crain, C. M., Kroeker, K. and Halpern, B. S. (2008). Interactive and cumulative effects of multiple human stressors in marine systems. *Ecology Letters* 11, 1304-1315.
9. Crawford, D. L. and Oleksiak, M. F. (2007). The biological importance of measuring individual variation. *Journal of Experimental Biology* 210, 1613-1621.
10. Dalziel, A. C., Rogers, S. M. and Schulte, P. M. (2009). Linking genotypes to phenotypes and fitness: how mechanistic biology can inform molecular ecology. *Molecular Ecology* 18, 4997-5017.
11. Elran, R., Raam, M., Kraus, R., Brekman, V., Sher, N., Plaschkes, I., Chalifa-Caspi, V. and Lotan, T. (2014). Early and late response of *Nematostella vectensis* transcriptome to heavy metals. *Molecular Ecology* 23, 4722-4736.
12. Griffen, B. D., Belgrad, B. A., Cannizzo, Z. J., Knotts, E. R. and Hancock, E. R. (2016). Rethinking our approach to multiple stressor studies in marine environments. *Marine Ecology Progress Series* 543, 273-281.
13. Gunderson, A. R., Armstrong, E. J. and Stillman, J. H. (2016). Multiple stressors in a changing world: The need for an improved perspective on physiological responses to the dynamic marine environment. *Annual Review of Marine Science*, Vol 8 8, 357-+.

14. Hand, C. and Uhlinger, K. R. (1992). The culture, sexual and asexual reproduction, and growth of the sea anemone *Nematostella vectensis*. *Biological Bulletin* 182, 169-176.
15. Hand, C. and Uhlinger, K. R. (1994). The unique, widely distributed, estuarine sea anemone, *Nematostella vectensis* Stephenson: a review, new facts, and questions. *Estuaries* 17.
16. Harvey, B. P., Gwynn-Jones, D. and Moore, P. J. (2013). Meta-analysis reveals complex marine biological responses to the interactive effects of ocean acidification and warming. *Ecology and Evolution* 3, 1016-1030.
17. Helm, R. R., Martin-Diaz, M. L. and Tarrant, A. M. (2018). Phylogenetic analysis of cnidarian peroxiredoxins and stress-responsive expression in the estuarine sea anemone *Nematostella vectensis*. *Comparative Biochemistry and Physiology Part A: Molecular Integrative Physiology* 221, 32-43.
18. Helm, R. R., Siebert, S., Tulin, S., Smith, J. and Dunn, C. W. (2013). Characterization of differential transcript abundance through time during *Nematostella vectensis* development. *BMC Genomics*. 14.
19. Hofmann, G. E., Burnaford, J. L. and Fielman, K. T. (2005). Genomics-fueled approaches to current challenges in marine ecology. *Trends in Ecology & Evolution* 20, 305-311.
20. Jackson, R. B., Linder, C. R., Lynch, M., Purugganan, M., Somerville, S. and Thayer, S. S. (2002). Linking molecular insight and ecological research. *Trends in Ecology & Evolution* 17, 409-414.

21. Kauffmann, A., Gentleman, R. and Huber, W. (2009). arrayQualityMetrics--a bioconductor package for quality assessment of microarray data. *Bioinformatics* (Oxford, England) 25, 415-6.
22. Langmead, B. and Salzberg, S. L. (2012). Fast gapped-read alignment with Bowtie 2. *Nature Methods* 9, 357-U54.
23. Leach, W. B. and Reitzel, A. M. (2019). Transcriptional remodeling upon light removal in a model cnidarian: losses and gains in gene expression. *Molecular Ecology*.
24. Levene, H. (1960). "Robust Tests for Equality of Variances," in Contributions to Probability and Statistics, ed. I. Olkin, Palo Alto, Calif.: Stanford University Press, 278-292.
25. Li, E. C., Wang, S. L., Li, C., Wang, X. D., Chen, K. and Chen, L. Q. (2014). Transcriptome sequencing revealed the genes and pathways involved in salinity stress of Chinese mitten crab, *Eriocheir sinensis*. *Physiological Genomics* 46, 177-190.
26. Li, T. D. and Brouwer, M. (2013). Field study of cyclic hypoxic effects on gene expression in grass shrimp hepatopancreas. *Comparative Biochemistry and Physiology D-Genomics & Proteomics* 8, 309-316.
27. Love, M. I., Huber, W. and Anders, S. (2014). Moderated estimation of fold change and dispersion for RNA-seq data with DESeq2. *Genome Biology* 15.
28. Lu, X., Kong, J., Luan, S., Dai, P., Meng, X. H., Cao, B. X. and Luo, K. (2016). Transcriptome analysis of the hepatopancreas in the Pacific white shrimp (*Litopenaeus vannamei*) under acute ammonia stress. *PLoS ONE* 11.

29. Maor-Landaw, K., Karako-Lampert, S., Ben-Asher, H. W., Goffredo, S., Falini, G., Dubinsky, Z. and Levy, O. (2014). Gene expression profiles during short-term heat stress in the red sea coral *Stylophora pistillata*. *Global Change Biology* 20, 3026-3035.
30. Maor-Landaw, K. and Levy, O. (2016). Gene expression profiles during short-term heat stress; branching vs. massive Scleractinian corals of the Red Sea. *PeerJ* 4.
31. McBryan, T. L., Anttila, K., Healy, T. M. and Schulte, P. M. (2013). Responses to temperature and hypoxia as interacting stressors in fish: Implications for adaptation to environmental change. *Integrative and Comparative Biology* 53, 648-659.
32. Mishra, Y., Jankanpaa, H. J., Kiss, A. Z., Funk, C., Schroder, W. P. and Jansson, S. (2012). *Arabidopsis* plants grown in the field and climate chambers significantly differ in leaf morphology and photosystem components. *BMC Plant Biology* 12.
33. Muller, W. E. G., Batel, R., Lacorn, M., Steinhart, H., Simat, T., Lauenroth, S., Hassanein, H. and Schroder, H. C. (1998). Accumulation of cadmium and zinc in the marine sponge *Suberites domuncula* and its potential consequences on single-strand breaks and on expression of heat-shock protein: a natural field study. *Marine Ecology Progress Series* 167, 127-135.
34. Oleksiak, M. F., Churchill, G. A. and Crawford, D. L. (2002). Variation in gene expression within and among natural populations. *Nature Genetics* 32, 261-266.

35. Oren, M., Tarrant, A. M., Alon, S., Simon-Blecher, N., Elbaz, I., Appelbaum, L. and Levy, O. (2015). Profiling molecular and behavioral circadian rhythms in the non-symbiotic sea anemone *Nematostella vectensis*. *Scientific Reports* 5, 11418.
36. Overgaard, J., Sorensen, J. G., Jensen, L. T., Loeschcke, V. and Kristensen, T. N. (2010). Field tests reveal genetic variation for performance at low temperatures in *Drosophila melanogaster*. *Functional Ecology* 24, 186-195.
37. Pearson, W. R., Wood, T., Zhang, Z. and Miller, W. (1997). Comparison of DNA sequences with protein sequences. *Genomics* 46, 24-36.
38. Przeslawski, R., Byrne, M. and Mellin, C. (2015). A review and meta-analysis of the effects of multiple abiotic stressors on marine embryos and larvae. *Global Change Biology* 21, 2122-2140.
39. Purugganan, M. and Gibson, G. (2003). Merging ecology, molecular evolution, and functional genetics. *Molecular Ecology* 12, 1109-1112.
40. Reitzel, A. M., Chu, T., Edquist, S., Genovese, C., Church, C., Tarrant, A. M. and Finnerty, J. R. (2013a). Physiological and developmental responses to temperature by the sea anemone *Nematostella vectensis*. *Marine Ecology Progress Series* 484, 115-130.
41. Reitzel, A. M., Herrera, S., Layden, M. J., Martindale, M. Q. and Shank, T. M. (2013b). Going where traditional markers have not gone before: utility of and promise for RAD sequencing in marine invertebrate phylogeography and population genomics. *Molecular Ecology* 22, 2953-2970.

42. Richards, C. L., Rosas, U., Banta, J., Bhambhra, N. and Purugganan, M. D. (2012). Genome-wide patterns of *Arabidopsis* gene expression in nature. *PLoS Genetics* 8, 482-495.
43. Satake, A., Kawatsu, K., Teshima, K., Kabeya, D. and Han, Q. M. (2019). Field transcriptome revealed a novel relationship between nitrate transport and flowering in Japanese beech. *Scientific Reports* 9.
44. Schaefer, R. B. and Piggott, J. J. (2018). Advancing understanding and prediction in multiple stressor research through a mechanistic basis for null models. *Global Change Biology* 24, 1817-1826.
45. Smith, S., Bernatchez, L. and Beheregaray, L. B. (2013). RNA-seq analysis reveals extensive transcriptional plasticity to temperature stress in a freshwater fish species. *BMC Genomics* 14.
46. Todd, E. V., Black, M. A. and Gemmell, N. J. (2016). The power and promise of RNA-seq in ecology and evolution. *Molecular Ecology* 25, 1224-1241.
47. Vanin, S., Bhutani, S., Montelli, S., Menegazzi, P., Green, E. W., Pegoraro, M., Sandrelli, F., Costa, R. and Kyriacou, C. P. (2012). Unexpected features of *Drosophila* circadian behavioural rhythms under natural conditions. *Nature* 484, 371-U108.
48. Waller, S. J., Knighton, L. E., Crabtree, L. M., Perkins, A. L., Reitzel, A. M. and Truman, A. W. (2018). Characterizing functional differences in sea anemone Hsp70 isoforms using budding yeast. *Cell Stress & Chaperones* 23, 933-941.
49. Warner, J. F., Guerlais, V., Amiel, A. R., Johnston, H., Nedoncelle, K. and Rottinger, E. (2018). NvERTx: a gene expression database to compare

embryogenesis and regeneration in the sea anemone *Nematostella vectensis*.

Development 145.

50. Williams, R. (1983). The starlet sea anemone: *Nematostella vectensis* Stephenson 1935. In: Wells SM, Pyle RM, Collins NM (eds) The IUCN invertebrate red data book. International Union for Conservation of Nature and Natural Resources, Gland, pp 43–46.

Figures

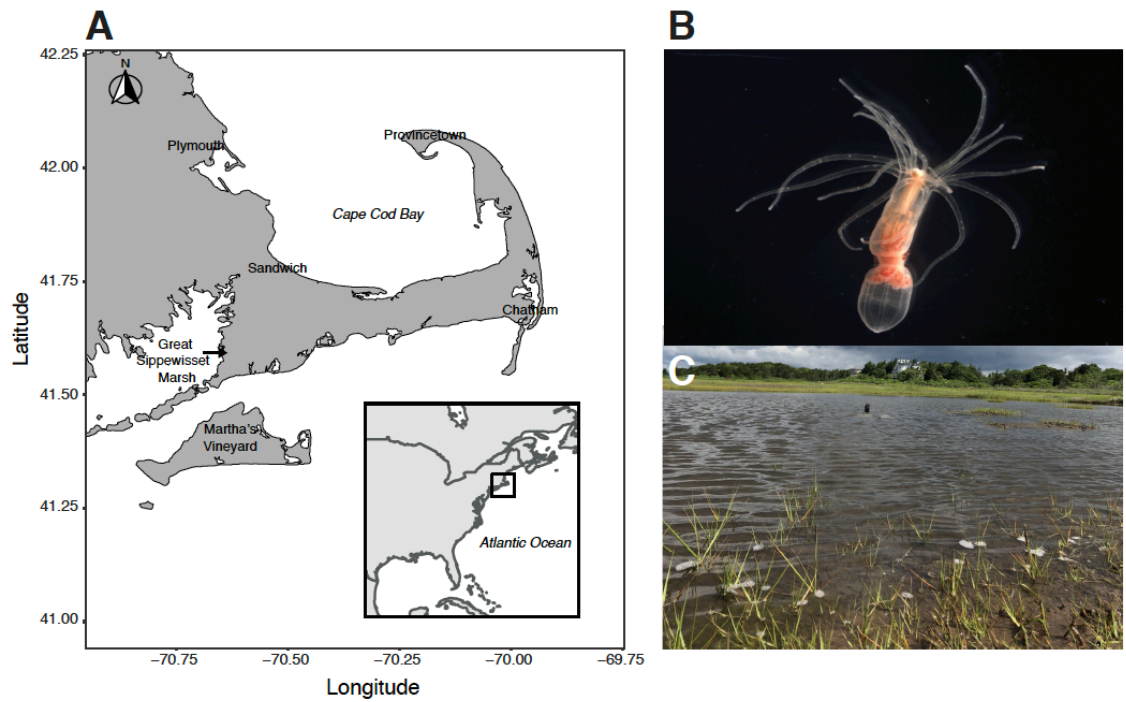


Figure 1. Map of field sampling site (A) and study species, adult *Nematostella vectensis* (B), at Great Sippewissett Marsh in Massachusetts (C).

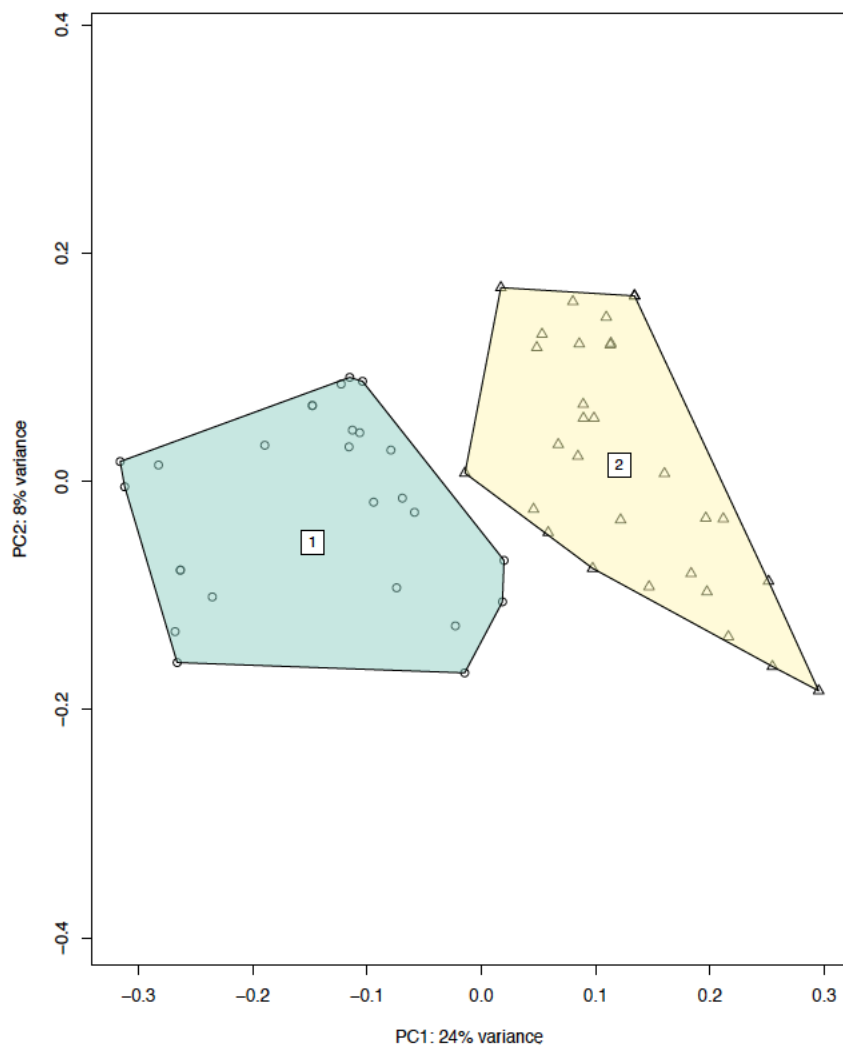


Figure 2. Principal Component Analysis (PCA) of samples collected between 08:00-12:00 (blue) and 13:00-17:00 (yellow).

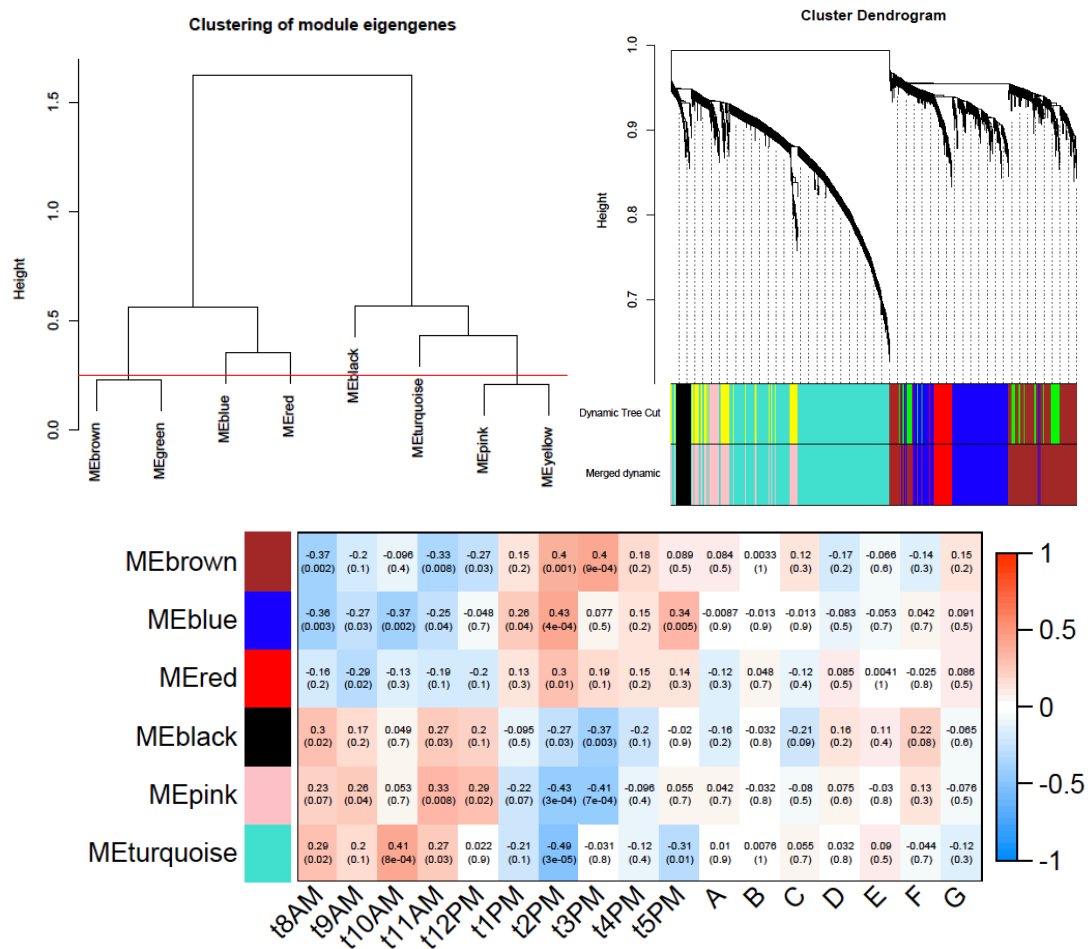


Figure 3. Weighted gene co-expression network analyses in this study. Gene dendrogram of modules based on correlation calculations from rlog transformed count data generated by DESeq2 and obtained by average linkage hierarchical clustering in WGCNA analysis. Colors of the dynamic tree cut represent the modules assigned for each gene, and the colors of the merged dynamic display the new modules after assigning a stringency threshold of 0.25 (A). Average linkage hierarchal cluster tree shows module eigengenes after clustering analysis. Each branch represents a meta-module that groups together the eigengenes that are positively correlated (B). Module-trait relationship heatmap and significance values of each module eigengene correlated to external traits from weighted gene co-expression network analysis (C). Gene co-expression network and module-trait relationships are represented by a heatmap of transcripts assigned to six modules (arbitrary colors on the left of the heatmap). Eigengenes were calculated for each module. The strength of the correlations between traits (time point and biological replicates) and gene expression, is indicated by the intensity of the colored blocks with red and blue indicating positive and negative correlations, respectively. The numbers in each block represent the Pearson's correlation between the module eigengene and the trait and corresponding p-values.

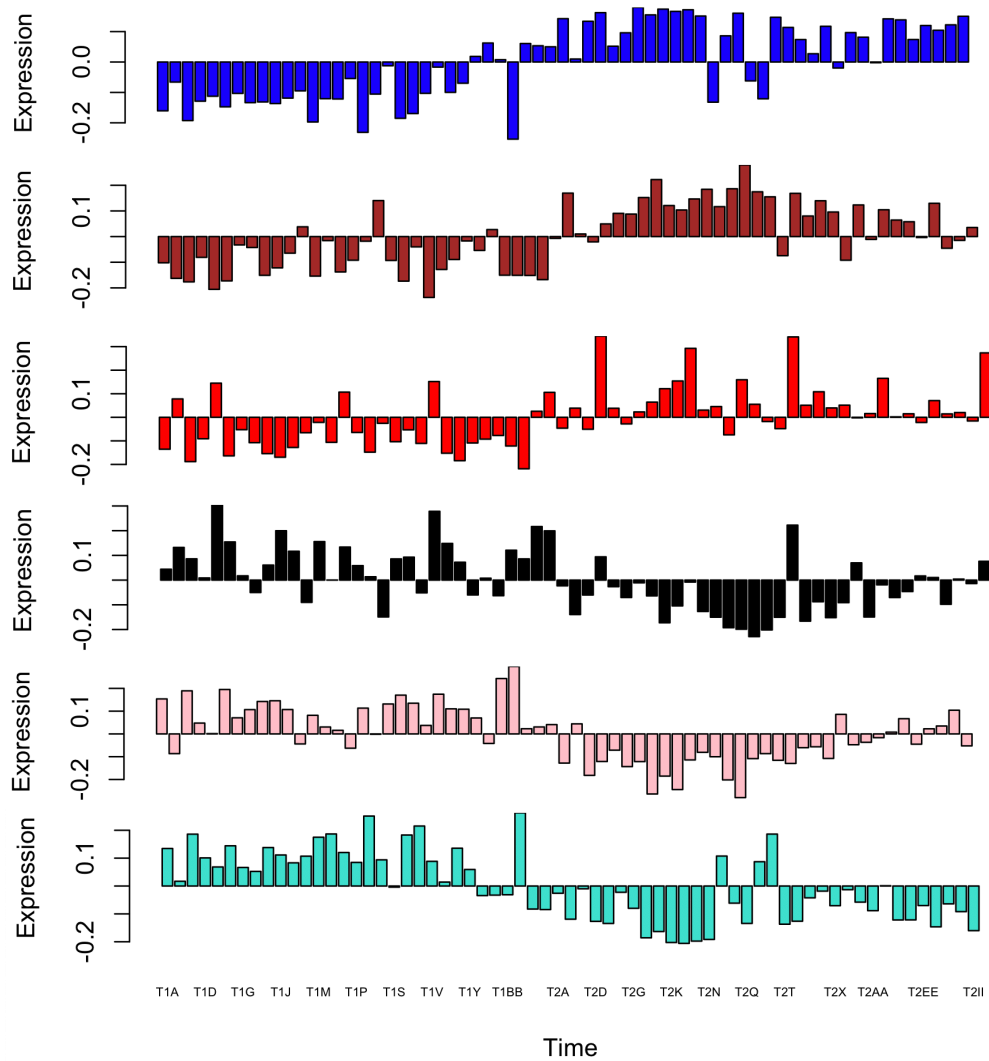


Figure 4. (A) Module eigengenes with up-regulation in the afternoon (blue, brown, red) and (B) in the morning (black, pink, turquoise) with eigengene expression on the Y-axis and time on the X-axis. Each bar represents a single replicate.

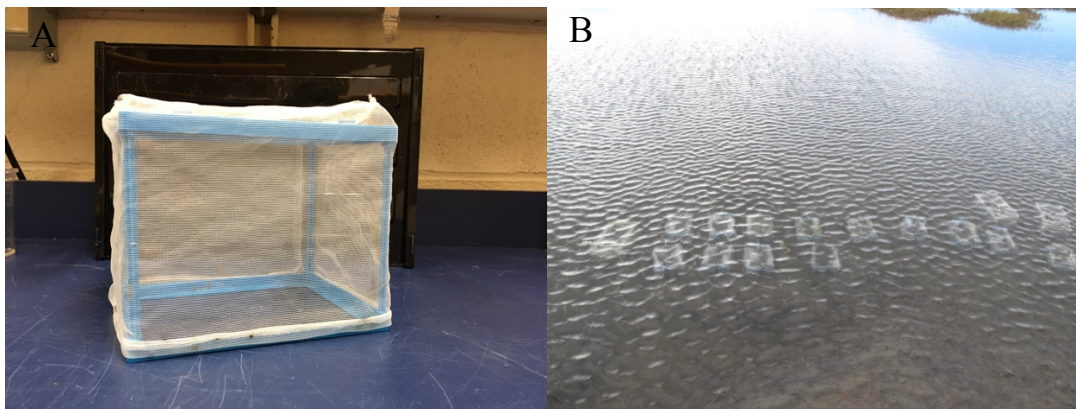


Figure S1. Small pen used for *Nematostella vectensis* (A) deployment and recapture (B).



Figure S2. Gene ontology (GO) enrichment analysis for differentially expressed genes between morning and afternoon samples in the Molecular Function category. AM up-regulated genes are shown in red. PM up-regulated genes are shown in blue.

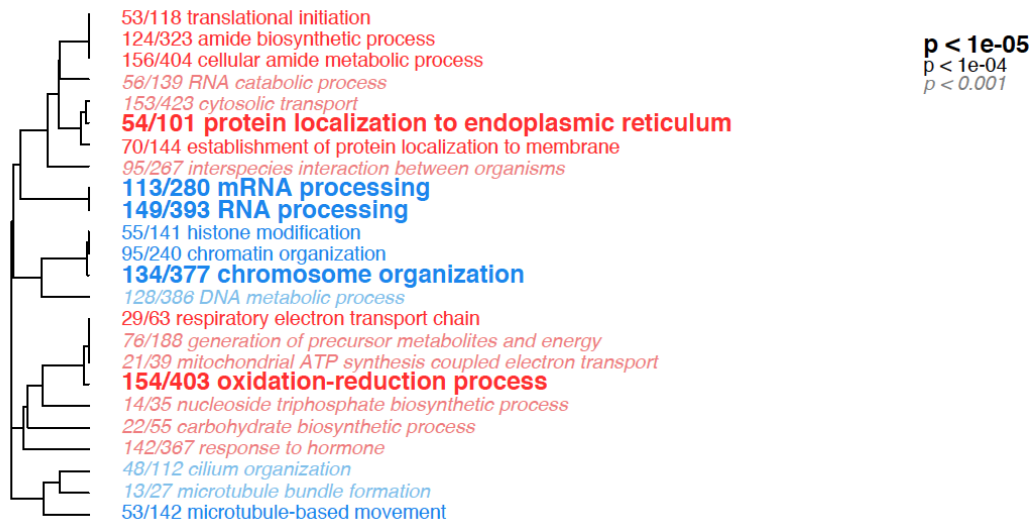


Figure S3. Gene ontology (GO) enrichment analysis for differentially expressed genes between morning and afternoon samples in the Biological Processes category. AM up-regulated genes are shown in red. PM up-regulated genes are shown in blue.

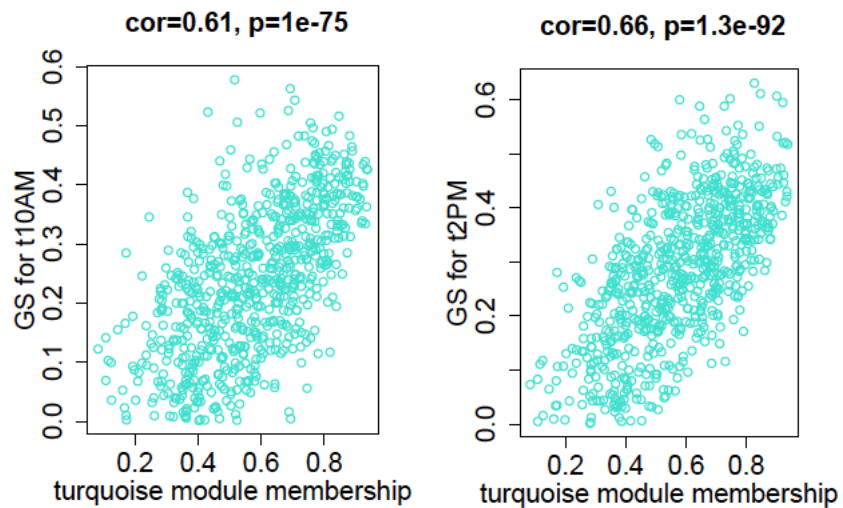


Figure S4. Gene significance scatter plots for the turquoise module. The plots represent gene significance (GS; y-axis) at t10AM (A) and t2PM (B) versus module membership (MM; x-axis). Gene significance and module membership are significant correlations that imply the genes of each module are highly correlated with the time of day sampled.

CONCLUSIONS

This dissertation uses an integrative approach at dissecting behavior and gene expression in the lab and in the field to better understand cyclic responses of the sea anemone, *Nematostella vectensis*. The first four chapters explore behavior and gene expression of *Nematostella* in laboratory conditions, where we manipulate light conditions and measure organismal responses. The last chapter examines environmental gene expression over time during the photoperiod of animals collected *in-situ*.

In chapter one, we hypothesized gene expression in *Nematostella* would dampen following light cue removal after established entrainment in light:dark conditions. Our results did not show a reduction in gene expression in the absence of diel light, but the opposite. Upon light removal, we measured up-regulation in several hundred genes that were not cycling in the presence of diel conditions. Several of these genes were identified to be involved in stress responses. Many candidate cnidarian circadian clock genes turned out to be rhythmically expressed in the presence of light:dark cycling, but as soon as the light cue was removed, this pattern was no longer present in this gene set suggesting that these ‘circadian’ genes are actually photoresponsive.

In chapter two, we hypothesized that *Nematostella* would show nocturnal behavioral patterns in response to different portions of the light spectrum (red, green, and blue) with gene expression patterns unique to each condition. Our results supported circadian behavioral activity in response to green and blue light, however in red light and constant dark conditions, *Nematostella* exhibited an activity pattern similar to circatidal behavior in other tidal organisms. Transcriptional responses of anemones in each light condition were similarly unique, but gene expression of animals under diel red light

showed the greatest differential expression between day and night sampling points.

Together, these behavioral and transcriptomic data suggest that *Nematostella* is capable of light entrainment in a broad range of wavelengths even without ocular photoreceptors.

In chapter three, we measure gene expression in three cell types of *Nematostella* to identify spatial patterns and potential circadian regulation. These data support that in *Nematostella*, neural cells contain the components of a complete clock that is capable of light entrainment.

In chapter four, we identified diel oscillations in microbial abundance of *Nematostella* under light:dark or dark:dark conditions. We identify specific bacterial OTUs that are differentially abundant in each light regime and suggests that there is a correlation between the photoperiod and bacterial partners within *Nematostella*.

In chapter five, *Nematostella* was sampled every hour for 10 hours in a natural setting and gene expression results showed that time-of-day and sampling strategy impact the interpretation of our transcriptomic results and that there is tremendous variability in gene expression patterns over a fine time scale in a dynamic habitat. Further, we were able to correlate transcriptional patterns to environmental data collected at the time of the experiment.

INTRODUCTION REFERENCES

1. Allada, R. and Chung, B. Y. (2010). Circadian organization of behavior and physiology in *Drosophila*. *Annual Review of Physiology* 72, 605-24.
2. Amoutzias, G., Veron, A., Weiner, J., Robinson-Rechavi, M., Bornberg-Bauer, E., Oliver, S. and Robertson, D. (2007). One billion years of bZIP transcription factor evolution: Conservation and change in dimerization and DNA-binding site specificity. *Molecular Biology and Evolution* 24, 827-835.
3. Brady, A. K., Snyder, K. A. and Vize, P. D. (2011). Circadian cycles of gene expression in the coral, *Acropora millepora*. *PLoS ONE* 6, e25072.
4. Buhr, E. D. and Takahashi, J. S. (2013). Molecular components of the mammalian circadian clock. *Handbook of Experimental Pharmacology*, 3-27.
5. Cyran, S. A., Buchsbaum, A. M., Reddy, K. L., Lin, M.-C., Glossop, N. R. J., Hardin, P. E., Young, M. W., Storti, R. V. and Blau, J. (2003). Vrille, Pdp1, and dClock form a second feedback loop in the *Drosophila* circadian clock. *Cell* 112, 329-341.
6. Darling, J. A., Reitzel, A. M. and Finnerty, J. R. (2004). Regional population structure of a widely introduced estuarine invertebrate: *Nematostella vectensis* Stephenson in New England. *Molecular Ecology* 13, 2969-2981.
7. Dodd, A. N., Salathia, N., Hall, A., Kévei, E., Tóth, R., Nagy, F., Hibberd, J. M., Millar, A. J. and Webb, A. A. R. (2005). Plant circadian clocks increase photosynthesis, growth, survival, and competitive advantage. *Science* 309, 630-633.

8. Dunlap, J. C. (1999). Molecular bases for circadian clocks. *Cell* 96, 271-290.
9. Frank, P. G. and Bleakney, J. S. (1978). Asexual reproduction, diet, and anomalies of anemone *Nematostella vectensis* in Nova Scotia. *Canadian Field-Naturalist* 92, 259-263.
10. Fritzenwanker, J. and Technau, U. (2002). Induction of gametogenesis in the basal cnidarian *Nematostella vectensis* (Anthozoa). *Development Genes and Evolution* 212, 99 - 103.
11. Genikhovich, G. and Technau, U. (2009a). In situ hybridization of starlet sea anemone (*Nematostella vectensis*) embryos, larvae, and polyps. *Cold Spring Harbor Protocols* 2009, pdb.prot5284-pdb.prot5284.
12. Genikhovich, G. and Technau, U. (2009b). Induction of spawning in the starlet sea anemone *Nematostella vectensis*, in vitro fertilization of gametes, and dejellying of zygotes. *Cold Spring Harbor Protocols* 2009, pdb.prot5281-pdb.prot5281.
13. Genikhovich, G., Technau, U. and Cold Spring Harbor Laboratory, P. (2010). The starlet sea anemone *Nematostella vectensis*: An anthozoan model organism for studies in comparative genomics and functional evolutionary developmental biology. *Emerging Model Organisms: Laboratory Manual*, Vol 2, 95-118.
14. Golden, S. S., Ishiura, M., Johnson, C. H. and Kondo, T. (1997). Cyanobacterial circadian rhythms. *Annual Review of Plant Physiology and Plant Molecular Biology* 48, 327-354.

15. Hand, C. and Uhlinger, K. R. (1992). The culture, sexual and asexual reproduction, and growth of the sea anemone *Nematostella vectensis*. *Biological Bulletin* 182, 169-176.
16. Hand, C. and Uhlinger, K. R. (1994). The unique, widely distributed, estuarine sea anemone, *Nematostella vectensis* Stephenson: A review, new facts, and questions. *Estuaries* 17, 501.
17. Hardin, P. E., Hall, J. C. and Rosbash, M. (1990). Feedback of the *Drosophila* period gene-product on circadian cycling of its messenger-RNA levels. *Nature* 343, 536-540.
18. Hardin, P. E., Hall, J. C. and Rosbash, M. (1992). Circadian oscillations in period gene messenger-RNA levels are transcriptionally regulated. *Proceedings of the National Academy of Sciences of the United States of America* 89, 11711-11715.
19. He, S., del Viso, F., Chen, C.-Y., Ikmi, A., Kroesen, A. E. and Gibson, M. C. (2018). An axial Hox code controls tissue segmentation and body patterning in *Nematostella vectensis*. *Science* 361, 1377-+.
20. Heath-Heckman, E. A. C., Peyer, S. M., Whistler, C. A., Apicella, M. A., Goldman, W. E. and McFall-Ngai, M. J. (2013). Bacterial bioluminescence regulates expression of a host cryptochrome gene in the squid-vibrio symbiosis. *mBio* 4.
21. Hemond, E. M. and Vollmer, S. V. (2015). Diurnal and nocturnal transcriptomic variation in the Caribbean staghorn coral, *Acropora cervicornis*. *Molecular Ecology* 24, 4460-73.

22. Hendricks, W. D., Byrum, C. A. and Meyer-Bernstein, E. L. (2012). Characterization of circadian behavior in the starlet sea anemone, *Nematostella vectensis*. *PLoS ONE* 7, e46843.
23. Hoadley, K. D., Szmant, A. M. and Pyott, S. J. (2011). Circadian clock gene expression in the coral *Favia fragum* over diel and lunar reproductive cycles. *PLoS ONE* 6, e19755.
24. Hoadley, K. D., Vize, P. D. and Pyott, S. J. (2016). Current understanding of the circadian clock within cnidaria. In the cnidaria, past, present and future: The world of Medusa and her sisters, eds. S. Goffredo and Z. Dubinsky), pp. 511-520. Cham: Springer International Publishing.
25. Horne, J. A. and Renninger, G. H. (1988). Circadian photoreceptor organs in *Limulus*. *Journal of Comparative Physiology a-Sensory Neural and Behavioral Physiology* 162, 127-132.
26. Ikmi, A., McKinney, S. A., Delventhal, K. M. and Gibson, M. C. (2014). TALEN and CRISPR/Cas9-mediated genome editing in the early-branching *metazoan* *Nematostella vectensis*. *Nature Communications* 5.
27. Jindrich, K., Roper, K. E., Lemon, S., Degnan, B. M., Reitzel, A. M. and Degnan, S. M. (2017). Origin of the animal circadian clock: Diurnal and light-entrained gene expression in the sponge *Amphimedon queenslandica*. *Frontiers in Marine Science* 4.
28. Karabulut, A., He, S., Chen, C.-Y., McKinney, S. A. and Gibson, M. C. (2019). Electroporation of short hairpin RNAs for rapid and efficient gene knockdown in

- the starlet sea anemone, *Nematostella vectensis*. *Developmental Biology* 448, 7-15.
29. Kneib, R. T. (1985). Predation and disturbance by grass shrimp, *Palaemonetes pugio holthius*, in soft-substratum benthic invertebrate assemblages. *Journal of Experimental Marine Biology and Ecology* 93, 91-102.
30. Konopka, R. J. and Benzer, S. (1971). Clock mutants of *Drosophila melanogaster*. *Proceedings of the National Academy of Sciences* 68, 2112-2116.
31. Layden, M. J., Rentzsch, F. and Rottinger, E. (2016). The rise of the starlet sea anemone *Nematostella vectensis* as a model system to investigate development and regeneration. *Wiley Interdisciplinary Reviews-Developmental Biology* 5, 408-428.
32. Leach, W. B., Macrander, J., Peres, R. and Reitzel, A. M. (2018). Transcriptome-wide analysis of differential gene expression in response to light:dark cycles in a model cnidarian. *Comparative Biochemistry and Physiology Part D: Genomics and Proteomics* 26, 40-49.
33. Levy, O., Appelbaum, L., Leggat, W., Gothlif, Y., Hayward, D. C., Miller, D. J. and Hoegh-Guldberg, O. (2007). Light-responsive cryptochromes from a simple multicellular animal, the coral *Acropora millepora*. *Science* 318, 467-470.
34. Maas, A. E., Jones, I. T., Reitzel, A. M. and Tarrant, A. M. (2016). Daily cycle in oxygen consumption by the sea anemone *Nematostella vectensis* Stephenson. *Biology Open* 5, 161-164.

35. Merlin, C., Gegear, R. J. and Reppert, S. M. (2009). Antennal circadian clocks coordinate sun compass orientation in migratory monarch butterflies. *Science* 325, 1700-1704.
36. Meuti, M. E., Stone, M., Ikeno, T. and Denlinger, D. L. (2015). Functional circadian clock genes are essential for the overwintering diapause of the Northern house mosquito, *Culex pipiens*. *Journal of Experimental Biology* 218, 412-422.
37. Moran, Y., Fredman, D., Praher, D., Li, X. Z., Wee, L. M., Rentzsch, F., Zamore, P. D., Technau, U. and Seitz, H. (2014). Cnidarian microRNAs frequently regulate targets by cleavage. *Genome Research* 24, 651-663.
38. Oren, M., Tarrant, A. M., Alon, S., Simon-Blecher, N., Elbaz, I., Appelbaum, L. and Levy, O. (2015). Profiling molecular and behavioral circadian rhythms in the non-symbiotic sea anemone *Nematostella vectensis*. *Scientific Reports* 5, 11418.
39. Panda, S., Hogenesch, J. B. and Kay, S. A. (2002). Circadian rhythms from flies to human. *Nature* 417, 329-335.
40. Peres, R., Reitzel, A. M., Passamaneck, Y., Afeche, S. C., Cipolla-Neto, J., Marques, A. C. and Martindale, M. Q. (2014). Developmental and light-entrained expression of melatonin and its relationship to the circadian clock in the sea anemone *Nematostella vectensis*. *EvoDevo* 5, 26.
41. Posey, M. H. and Hines, A. H. (1991). Complex predator-prey interactions within an estuarine benthic community. *Ecology* 72, 2155-2169.
42. Putnam, N., Srivastava, M., Hellsten, U., Dirks, B., Chapman, J., Salamov, A., Terry, A., Shapiro, H., Lindquist, E. and Kapitonov, V. (2007). Sea anemone

genome reveals ancestral eumetazoan gene repertoire and genomic organization. *Science* 317, 86 - 94.

43. Reinke, A. W., Baek, J., Ashenberg, O. and Keating, A. E. (2013). Networks of bZIP protein-protein interactions diversified over a billion years of evolution. *Science* 340.
44. Reitzel, A. M., Behrendt, L. and Tarrant, A. M. (2010). Light entrained rhythmic gene expression in the sea anemone *Nematostella vectensis*: the evolution of the animal circadian clock. *PLoS ONE* 5, e12805.
45. Reitzel, A. M., Chu, T., Edquist, S., Genovese, C., Church, C., Tarrant, A. M. and Finnerty, J. R. (2013a). Physiological and developmental responses to temperature by the sea anemone *Nematostella vectensis*. *Marine Ecology Progress Series* 484, 115-130.
46. Reitzel, A. M., Darling, J. A., Sullivan, J. C. and Finnerty, J. R. (2008). Global population genetic structure of the starlet anemone *Nematostella vectensis*: multiple introductions and implications for conservation policy. *Biological Invasions* 10, 1197-1213.
47. Reitzel, A. M., Tarrant, A. M. and Levy, O. (2013b). Circadian clocks in the cnidaria: environmental entrainment, molecular regulation, and organismal outputs. *Integrative and Comparative Biology* 53, 118-30.
48. Renfer, E. and Technau, U. (2017). Meganuclease-assisted generation of stable transgenics in the sea anemone *Nematostella vectensis*. *Nature Protocols* 12, 1844-1854.

49. Reppert, S. M. (2000). Cellular and molecular basis of circadian timing in mammals. *Seminars in Perinatology* 24, 243-246.
50. Reppert, S. M. and Weaver, D. R. (2002). Coordination of circadian timing in mammals. *Nature* 418, 935-941.
51. Rosbash, M. (2009). The implications of multiple circadian clock origins. *PLoS Biology* 7, e1000062.
52. Schwaiger, M., Schönauer, A., Rendeiro, A. F., Pribitzer, C., Schauer, A., Gilles, A. F., Schinko, J. B., Renfer, E., Fredman, D. and Technau, U. (2014). Evolutionary conservation of the eumetazoan gene regulatory landscape. *Genome Research* 24, 639-650.
53. Sebens, K. P. and DeRiemer, K. (1977). Diel cycles of expansion and contraction in coral reef anthozoans. *Marine Biology* 43, 247-256.
54. Sebé-Pedrós, A., Saudemont, B., Chomsky, E., Plessier, F., Mailhé, M.-P., Renno, J., Loe-Mie, Y., Lifshitz, A., Mukamel, Z., Schmutz, S. et al. (2018). Cnidarian cell type diversity and regulation revealed by whole-organism single-cell RNA-Seq. *Cell* 173, 1520-1534.e20.
55. Shearer, M., Suwailem, A. M. and Rowe, G. A. (1997). The anemone, *Nematostella vectensis*, in Britain: considerations for conservation management. *Aquatic Conservation: Marine and Freshwater Ecosystems* 7, 13-25.
56. Suga, H., Schmid, V. and Gehring, W. J. (2008). Evolution and functional diversity of jellyfish opsins. *Current Biology* 18, 51-55.
57. Vize, P. D. (2009). Transcriptome analysis of the circadian regulatory network in the coral *Acropora millepora*. *Biological Bulletin* 216, 131-137.

58. Williams, R. (1983). The starlet sea anemone: *Nematostella vectensis* Stephenson 1935. In: Wells SM, Pyle RM, Collins NM (eds) The IUCN invertebrate red data book. *International Union for Conservation of Nature and Natural Resources, Gland*, pp 43–46.
59. Wolenski, F. S., Layden, M. J., Martindale, M. Q., Gilmore, T. D. and Finnerty, J. R. (2013). Characterizing the spatiotemporal expression of RNAs and proteins in the starlet sea anemone, *Nematostella vectensis*. *Nature Protocols* 8, 900-915.
60. Yuan, Q., Metterville, D., Briscoe, A. D. and Reppert, S. M. (2007). Insect cryptochromes: gene duplication and loss define diverse ways to construct insect circadian clocks. *Molecular Biology and Evolution* 24, 948-955.
61. Zemach, A., McDaniel, I. E., Silva, P. and Zilberman, D. (2010). Genome-wide evolutionary analysis of eukaryotic DNA methylation. *Science* 328, 916-919.
62. Zhu, H., Sauman, I., Yuan, Q., Casselman, A., Emery-Le, M., Emery, P. and Reppert, S. M. (2008a). Cryptochromes define a novel circadian clock mechanism in monarch butterflies that may underlie sun compass navigation. *PLoS Biology* 6, e4.